Department of Mechanical Engineering

EF900 – Individual MSc Project

Identification and Evaluation of Critical Parameters Affecting Photovoltaic Performance in Buildings

Author: Ioannis Tsironis

Supervisor: Dr Paul Strachan

A thesis submitted in partial fulfilment for the requirement of degree in Master of Science in Energy Systems and the Environment

2010

Copyright Declaration

This thesis is the result of the author's original research. It has been composed by the author and has not been previously submitted for examination which has led to the award of a degree.

The copyright of this thesis belongs to the author under the terms of the United Kingdom Copyright Acts as qualified by University of Strathclyde Regulation 3.50. Due acknowledgement must always be made of the use of any material contained in, or derived from, this thesis.

Signed: Ioannis Tsironis   Date: 9th November 2010

Abstract

The aim of this project is to make a general review of PV technology, identify and evaluate the most significant (often interactive) parameters that affect the PV system performance and investigate in depth the 2 most important: the array inclination and orientation.

Chapter 2 states the necessity to satisfy our energy demands and reduce CO_2 emissions by using renewable energy systems. PV play an important role towards that direction. Chapter 3 analyses the effect of the various solar angles regarding the incident solar radiation on a PV surface and how the global solar radiation is divided into its direct and diffuse components. Chapter 4 makes a brief analysis of PV cell technology, the various PV types, their environmental impact and financial aspects. Additionally, the basic components of a PV system are presented as well as the literature concerning the parameters affecting PV performance when connected to the dwelling's load and to the grid. Chapter 5 constitutes an introduction for chapters 6 and 7 regarding the widely recognised research oriented simulation tool Merit (University of Strathclyde) and the developed Excel tool, both of which are used in order to investigate the potential energy yield of PV systems.

Chapter 6 refers to a case study of 30 semi-detached dwellings in Troon. It focuses on the evaluation of actual climatic input and power PV output data. A climatic – demand - supply data file concerning one dwelling has been selected. Global solar radiation on a horizontal surface has been introduced to a developed Excel sheet designed to split it into its diffuse and direct / direct normal components since such a data form is required by the majority of current available simulation tools. In addition, the created Excel tool provides realistic and relatively agreeable results compared to those of the actual case study. Indicatively, it overestimates by 9.44% the measured annual PV array output (957.9kWh compared to the measured 867.5kWh). Merit's results are higher than the tool's results. The PV array in Troon is orientated 17° east of south and inclined 45° from the horizontal plane. An inclination of 35° (optimal inclination) would increase the PV array output by 3.85% (orientation angle γ fixed at 17° east of south). Furthermore, if PV were due south (optimal orientation), an 8.67% increase in the potential energy yield would appear (inclination angle equal to 45°).

In chapter 7, it is estimated the PV system performance and how it is affected by orientation and inclination in 4 different climate regions. These are Glasgow (included in the less fortunate solar gain zone of northern Europe as illustrated in maps in literature), Oban (a coastal Scottish area), Jersey (a sunny island in southern England with similar solar radiation levels to central Europe) and Athens (a typical southern European climatic region). The tool

results are in close agreement with Merit and PVGIS (4-6% / less than 1% deviation with Merit concerning northern / southern regions respectively and 3-5% / 1.5% divergence with PVGIS regarding horizontal / optimal inclined PV systems). The only noticeable deviation of approximately 15% has been noted in case of vertically inclined systems when comparing the tool with PVGIS. According to the developed tool, an optimal inclined and south orientated PV system in Athens generates 1261.2kWh, meaning 23.7% / 39.9% / 43.36% more electricity than in Jersey / Glasgow / Oban respectively. Orientation when varying array direction 90° from due south has lead to a maximum energy output decrease of 16-20% and no correlation between latitude and orientation has been identified.

Finally, in chapter 8, the main project outcomes and various significant issues that need to be further dealt with regarding PV systems are presented.

Acknowledgements

I would like to acknowledge first and foremost my supervisor Dr Paul Strachan for his diligent support and guidance throughout this project.

I would like to thank Dr Jun Hong and Amos Madhlopa for their useful advice.

My thanks also go to Andrew Marnie at South Ayrshire Council for his help in providing the data which I used in the Troon case study.

I would lastly like to express my gratitude to my family for their encouragement and continued support throughout this Master's course.

1 Table of Contents

2 Introduction

2.1 Global warming

Reducing energy consumption in the building sector based on fossil fuel can play an important role regarding necessary cuts in current carbon emissions. This should be primarily dealt with through the reduction of energy consumption by improving thermal performance of new buildings as well as retrofitting measures regarding existing older constructions. The reduced fossil fuel consumption could be then minimized by exploiting local renewable energy sources e.g. solar, wind etc.

2.2 Building sector – energy demand profiles

Roughly 27% of Britain's energy consumption is attributed to the housing sector [1]. More general, in the European Union, the buildings are responsible for about 40% of the total energy demands. Therefore, the CO_2 emissions can be decreased in a large scale by reducing their consumption. On the 14th of February 2007 the European Parliament agreed that CO_2 emissions should be decreased by 25% [2]. It is much easier to adopt regulations concerning the new dwellings than achieving improvements in the existing ones. This is quite a challenging task, taking into account that the old ones vary significantly not only concerning their age and their condition but also concerning their construction method and maintenance through the years.

According to the Select Committee on Environmental Audit, if the dwellings' CO_2 emissions are regulated, they could constitute above 55% of the UK's objective concerning CO_2 emissions in 2050 [3]. The objective is to cut the total emissions by 60%. In December 2006, the UK's government announced through the Pre-Budget report that their target is all the new buildings should be "zero-carbon" by 2016 [4]. A motivation towards that direction was that everybody who would manage to achieve that goal would receive a Stamp duty land tax exemption until 2012 if the building's value was less than 500,000£ [5]. For Scotland, this aim was set on 2017.

In 2006, it was introduced that when an old building is expanded or renovated it is compulsory to improve its energy efficiency. In addition to this, since 1st of May 2007 in Scotland all the dwellings that are sold or let must hold an Energy Performance

Certification [6]. It is expected that all the buildings, the new ones as well as the old ones, would be renovated so as to satisfy the minimum specific energy requirements.

All the buildings in the future would have a certificate demonstrating their energy efficiency and their CO_2 emissions and thus their impact on the environment. The energy efficiency and the environmental impact rating according to which a structure is valuated are shown below.
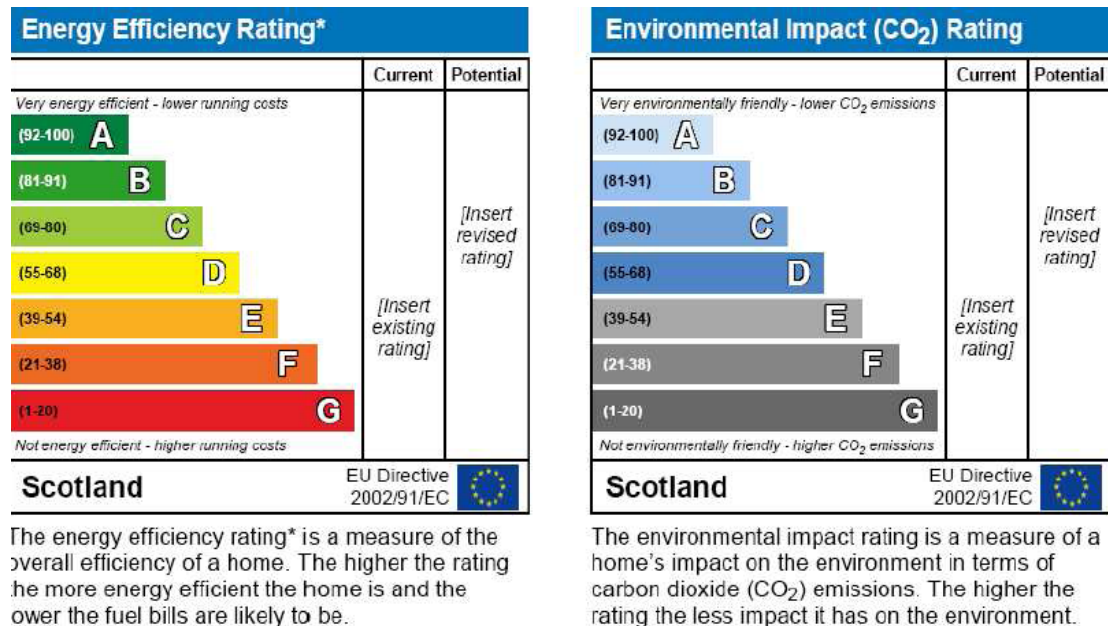
Figure 1: energy efficiency and environmental impact rating

2.3   Renewable energy

There are a lot of different methods that exist in order to achieve energy efficient buildings such as exploit passive solar gains and natural lighting, using effectively the natural convection, applying smart control systems etc. For sure, the most widespread method is the introduction of renewable energy systems into them.

It is very important to develop methods evaluating the energy output potential of contemporary renewable technologies. This way it may be possible to analyse scenarios regarding the future energy supply and implement in a rationale manor legal and financial frameworks to support the developing industrial production of such technologies. Some important aspects which are explored by researchers currently are: the estimated annual electricity generation of a grid connected installation; potential of a renewable technology electricity generation; specification of required

installed capacity to match a certain percentage of a county's power load through this renewable technology.

2.4 Solar energy

The sun provides the bigger amount of energy on the earth than any other source. The amount of solar energy reaching the earth each year is $6*10^{24}$ J, meaning around 12,000 times more than our energy consumption [7]. The tremendous amounts of energy which are released from the sun owe their origin to the existence of thermonuclear reactions – fusion in its interior. Its effective blackbody temperature is 5762 K [8]. The sun – earth relationships are shown in the following graph.
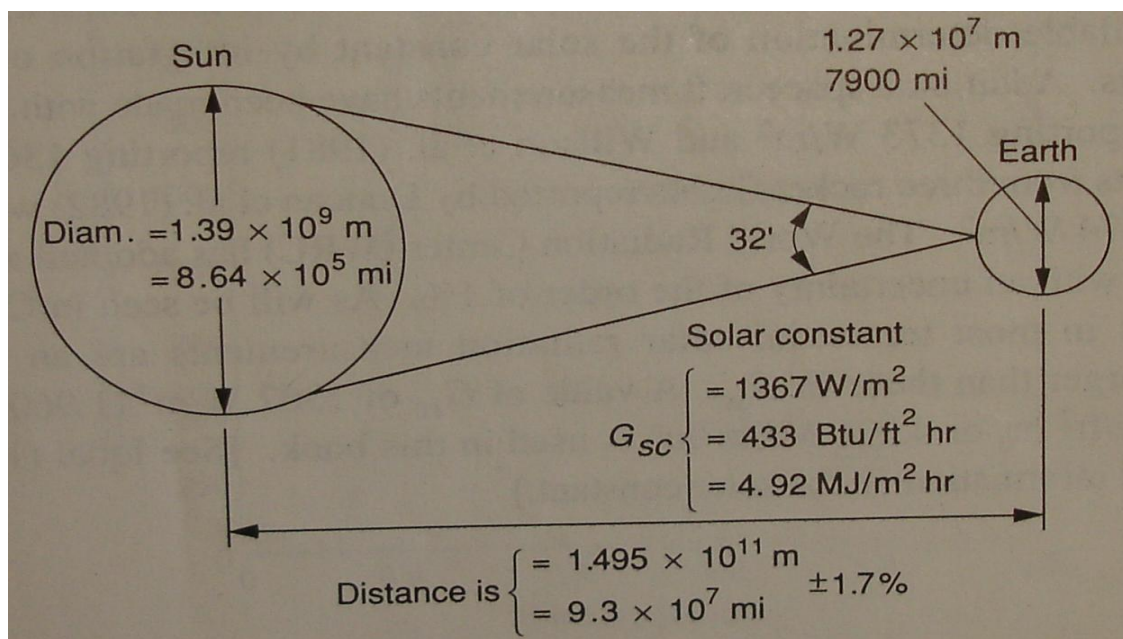
Figure 2: sun – earth relationships [9]

The engineers must possess the know how to estimate the intensity and the effects of solar radiation in order to try to control and utilize it in the best possible way. An interesting way to exploit the available energy from the sun is to convert it into DC current through PV technology. In order to analyse regional and national differences regarding solar energy resources and to assess PV potential, relevant databases have been developed in the former decade.

2.5 Context of study / Rationale

In this project the installation of PV systems is investigated and analysed. First of all, the parameters influencing the distribution of solar irradiation upon a PV surface are

set out. The global solar radiation can be divided into direct and diffuse and the share of its components depends mainly upon the clearness index and the location of the PV installation. PV cells whose technology and different types are examined in the relative chapter are electrically connected in order to create PV modules. PV arrays are formed by a number of interconnected PV modules and constitute the major part of a PV system. PV panels can also be utilised as construction materials in the building envelope (alongside being mounted on the top of the roof) and are known as BIPV. In addition, if the thermal losses of PV systems are further utilised as thermal energy for space heating, then BIPV-T are introduced. The financial incentives for adopting PV installations and the environmental impact of PV are also presented.

There are various parameters that affect the PV system performance. The target of this project is to identify and evaluate the significance of these parameters. For instance, PV temperature is one of them (wind speed and direction as well as local microclimate conditions should be considered). The array inclination and orientation are then identified as the two most important factors influencing PV performance and therefore analysed in much more depth for different regions.

The PV performance can be evaluated through widely recognized simulation tools either research oriented i.e. Merit or commercial i.e. PVGIS. The aim of this study is to create a simplified calculation Excel tool through extensive parameter (affecting PV systems) overview and modification /selection of incorporated equations (found in literature). The developed tool provides realistic and relatively agreeable results compared to those of the widely accepted simulation programs. Its reliability and accuracy is examined by comparing its results with data from an actual case study. Moreover, the obtained tool's results are further verified for 4 European regions with different climatic characteristics. The obtained results can also be used in order to determine the extent of influence of array inclination and orientation upon PV performance.

3 Solar energy

3.1 General solar angles

Every day earth makes a rotation about its axis, when it needs around a year to complete a revolution about the sun. The rotation axis of the earth has a tilt angle of 23.5° compare to the earth's orbit about the sun. The above characteristics are significantly important regarding how solar radiation is distributed over the earth's surface.

In order to estimate the solar radiation incident on a specific location on the earth's surface at a certain moment in time the main parameters required are latitude **l**, declination angle **δ** and the hour angle **h**.
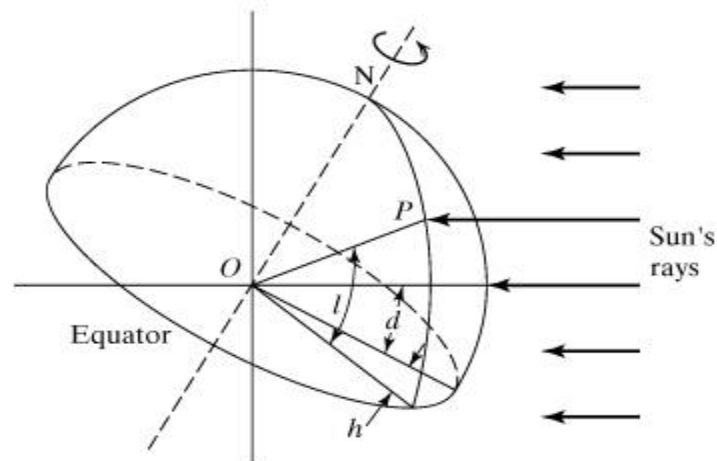
Figure 3: latitude l, declination angle δ, hour angle h

- Latitude **l**: angle North or South of the equator, -90° ≤ l ≤ 90° with north positive

- Declination **δ**: the angular position of the sun at solar noon with respect to the plane of equator, -23.45° ≤ δ ≤ 23.45° with north positive

$$\delta = \delta_o * \sin\left[\frac{360*(284+n)}{365}\right] \quad \text{\{1\}}$$

n=day of the year and δ_o=23.5

- Hour angle **h**: the angular displacement of the sun east or west of the local meridian due to rotation of the earth on its axis. Before noon the hour angle is negative and after noon positive, changing by 15° per hour

$$h = 15 * [t_{sol} - 12] \quad \text{\{2\}}$$

$$t_{sol} = t_{ref} + \left[\frac{4(L_{ref} - L) + E}{60} \right] \quad \text{\{3\}}$$

t_{sol} is the solar time for the longitude L, longitude is the angle East or West from prime meridian (Greenwich) in hourly fraction

t_{ref} is the unadjusted reference time (for the UK this is GMT)

L_{ref} is the reference longitude for t_{ref} Greenwich = 0°

E is correction in mins

$$E = 9.87 \sin(2B) - 7.35 \cos B - 1.5 \sin B \quad \text{\{4\}}$$

$$B = \frac{360(n - 81)}{364} \quad \text{\{5\}}$$

Solar altitude **β** and solar azimuth **γ$_s$** can be calculated for any point P on the earth's surface and at any time t in order to define the position of the sun in the sky from the latitude **l**, the sun's declination angle **δ** and the hour angle **h**
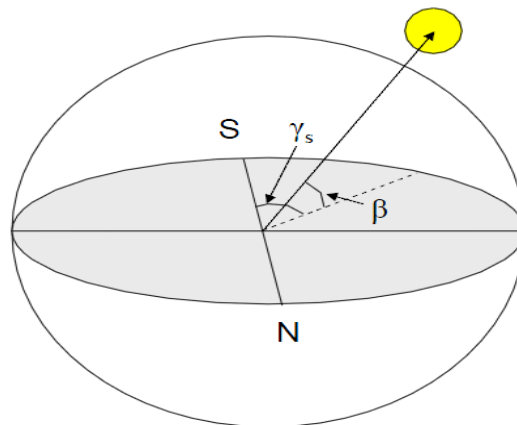
Figure 4: solar azimuth angle γ$_s$ and elevation angle β [10]

- Solar altitude **β**: the angle between the solar radiation and the horizontal

$$\beta = \sin^{-1}(\cos l \cos h \cos \delta + \sin l \sin \delta) \quad \text{\{6\}}$$

13

- Zenith angle θ_Z: angle between beam radiation and the vertical, the complement of solar altitude β

$$\theta_Z = 90 - \beta = \cos^{-1}\left(\cos l \cos h \cos \delta + \sin l \sin \delta\right) \quad \text{\{7\}}$$

- Solar azimuth γ_s: angular displacement from south of the projection of beam radiation on the horizontal plane

$$\gamma_s = \cos^{-1}\left(\frac{\sin l \cos h \cos \delta - \cos l \sin \delta}{\cos \beta}\right) \quad \text{\{8\}}$$

Also the position of the surface relative to the sun should be defined

- Surface azimuth angle γ: the deviation of the projection on a horizontal plane of the normal to the surface from the local meridian, $-180° \leq \gamma \leq 180°$; with zero due south, east negative and west positive
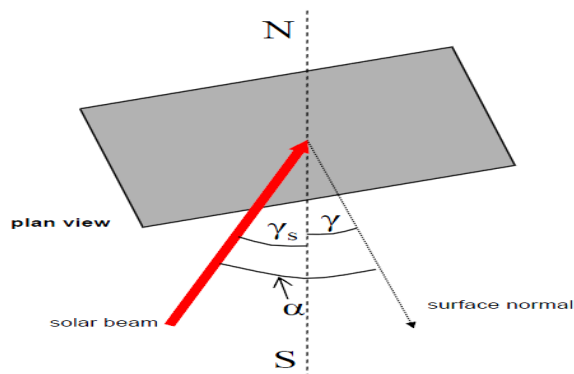
Figure 5: solar azimuth angle γ_s, surface azimuth angle γ, surface-solar azimuth angle α [10]

- Surface – solar azimuth angle $\boldsymbol{\alpha}$: angle between the incident beam radiation and the surface normal

$$\alpha = \left|\gamma - \gamma_s\right| \quad \text{\{9\}}$$

Then the position of the surface in question and the horizontal or the vertical should be defined, as well as the angle of incidence.

- Tilt angle **Φ** : angle between the vertical and the plane of the surface

- Slope **τ**: angle between the horizontal and the plane of the surface, the complement of the tilt angle φ

$$\tau = 90 - \Phi \quad \{10\}$$

- Angle of incidence **θ**: the angle between the beam radiation and the normal

$$\theta \approx \cos^{-1}\left(\cos\beta\cos\alpha\cos\Phi + \sin\beta\sin\Phi \right) \quad \{11\}$$
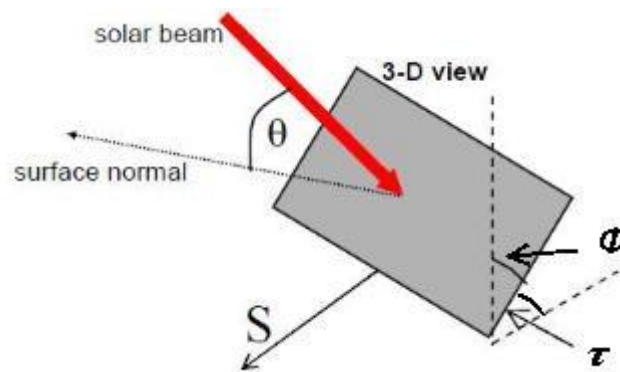
Figure 6: tilt angle φ, slope τ, angle of incidence θ [10]

3.2 Diffuse - Direct radiation

The total solar radiation that reaches the earth's surface (global solar radiation) **I$_t$** can be divided into 2 components; direct beam radiation **I$_b$** and diffuse radiation **I$_d$**. Direct beam radiation is the one that reaches the surface directly from the sun, while diffuse reaches the plane after having been scattered by the earth's atmosphere.

$$I_t = I_b + I_d \quad \{12\}$$

It is very important to measure the available amount of solar radiation incident on a surface. There is a variety of devices that can be used in order to achieve that. The most commonly used one is the pyranometer that measures the broadband solar irradiance **I$_t$** (W/m^2) on a planar surface. Also there are the shaded pyranometers and the integrated ones. A shaded pyranometer blocks out the direct beam component of

the total irradiance through shade, thus metering the diffuse solar irradiance on a horizontal surface I_{dH} (W/m^2). Furthermore, a integrated pyranometer measures usually the total and diffuse solar radiation on a horizontal surface, I_{tH} and I_{dH} respectively. Whenever, there is no index, the index H for a horizontal plane is considered. Alternatively, a pyrheliometer could be utilised. Pyrheliometer is usually mounted upon a sun tracker in order to track the sun during the day and meters the direct beam solar radiation I_b (W/m^2).

The direct solar radiation falling on a surface tilted at an angle Φ can be evaluated from the measured direct beam radiation I_b by using the equation,

$$I_{b\Phi} = I_b\left(\cos\beta\cos\alpha\cos\Phi + \sin\beta\sin\Phi\right) \quad \{13\}$$

whereas the diffuse radiation falling on that surface is calculated from the measured value of I_{dH} through

$$I_{d\Phi} = I_{dH}\frac{1+\sin\Phi}{2} = I_{dH}\frac{1+\cos\tau}{2} \quad \{14\}$$

If the surface is perpendicular to the solar beam, the incident solar radiation is defined as direct normal solar radiation I_{bN} (W/m^2). The direct normal solar radiation is used as an input to a lot of programs that estimate the PV performance.

$$I_b = I_{bN}\cos\theta \quad \{15\}$$

3.3 Sky clearance index

The density of solar energy reaching the outer atmosphere of the earth (extraterrestrial radiation) on a surface perpendicular to the direction of propagation of the radiation, at mean earth-sun distance, is known as the solar constant **Gsc** and has a value of 1353 W/m^2 [11].

The extraterrestrial radiation, measured on a plane normal to the solar radiation on the nth day of the year can be estimated by the equation

$$G_{on} = G_{sc}\left(1 + 0.033\cos\frac{360n}{365}\right)\{16\}$$

16

The solar radiation incident on a horizontal surface outside of the atmosphere at any point of time can be estimated by the above equation {16} and the zenith angle θ_Z.

$$G_{on} = G_{sc}\left(1 + 0.033\cos\frac{360n}{365}\right)\cos\theta_z \quad \{17\}$$

By combining equations {17} and {7}, the result is:

$$G_{on} = G_{sc}\left(1 + 0.033\cos\frac{360n}{365}\right)\left(\cos l\cosh\cos\delta + \sin l\sin\delta\right) \quad \{18\}$$

As the majority of the available data and calculating programs are of an hour time step, it is quite interesting to calculate the extraterrestrial radiation on a horizontal plane for an hour interval by integrating the equation {18} between the hour angles h_1 and h_2.

$$I_o = \frac{12*3600}{\pi}G_{sc}\left(1 + 0.033\cos\frac{360n}{365}\right)\left[\cos l\left(\sin h_2 - \sin h_1\right)\cos\delta + \frac{\pi(h_2 - h_1)}{180}\sin l\sin\delta\right]$$

{19}

The atmospheric conditions and air mass responsible for solar radiation scattering and absorbtivity are also time dependent. A standard "clear sky" should be defined and a hourly radiation estimated (received on a horizontal plane depending on the conditions in relation to this "clear sky"). Therefore, days or even hours could be divided into sunny or cloudy through the clearness index K_t, $0 \leq K_t \leq 1$. K_t is equal to 1 for an extremely clear sunny hour/day and equal to 0 for a very cloudy one.

The hourly clearness index K_t is defined as the ratio of the total solar radiation to the extraterrestrial radiation for that specific hour.

$$K_t = \frac{I}{I_o} \quad \{20\}$$

Measured data provide global solar radiation values on a horizontal surface. Therefore, the clearness index can be applied for estimating the ratio of diffuse to global radiation by using either the Orgill and Hollands correlation or the Erbs et al. [12].

The Orgills and Hollands correlation is:

$$\frac{I_d}{I} = \begin{cases} 1.0 - 0.249k_T & \text{for } k_T < 0 \\ 1.557 - 1.84k_T & \text{for } 0.35 < k_T < 0.75 \\ 0.177 & \text{for } k_T > 0.75 \end{cases}$$

{21}

, whereas the Erbs et al. is

$$\frac{I_d}{I} = \begin{cases} 1.0 - 0.09k_T & \text{for } k_T \le 0.22 \\ 0.9511 - 0.1604k_T + 4.388k_T^2 \\ \quad - 16.638\ k_T^3 + 12.336\ k_T^4 & \text{for } 0.22 < k_T \le 0.80 \\ 0.165 & \text{for } k_T > 0.80 \end{cases}$$

{22}

3.4   Diffuse/direct radiation in cities

Diffuse-direct solar radiation ratios in urban and rural locations seem to be significantly different. Researchers have observed a considerable decrease in solar radiation and sun shine hours' duration in the case of urban environments (usually warmer climatic regions). This result is justified by the fact that increased scattering and solar energy absorption takes place attributed namely to exhaust gases and various particles appearing in cities especially in summer (car emissions, factory chemicals, pollen, dust and mold spores) [13].

Specifically Landberg [14] has mentioned a 10-20 % sun shine duration reduction in industrial cities compared to neighboring areas. Oke has presented work estimating a solar radiation reduction of up to 30% in case of polluted days and a low solar elevation [15]. It is generally accepted that urban pollution affects both spectral composition and direction of incoming radiation. Increased scattering reduces visibility and generally increases diffuse solar radiation levels in expense of direct.

Furthermore, Hufty [16] mentions a 55 minute loss in sun shine hours /day in case of high pollution levels in Belgium and a 16% reduction in London compared to surrounding areas [17]. Unsworth and Monteith have found solar radiation flux in urban areas to be 82% that of the minimum in rural [18]. Losses in Montreal and

Toronto have been estimated at 9% and 7% respectively [19] when in Tokyo vary between 12% and 30% [20]. In the USA relative percentages show a 30-50% decrease in direct solar radiation according to atmospheric turbidity when solar diffuse increases by 40-70% [21]. The result in the USA is that global radiation seems to be reduced by a 10-20%.

3.5   Solar data bases

The exploitation of solar energy is directly related to geographical variability and time dynamics. The geographic analysis of solar availability can improve estimations of PV potential contribution to the future world energy demand and financial structures thus contribute to the set up of most effective policies.

Various data bases and estimation tools are available worldwide in order to estimate solar energy measured values with different levels of accuracy and resolution i.e. Meteonorm, European solar radiation atlas, NASA SSE, SODA, Satel-Light, etc [22].

However, the distributed nature of solar electricity generation and dependency on geographic coordinates raise questions on how to better utilise, evaluate and communicate results and conclusions to various community groups i.e. engineers, scientists, policy makers, research and education institutes, potential investors and the public in general. Some of these questions involving different groups of experts and non experts would be related to:

- Improved map based interface 'friendlier' to non professionals

- Climate / geographic data at higher spatial resolution for experts (i.e. integrated in a GIS system)

- Open data / software architecture

In order to deal with the above issues, the Photovoltaic Geographic Information System PVGIS has been developed at the joint Researched Centre of the European Commission in 2001. PVGIS is based on long-term expertise from laboratory research, testing and monitoring utilising geographical knowledge. It is capable of assessing performance of PV systems in various geographical regions and supporting policy making in the European Union. Interactive access to the data, maps and tools is provided through the web interface.

4   Photovoltaic panels

4.1   Photovoltaic technology

Photovoltaics generate electric power by using solar cells to convert solar radiation into electricity. They make use of the "photoelectric effect". Photoelectric effect refers to photons of light that strike atoms, liberating thus electrons into a higher state of energy in which they are capable of conduction and thus electricity is created.

Electrons are normally form "valence bonds" with the adjoining atoms in the valence band and thus cannot move. All the materials have a fundamental property, known as band gag E_g, which is the energy gap between the valence band and the conduction band. A large number of electrons should move from the valence to the conduction band in order electric current to be created. Every photon's energy is proportional to its frequency f,

$$E = hf = h\frac{c}{\lambda} \quad \{23\}$$

A photon that has energy greater than the band gap and knocks an electron, creates one electron–hole pair and its excess energy is dissipated as heat.
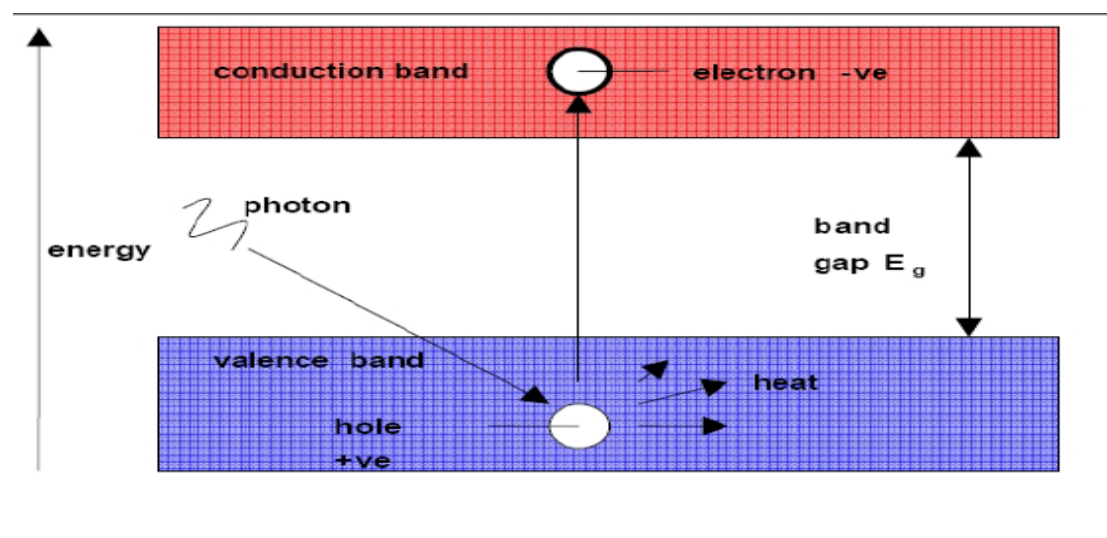

Figure 7: valence band, conduction band and energy gap [10]

A "special" material with properties that promote the flow of current and prevents recombination is required since under normal circumstances the electrons and the holes would be re-combined quickly resulting into no current flow. Silicon is one of

these "special" materials. If silicon is doped with different impurities we can create a material with p (positive charge) and n (negative charge) regions. These p-n junctions act as a filter, reduce recombination and create a semiconductor.

4.2   Photovoltaic cells, modules, arrays

4.2.1 Theory of cell operation

The combination of doped silicon and metal contacts creates a PV cell, or in other words a semiconductor device that generates electricity directly from solar radiation. Direct solar radiation is mostly responsible for the energy generated. Nevertheless, lower energy yields are possible under overcast conditions.

An ideal solar cell can be modelled by a current source in parallel with a diode. Practically, there is no ideal solar cell, thus a shunt resistance R_{SH} and a series resistance R_s should be added. The equivalent electrical circuit of a PV cell is shown in the following figure
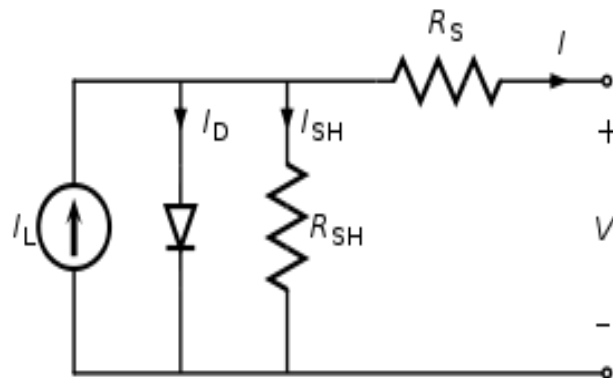
Figure 8: PV cell - equivalent electric circuit [23]

In the absence of a photon flux reaching the p-n junction, a "dark current" I_0 may occur described by the following equation:

$$I_0 = 4 \left(\frac{2\pi e m_e}{h^2} \right)^3 \left(\frac{\mu_h \mu_e}{L_h \sigma_e} \right) \left[\left(\frac{kT}{e} \right)^4 \exp\left(\frac{eV_g}{kT} \right) \right] \quad \{24\}$$

e= electron charge, $1.602*10^{-19}$Cb

h= Plank constant,$6.626*10^{-34}$kg

k= Boltzmann constant, 1.381 J/K

m_e= electron mass, 9.109×10^{-31} kg

μ_e= electron diffusion velocity

σ_e=electrical conductivity for electrons

V_g= band gap

T= cell temperature

μ_h= hole diffusion velocity

The current that flows through the diode is:

$$I_D = I_0 \left\{ \exp \left[\frac{e(V + IR_s)}{kT} - 1 \right] \right\} \quad \{25\}$$

The current that flows through the shunt resistance is

$$I_{SH} = \frac{V + IR_s}{R_{SH}} \quad \{26\}$$

The I_L is the source current for the PV cells or in other words the photo generated current. An equation in order to calculate I_L will be introduced at a later point.

The current produced by the solar cell is equal to:

$$I = I_L - I_D - I_{SH} = I_L - I_0 \left\{ \exp \left[\frac{e(V + IR_s)}{kT} - 1 \right] \right\} - \frac{V + IR_s}{R_{SH}}$$

$\{27\}$

The parameters I_o, R_S and R_{SH} cannot be measured directly and they depend on the physical size of the PV cell. A PV cell with twice the area of another has double I_o since the junction area through which the current can leak is doubled. In contrast it has half the R_S and R_{SH} due to the fact that the area across which current can flow is doubled.

22

PV cells have also other important characteristics that are provided by the manufacturer such as maximum nominal power P_{max}, short circuit current I_{SC}, open circuit voltage V_{OC}, current at maximum power point (I_{max} or I_{MPP}), voltage at maximum power point (V_{max} or V_{MPP}) and module's efficiency. The electrical characteristics of the PV cells are provided through I-V curves
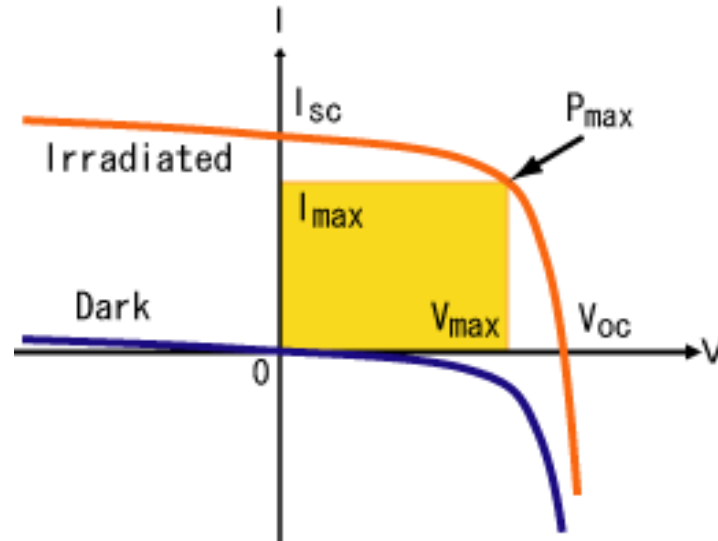
Figure 9: I-V curve for a PV cell [24]

The target is the PV to operate as close as possible to P_{max} and in order to achieve that we change the system's voltage.

Open circuit voltage V_{OC} is defined as the voltage occurred when the cell operates at open circuit, meaning actually that I=0. The open circuit voltage is equal to (assuming that the shunt resistance R_{SH} is very high):

$$V_{OC} \approx \frac{kT}{e} \ln\left(\frac{I_L}{I_0} + 1 \right) \quad \text{\{28\}}$$

Short circuit current I_{SC} is the flowing current when the cell operates at short circuit, meaning that V=0. If a PV cell is of high quality (high R_{SH}, low R_S and I_o), then $I_{SC} \approx I_L$.

Both the open circuit voltage and short circuit current are affected by the incident solar radiation and the cell temperature (analysis in 4.3.4 PV temperature influence in cell performance).

The following graphs show how the I-V curves are modified when the series resistance R_S and the shunt resistance are changed respectively.
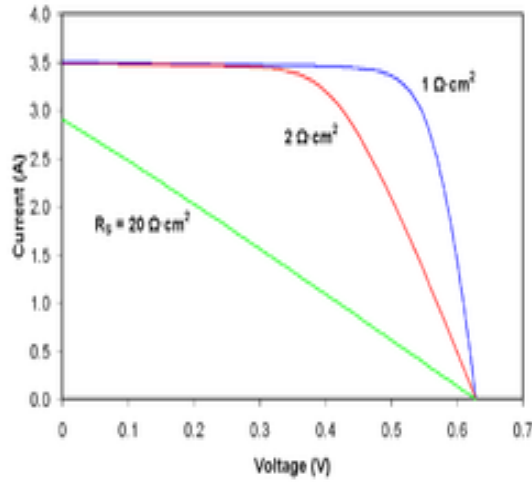
Figure 10: I-V curve regarding R_S **Figure 11**: I-V curve regarding R_{SH}
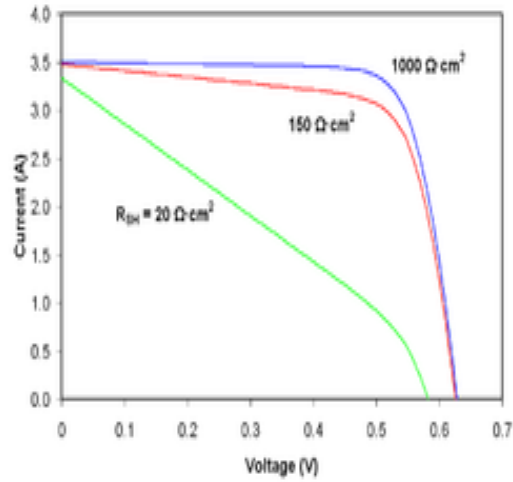
The series resistance loss are given by the equation $P = I^2 R_s$ {29}, proving that they become significant important at high radiation levels.

The solar cell's efficiency is given as the ratio of the maximum power point P_{max} divided by the incident solar radiation

$$\eta = \frac{P_{max}}{P_{in}} = \frac{V_{MPP}I_{MPP}}{J * A_c} = \frac{V_{oc} I_{sc} FF}{J * A_c} \quad \{30\}$$

J is the solar radiation in W/m^2, A_c is the solar cell's area in m^2 and FF is the Fill Factor

$$FF = \frac{V_{MPP}I_{MPP}}{V_{oc}I_{sc}} \quad \{31\}$$

The FF is affected by the shunt and the series resistance. If R_{SH} is increased and R_S decreased, the FF augments; leading to a higher efficiency n and the cell operates close to its maximum power point.

PV MODULES

The required amount of power is usually much higher than a single PV cell can deliver. Therefore, several cells are electrically connected together and a PV module is formed. A standard PV module is formed from cells sealed between glass and a

backing sheet held in a rigid aluminium frame. While the basic cell structure is standard, these can also be contained in a range of other fabrications to create modules suitable in various different applications. The manufacturers sell PV modules; therefore the provided technical characteristics refer to PV modules and not PV cells. The PV panels are rated through their 'peak power output' Wp meaning the power generated by the module at standard test conditions (STC). STC refer to a solar irradiance $1000W/m^2$ at a temperature of 25°C with an air mass 1.5 – AM1.5.

PV modules must be able to sustain harsh environmental conditions such as rain, heat, cold. Also diodes are used in order to avoid overheating caused by partial shading (bypass diodes). The PV modules have a life cycle of 25-30 years and their manufacturers provide warranties (every single PV module has its own warranty) that guarantee electrical generation during their life expectancy. A general guarantee is: 90% power output over 10 years and 80% over 25 years. Moreover, the PV panels can be recycled, offering the chance to reuse the materials that were used during their production procedure.

PV ARRAYS

Solar arrays are formed by a number of interconnected PV modules. Each of them comprises a number of interconnected solar cells. The PV modules in a PV array are firstly connected in series so as to obtain the desired voltage and then the "individual strings" are connected in parallel in order to provide the required current to our system.

Moreover, the photocurrent I_L in equation 27 is proportional to the solar irradiance J, introduced in equation 30 and is given by

$$I_L = \frac{J I_{sc}}{J_{STC} m} = \frac{I_{sc} J_{STC} r_0}{J * r} + 10^{-4} I_{sc} \left(T - T_{STC} \right) * A_P \quad \{32\}$$

J = solar irradiance

I_{SC} = short circuit current

J_{STC} = STC solar irradiance, $1000W/m^2$

T_{STC} = STC temperature, 25°C

m = parallel branches of cells

r_o = reflection loses at zero incidence angle

r = reflection losses

T = panel temperature

A_p = modules area

The power at maximum power point can be calculated by the following equation.

$$P_{\max} = \left\{ V_{MPP}I_D \left[\exp\left(\frac{eV_{MPP}}{kT * DF} - 1 \right) \right] - V_{MPP}I_L \right\} n * m * p \quad \{33\}$$

The symbol used in the equation are explained before apart from

n = number of cells in series

p = number of panels

DF = diode factor

$$DF = \frac{\dfrac{e}{kT_{STC}}\left(V_{MPP} - \dfrac{V_{oc}}{n} \right)}{\ln\left(\dfrac{I_{sc} - I_{MPP}}{I_{sc}} \right)} \quad \{34\}$$

A simpler equation for calculating $P_{\max}$ is:

$$P_{\max} = P_{STC} \frac{J}{J_{STC}} \left[1 - \beta\left(T - T_{STC} \right) \right] * p \quad \{35\}$$

β is the temperature coefficient explained in 4.3.4 - PV temperature influence in cell performance

4.2.2 PV cell types

The procedure which is undertaken in order to acquire a PV system is shown briefly in the following figure.

Figure 12: PV production procedure

There are various types of PV. The most commonly used are the crystalline ones. However the thin film technology develops rapidly. The 3 main issues concerning the different technologies are; their efficiency, their cost and the required area (if a problem concerning the available area arises). A brief analysis concerning some of the most common PV cells will be undertaken.

➢ **CRYSTALLINE PVs**

    ✓ Monocrystalline (sc-Si)

    ✓ Polycrystalline (mc-Si)

    ✓ Ribbon silicon (ribbon-sheet c-Si)

The monocrystalline have an efficiency of 16-17% but they are more expensive compared to the polycrystalline ones whose efficiency is 14-15%. The higher effieciency of monocrystalline PVs means that they produce the maximum power output per m^2. Furthermore, when harsh environments must be faced, they are significantly more reliable. The ribbon silicon ones have even a lower efficiency than the polycrystalline (n=12-13%) but their major advantage is that 50% less Si is required in order to be manufactured.

➢ **THIN FILM PVs**

Their efficiency is low, n=8-12%. This means that they require a larger area in order to produce the same power output as the crystalline ones, almost the double actually. Despite this drawback they have become quite popular because they have some outstanding advantages. They use only 1% or no silicon. They "suffer" less from shading effects since there are modules that have bypass diodes between each cell. They absorb a wider range of the solar spectrum (they perform better in "low light" conditions). This characteristic has 2 benefits. They can be used in overcast conditions, in areas where there isn't much sunlight making a better usage of the available diffuse radiation. Also their deposited layer can be extremely thin, thus their manufacturing costs are quiet cheap, making them much cheaper than the crystalline ones. They are also lighter, so they can be integrated into buildings easier. At the same time, they are much less influenced by high temperatures, so they don't face overheating problems in a large scale. There are 4 major categories of thin films concerning the active material which is used:

✓ Amorphous silicon (a-Si)

✓ Cadmium telluride (CdTe)

✓ Copper indium/gallium Diselenide/disulphide (CIS, CIGS)

✓ Multi junction cells

The a-Si is by far the most commonly applied thin film category. It is less durable than crystalline silicon [25]. Also, there are double junction and triple junction a-Si PV cells.

➢ **HYBRID PVs**

They combine thin-film silicon technology with the monocrystalline one. Layers of different technologies, such as a-Si, sc-Si, a-Si, are combined together in order to produce cells that possess the best features of the 2 technologies. As a consequence, they have the previous mentioned advantages for the combined technologies, resulting in efficiency around 19% but they are extremely expensive up until now.

The following table makes a brief comparison of the PV technologies concerning different aspects.

	Monocrystalline	Polycrystalline	Thin Film	Hybrid
Cell Efficiency at STC	16 - 17%	14 - 15%	8 - 12%	18 - 19%
Module Efficiency	13 - 15%	12 - 14%	5 - 7%	16 - 17%
Area needed for modules per kWp	$7m^2$	$8m^2$	$\sim 16m^2$	$\sim 6m^2$
Annual energy generated / m^2 (south-facing, 30° tilt)	107 kWh/m^2	100 kWh/m^2	≈ 51 kWh/m^2	≈ 146 kWh/m^2
Annual energy generated / kWp (south-facing , 30° tilt)	750 kWh/kWp	750 kWh/kWp	800 kWh/kWp	900 kWh/kWp
Annual CO_2 savings / m^2	46 kg/m^2	40 kg/m^2	22 kg/m^2	60 - 65 kg/m^2
Annual CO_2 savings / kWp	323 kg/kWp	323 kg/kWp	344 kg/kWp	387 kg/kWp

Table 1: Characteristics of the different PV technologies **[26]**

4.2.3 Performance comparisons

The market regarding photovoltaic panels has grown rapidly the last years with various technologies competing for market share.

PV technologies exhibit various responses related to insolation, spectral preferences and temperature. PV performance under overcast sky conditions is a significant parameter especially in northern climatic regions. It is very important that the most effective technology is being chosen for each climatic region.

Oxford University has researched the efficiency of a broad variety of PV cell types for a northern and southern European climatic region and has come up with results presented in the following figures:

Energy output:

Name	Technology	Wp (W)
Unisolar US64	a-Si (Triple Junction)	512
ASE 30 DG-UT	a-Si (Double Junction)	540
Solarex Millennia	a-Si (Double Junction)	516
Intersolar Gold	a-Si (Single Junction)	504
Evergreen ES 112	mc-Si (Ribbon)	560
Astropower APX-80	mc-Si (APEX Si film)	640
Solarex MSX 64	mc-Si	640
ASE 300 DG UT	mc-Si (EFG)	600
BP Solar 585	sc-Si	595
Siemens ST40	CIS	560
BP Solar Apollo	CdTe	500[†]

[†] BP Solar Apollo sub-array is 560 Wp in Begbroke.

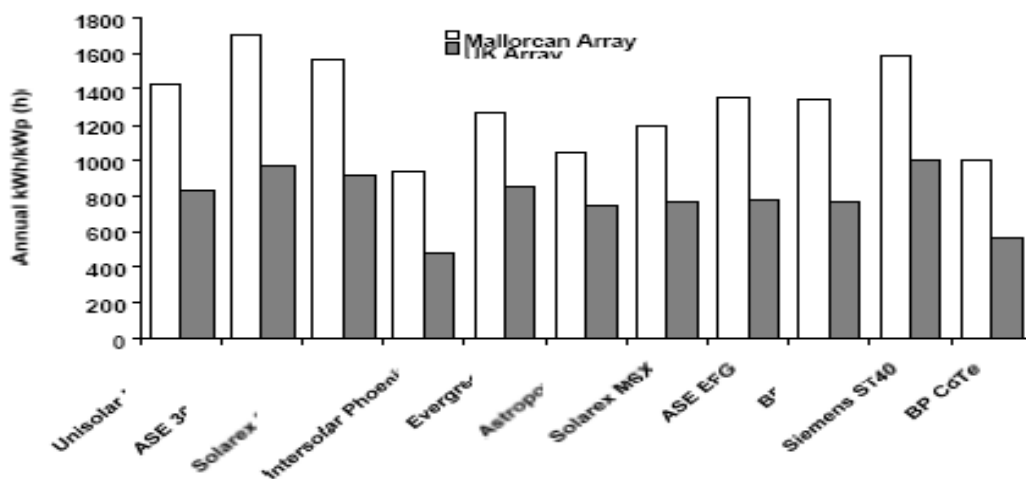**Table 2:** products under test by Oxford University [27]

Figure 13: Annual kWh/kWp for each sub array (UK & Mallorca) [27]

In the southern European region, multi-junction amorphous silicon and copper indium diselenide generate the highest energy yields (1400-1700 kWh/kWp) in a yearly basis. Crystalline silicon technologies typically generate 1200-1400 kWh/kWp annually with the lowest yields being those of amorphous silicon single junction and cadmium telluride.

In northern Europe copper indium diselenide performs best followed by double and triple junction amorphous silicon. Crystalline silicon arrays seem to maintain the most stable output. Cadmium telluride and amorphous single junction perform similarly worse than the above in this region.

Average annual energy generated from each sub array after normalisation (manufacturer's rated peak power) is illustrated bellow [27]:

Sub-array		kWh/kWp Mallorca (h)	kWh/kWp UK (h)	%
Unisolar US64	a-Si	1429	838.6	58
ASE 30 DG-UT	a-Si	1706	968.8	56
Solarex Millennia	a-Si	1555	904.1	58
Intersolar Gold	a-Si	937	479.2	51
Evergreen	mc-Si	1265	841.4	66
Astropower	mc-Si	1036	736.3	71
Solarex MSX 64	mc-Si	1201	765.9	63
ASE 300 DG UT	mc-Si	1352	784.7	58
BP Solar 585	sc-Si	1341	773.8	58
Siemens ST40	CIS	1590	1003.9	63
BP Solar Apollo	CdTe	1007	558.8	56

Table 3: Normalised power outputs Mallorca- UK [27]

We can therefore conclude that relative performance of crystalline silicon technologies and CIS in northern regions compared to a southern are greater than those of amorphous silicon. This would mean that narrower band gap materials with larger temperature coefficients benefit from the lower temperature operating conditions in northern regions and so are better suited for such regions.

From the above figures it should furthermore be noted that double junction amorphous silicon seems to be more efficient than triple junction. This could be justified by internal layers not shunted correctly. In addition, multi junction cells require current matching. Triple junction cells may be more susceptible to ambient light spectrum variation compared to double junction.

Power compared to insolation levels

Oxford University researched furthermore the performance of the above mentioned cell technologies relative to insolation levels during day time for the climatic region of Mallorca and came up with the following:
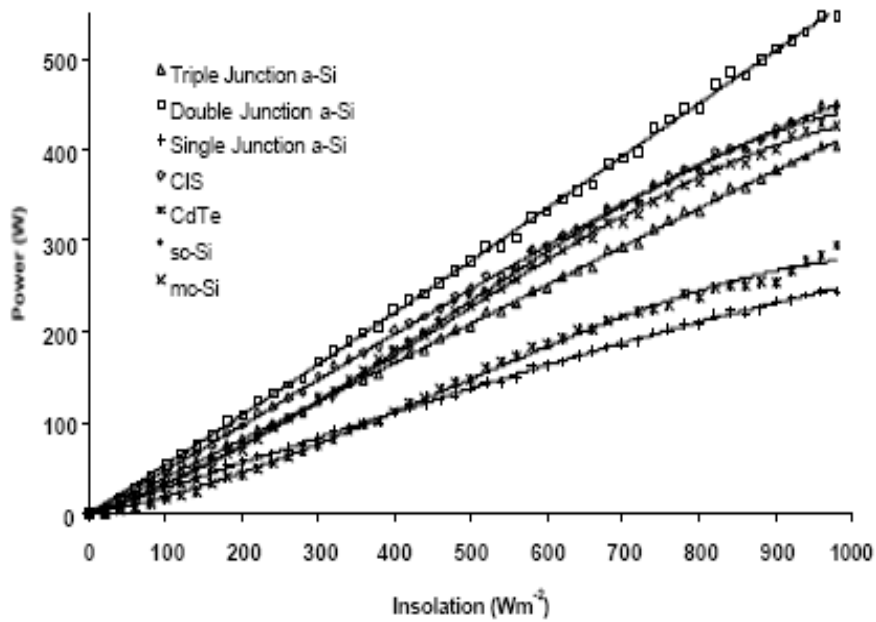
Figure 14: power output variation relative to insolation for the above mentioned technologies [27]

Power generated by amorphous silicon responds linearly to insolation increase where crystalline silicon and cadmium telluride technologies maintain s-shaped profiles. What is important is that at high insolation levels crystalline silicon, cadmium telluride and copper indium diselenide drop off compared to amorphous silicon. This was anticipated since higher insolation leads to higher temperatures which effect amorphous silicon the least (amorphous silicon has a larger band gap and smaller negative temperature coefficients when compared to small and mid band gaps of crystalline silicon and cadmium telluride).

At low insolation levels amorphous silicon and copper indium diselenide perform better than crystalline silicon and cadmium telluride. a-Si and CIS based on their absorption profiles are able to capture shorter wavelengths of the visible spectrum area (400-500 nm). Low insolation and such wavelengths are observed in overcast skies when as a result these technologies prove to be more efficient (light received is primarily from diffuse radiation [28]).

Low insolation conditions do occur also in dusk and dawn. The position of the sun in the sky in this case is low. Solar radiation travels longer till the earth's surface and lower visible and ultraviolet wavelengths are further absorbed (increase in Rayleigh scattering). This loss is not very important since especially in summer this part of the day direct sun light would fall behind the array plane.

Energy and insolation levels

Another useful figure provided by the University of Oxford illustrates the insolation frequency together with the various technologies specific yields generated relative to insolation.
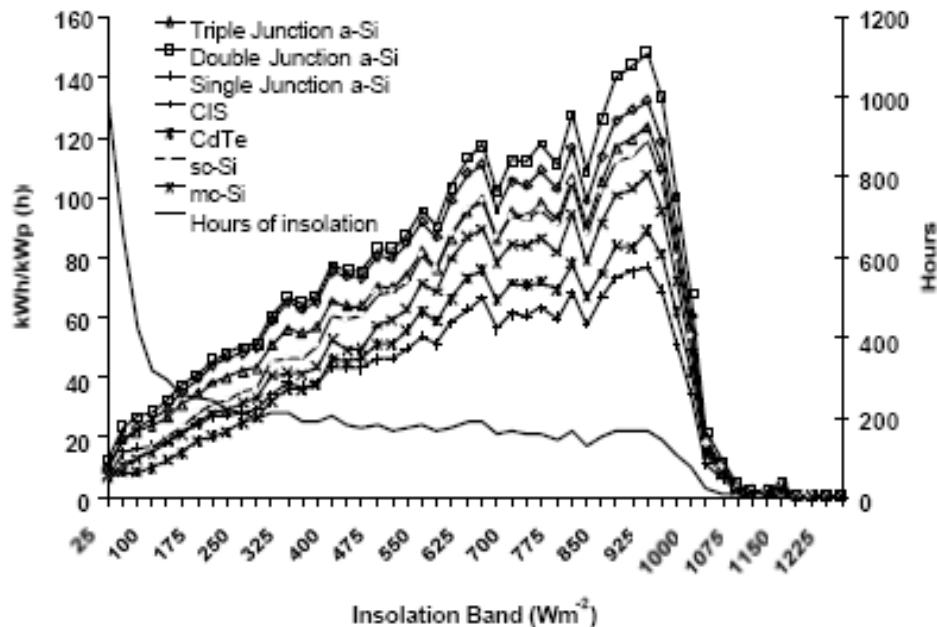

Figure 15: Insolation frequency and sub array energy output (Mallorca) [27]

Obviously most energy is generated between 500 and 900 W/m^2. However the better performance of amorphous silicon and copper indium diselinide provides higher energy returns at 0-400 W/m^2. Crystalline silicon and cadmium telluride provide better yields in moderate insolation levels 400-800 W/m^2 where there is usually adequate sun light but not enough to result in cell overheating. At higher temperatures amorphous silicon is affected less from temperature rise and maintains better efficiencies.

At higher latitudes where lower insolations are more common good spectral response to lower visible and ultraviolet wavelengths is quite important [29].

Solar spectrum variation

Evaluating the influence of hourly variation of the solar spectrum has been proven to be a quite complicated procedure. It has been observed that in the case of AM (air mass) maintaining a value of 1.5 (standardised by ASTM [30]), used as reference

concerning panel power specification, the yearly panel energy yield is relatively independent of spectrum variation. Performance variations in a daily and seasonal basis seem to be averaged out when looking at a whole year. A-Si modules seem to be mostly effected despite the annual yield is not affected more than 3% [31].

Although the annual effect of spectrum variation may seem small, it is still useful to notice its influence on the short circuit current in a daily basis i.e. in Albuquerque illustrated in the following figure.
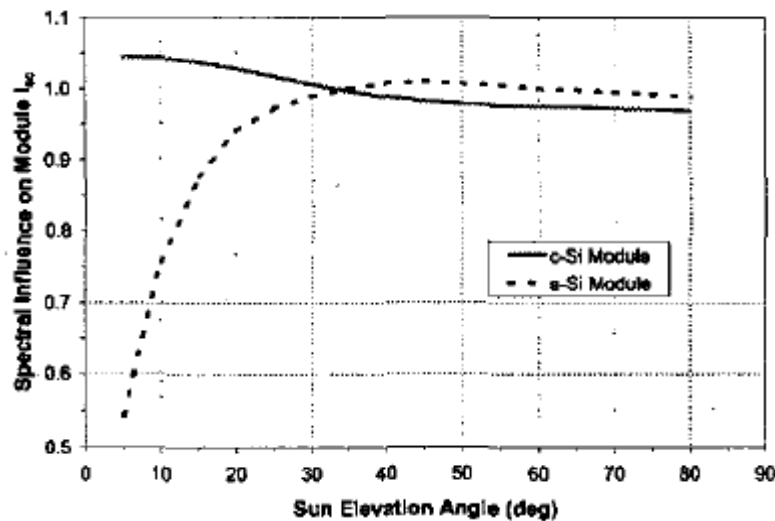

Figure 16: Solar spectrum variation effect on module Isc with daily solar angle elevation in a daily basis (Albuquerque) [31]

mc-Si and a-Si modules seem to be dependent on the specific spectral response characteristics of the module cells. The above figure should be considered when making field measurements since it is important to understand that the resulting error relative to ASTM standard reporting condition depends on time of day in which measurements have been taken.

Obviously there is a similar seasonal effect since in summer, the sun maintains higher elevation angles (when the air mass is lower) in contrast to the winter period (when the air mass is greater).

This effect has been further investigated through comparing monthly energy yields for mc-Si and a-Si modules on latitude inclination through a year.
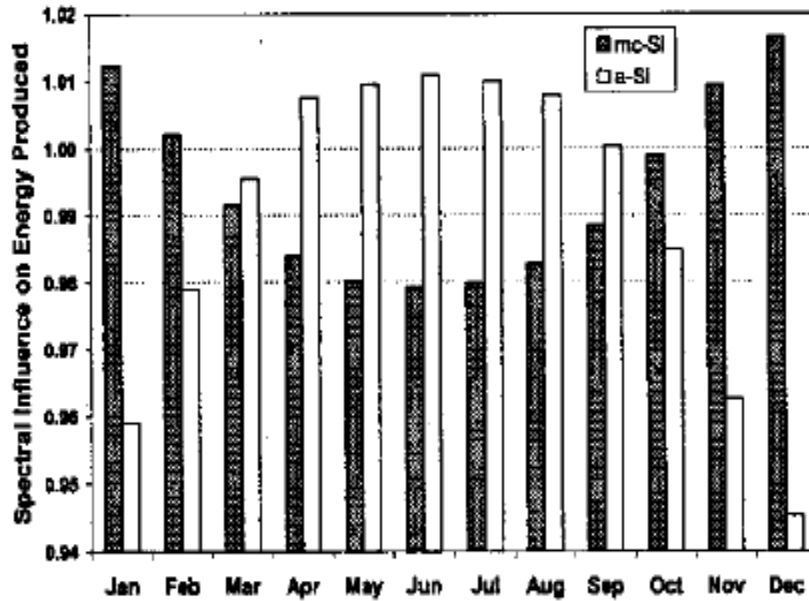
Figure 17: monthly solar spectrum variation effect on mc-Si/a-Si modules on latitude inclination in Albuquerque (yields considering spectrum variation divided by yields with no solar dependence) [31]

The magnitude of the effect of spectral variation is observed to be noticeably larger in the case of a-Si. This cell technology has been monitored in a long term and has kept on being a subject of technical debates up to these days [32].

Overcast sky effect

The extent at which the sky is covered with clouds is strongly related with PV output. This can be determined by using the clearness index, K_t which is basically the ratio of observed insolation to that outside the earth's atmosphere modified regarding elevation (this is calculated from time of year and day and latitude). The clearness index can be evaluated by equation {20} in chapter 3.3-Sky clearness index.

As shown below in the plot relating K_t with cell efficiencies, it is evident that crystalline silicon and cadmium telluride performs better under high K_t values (meaning clear skies) in contrast to amorphous silicon which performs better under overcast skies. Copper indium diselenide varies less but also performs better under overcast sky conditions. This is the reason why the two latter perform well in Mallorca and should perform even better in a northern climatic region.
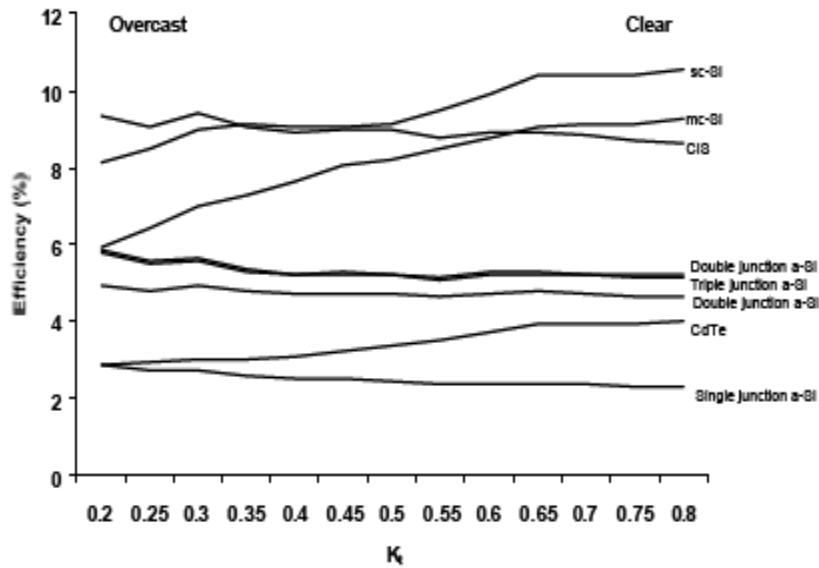
Figure 18: Overcast sky effect on different PV technologies

4.3 Photovoltaic system

PV modules are the major part of a PV system. However, a PV system consists also of other important components such as inverter, battery tank, wirings and fuses. The PV systems can be divided into two categories; the stand-alone (off-grid) and the grid connected.

Stand-alone (off-grid) PV systems are convenient for dwellings which are not connected to the national grid. These systems can be very cost effective if the building is far away from the grid and the cost for becoming grid connected is unbearable. PV produce the required electrical power, cover the dwelling's demand and the surplus electricity is stored into a battery tank. This stored electricity can be utilised later on, when the PV cannot meet the demand. The PV panels generate DC current which is used for DC appliances as well as lighting. Also the power that is drawn from the battery is DC ELV- Direct Current Extra Low Voltage, so an inverter is applied in order to convert DC current to AC. AC current is used by the majority of the typical appliances.

The batteries have some specific important characteristics like capacity C in Ah, state of charge SOC, depth of discharge DOD, life expectancy in cycles, rate of charge and discharge, cut off voltage etc. Batteries must not be discharged. Their lifetime is reduced the more frequently the battery is drained, therefore over draining should be avoided. A good approach to exceed battery's life expectancy is to be maintained,

whenever it is possible, maximum charged. This thesis doesn't focus on stand-alone PV systems thus batteries won't be further analysed.

Grid connected PV systems represent nowadays the majority of the PV installations. These systems don't use batteries for storage. PV are the main energy supplier and the national grid is used as back up. PV system generates electricity, cover the dwelling's electrical energy requirements and then sell the superfluity to the grid under a specific fixed price. The national grid is obliged to buy the surplus energy for a fixed time interval. In addition, when the dwelling's electrical demand cannot be covered by our PV installation, electricity is sent by the grid. An inverter is essential to all these systems. Inverters are electronic devices that convert DC to AC power. On the AC side, the inverter must limit the feed-in voltage to the grid to levels that aren't higher than the grid's voltage and be synchronized to the grid's frequency. The electricity must be supplied always in sinusoidal form. Inverters are also designed to detect power cuts and automatically turn off the PV system (most of their control systems are there to monitor and respond accordingly under such circumstances). When power is back on, the system is automatically switched on usually after a delay of 3 minutes. The inverter's AC output passes through a meter in order to measure the electricity sent to the grid. This meter should run in both directions in order to quantify also the electricity that is received by the grid. The inverter's efficiency is very high and is included in the final power output P, of a PV system (equation {36}). A typical efficiency is about 95%.

$$P = I * V * m * n * N * n_{inv} \quad \{36\}$$

n = number of cells in series

m = parallel branches of cells

N = number of modules in the PV system

n_{inv} = inverter's efficiency

This thesis deals with grid connected PV systems and a schematic of a grid connected installation is shown below.
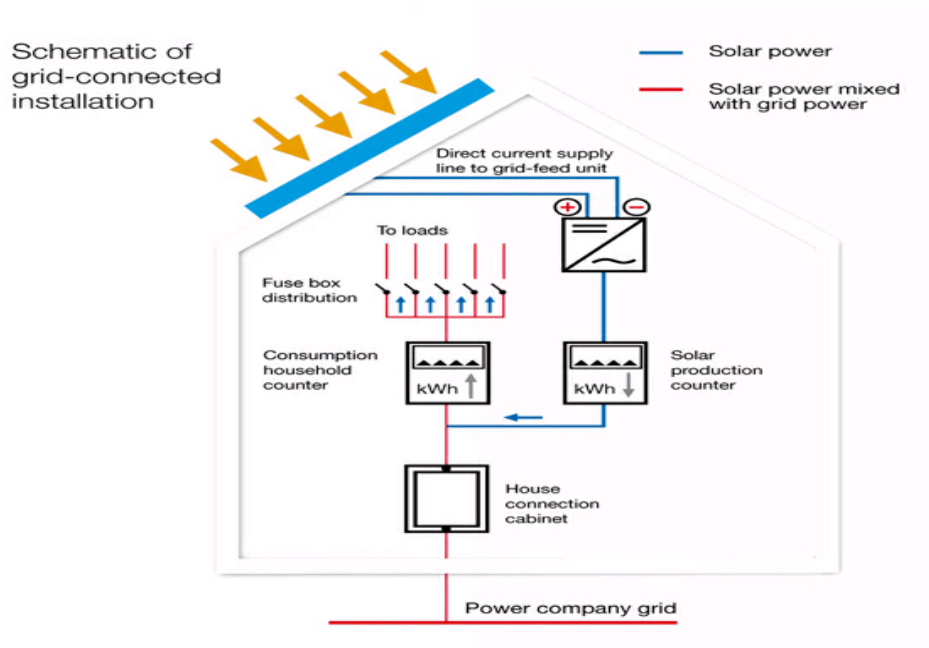
Figure 19: schematic of grid-connected PV installation [33]

4.4 Parameters affecting PV system performance when connected to the grid and building load

The following schematic presents the basic components of a grid connected PV system meaning the output of the solar system is fed directly into the building's existing electricity supply. On a sunny day power generated reduces electricity acquired by the electricity company. In case power generated exceeds a building's demand, excess energy may be exported to the grid.
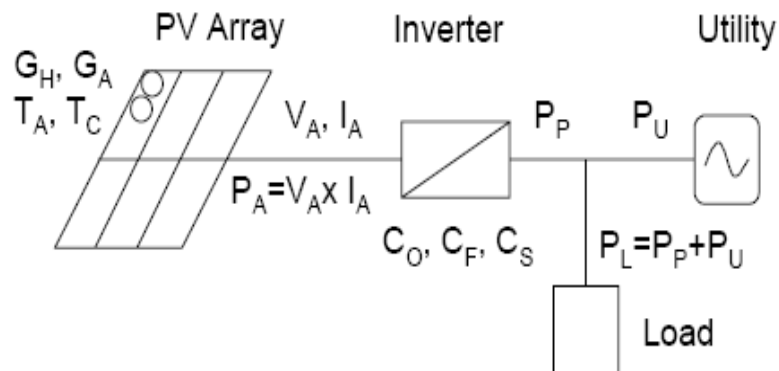

Figure 20: measurements of Japanese quality assurance organisation (JQA) PV monitoring program [34]

The basic measured items by researchers, as for example in the case of a project of 100 residential PV system installations followed through by the Japanese Quality Assurance organisation (JQA) in 2000, are shown below:

Measuring Item	Symbol	Unit
Global irradiance	G_H	kW/m^2
In-plane irradiance	G_A	kW/m^2
Ambient temperature	T_A	°C
Module temperature	T_C	°C
Array output voltage	V_A	V
Array output current	I_A	A
Array output power	P_A	kW
Inverter output power	P_P	kW
Receiving power	P_U	kW
Load power	P_L	kW
Inverter operating time	t_O	times/min.
Inverter trouble time	t_F	times/min.
Inverter operation frequency	t_S	times/min.

Table 4: measured parameters by JQA [34]

In order to meet the highest performance levels that PV cells can offer it is crucial to have a good broader understanding of the whole system. Solar panels may often be put to blame in cases of low efficiencies when often other parts of the system are actually responsible i.e. poor components, inefficient system architecture, wrong choice of PV cells for a certain location and climate region, poor installation etc.

4.4.1 System Longitude latitude

In more detail, the performance of a PV array is related primarily to the geographical coordinates of the location where it is positioned. A higher latitude i.e. UK would mean longer days (summer period) compared to lower latitudes i.e. Mallorca. However the effect of the bigger daylight hour would be counteracted by greater cloud coverage even in summer months as can be observed in the following figure [27].
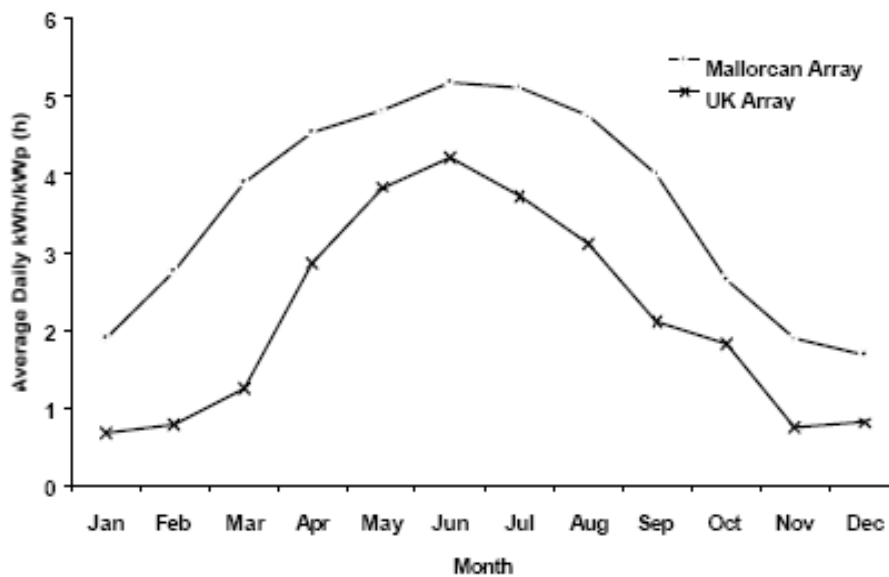
Figure 21: Daily kWh/kWp of arrays positioned in the UK and Mallorca [27]

4.4.2 Orientation

Generally PV must face south in the northern hemisphere and north in the southern. Azimuth, meaning the deviation of a cell's surface direction from the true South generally reduces the optimum energy yield. Deviations of the true south move the peak output curve towards the deviation direction (either East or West of true South). Obviously, the steeper the inclination of a cell surface would lead to higher deviation effects (considerably greater for crystalline PV cells).

An investigation in the advantages of installing PV cells on western and eastern surfaces has been considered by Omer [35] in order to match typical domestic morning and afternoon energy demands [36].Unfortunately annual energy generation in this case would be significantly less and would not support the viability of such an investment.

4.4.3 Array Inclination

The tilt angle at which a PV cell is positioned is of great relevance to its final annual energy yield. This is basically related to a location's latitude. However shallower/ steeper angles than the local latitude, would provide higher yields in summer/ winter respectively. The most efficient inclination of a system's panels should be closely related to the demand type/ energy requirements in each case investigated.

Panel inclination is very important especially in the case of crystalline PV technologies as these are more sensitive to incident solar radiation, dust, dirt compared to amorphous silicon.

The annual global irradiation [kWh/m^2] absorbed by PV panels (south oriented and optimally inclined regarding their location in Europe is illustrated in the following map, as well as the generated electricity by a 1kWp PV system with a 0.75 performance ratio. Performance ratio will be analysed later on.
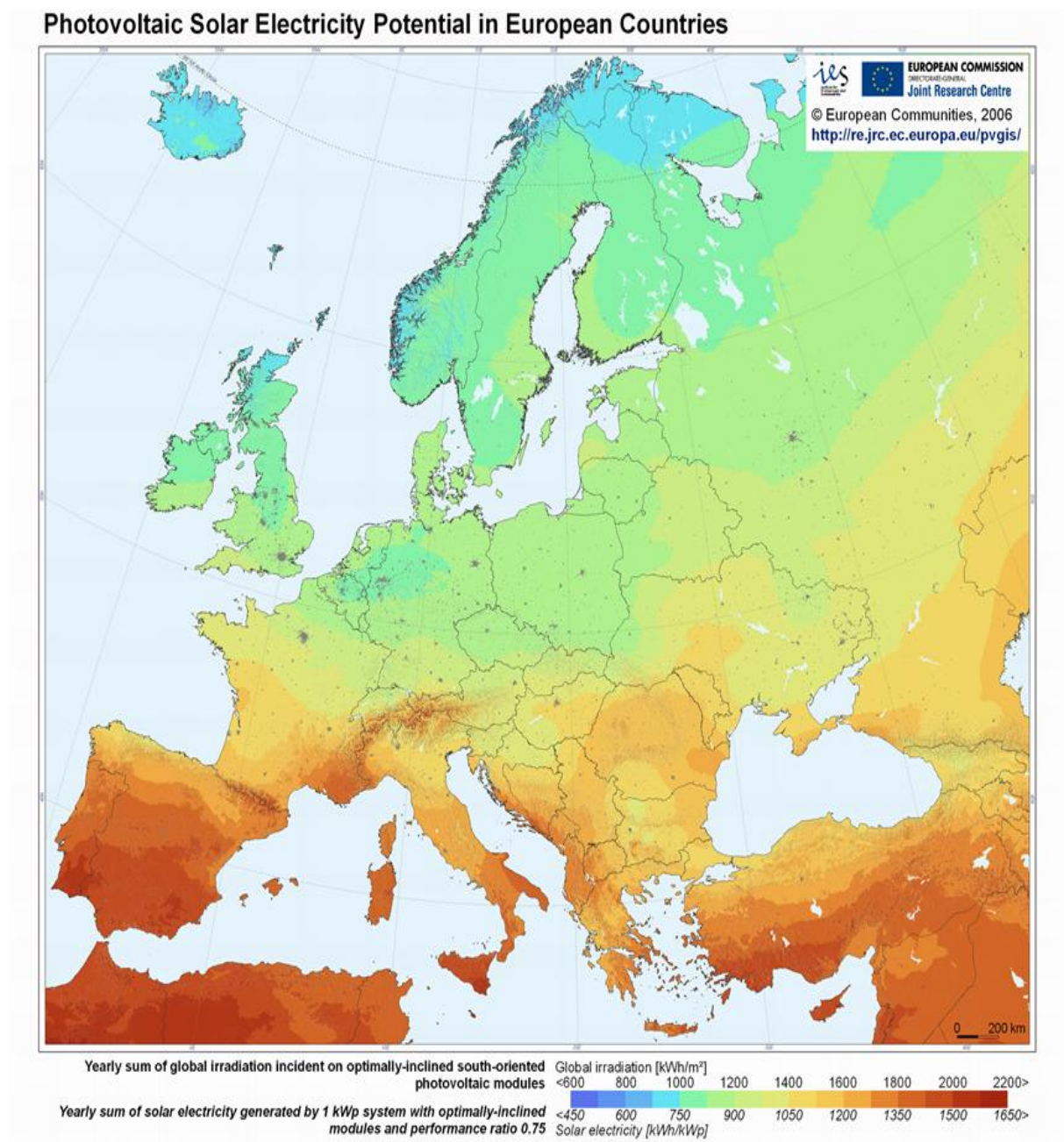

Figure 22: annual solar gains & electricity generation kWh /kWp (modules on an optimal inclined and orientated surface) [37]

Analysis of the effect of module inclination in European climatic conditions

Suri and Huld [38] have focused in comparing the potential of installing PV systems mainly in residential areas around Europe. Results reveal significant differences in the 25+5 EU states related to latitude, local climatic variations and continentality.

A generally accepted equation regarding energy generated by PV systems in a yearly basis is the following:

$$E = P_k * PR * G \quad \text{\{37\}}$$

P_k: the unit peak power (characterising the nominal power output at standard conditions usually assumed to be 1 kWp)

PR: performance ratio (actual efficiency of PV module is a percentage of P_k relative to cell temperature increase over 25°C, losses relative to angular /spectral variation and system losses in inverters-cables [39] usually a value of 0.75 is representative for mono & polycrystalline systems)

G: yearly sum of global irradiation on the inclined plane of the PV module (kWh/m^2)

In this way neither PV conversion efficiency nor module surface area is required.

The high potential of installing such systems on buildings especially in high populated locations leads researchers to focus on categorising their results concerning module inclination. The two following maps outline geographic regions of solar energy generation in kWh per kWp based on the local climatic conditions and the above equation, when panels are installed horizontally and at optimal inclination [38]:
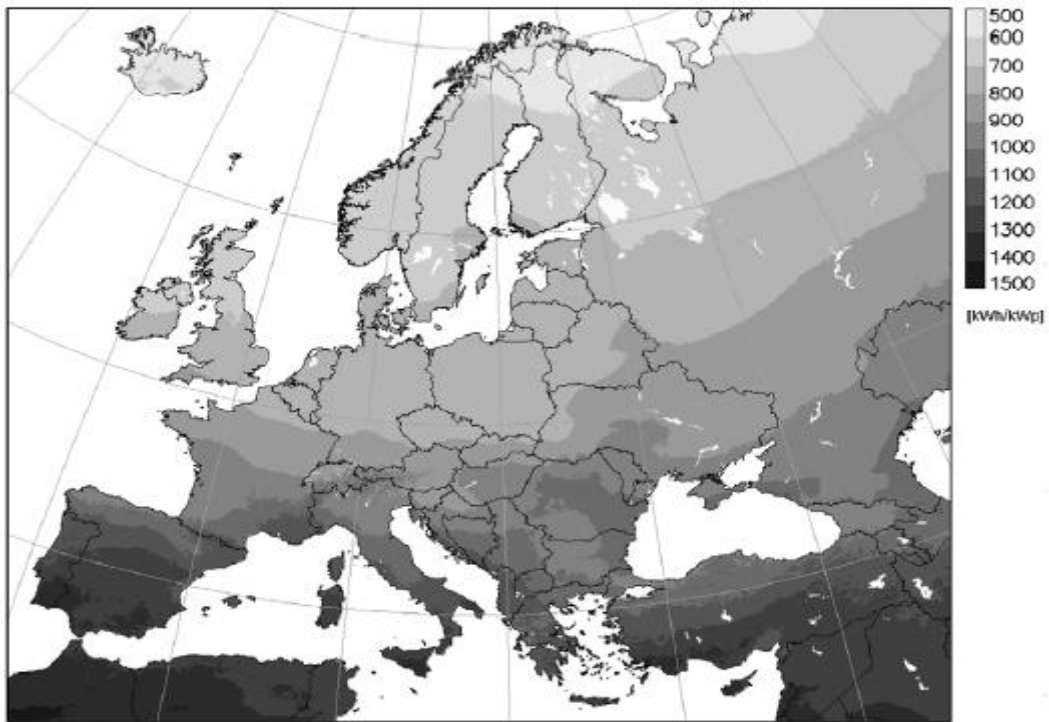
Figure 23: annual electricity generation kWh /kWp (panels on a horizontal surface) [38]
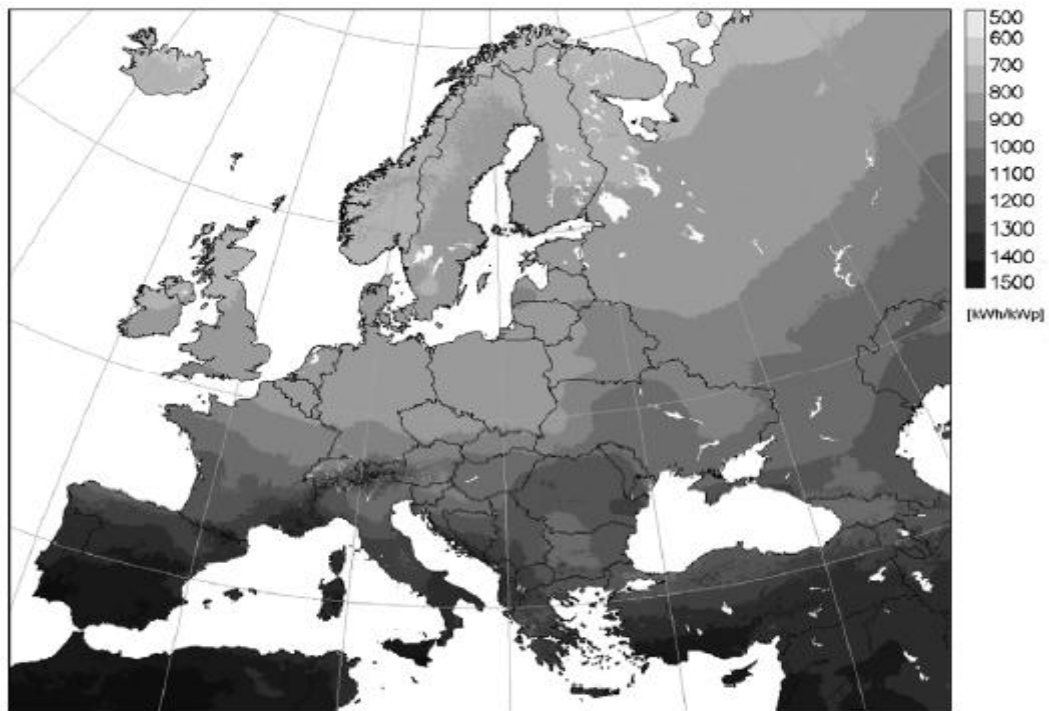
Figure 24: annual electricity generation kWh /kWp (panels on an optimal inclined surface) [38]

Regional data have been then acquired for a horizontal, optimally inclined and vertical surface concerning building installations for the 25+5 EU states in order to compare the potential between them as well as between local internal regions.

Extreme values have been illustrated by dash lines which however cannot be very helpful. The upper / lower parts of the boxes show 5% minimum / 95% maximum occurrence probability of power generated in urban residential areas (in order to eliminate rare values usually in locations like deep valleys or high mountains) [38].
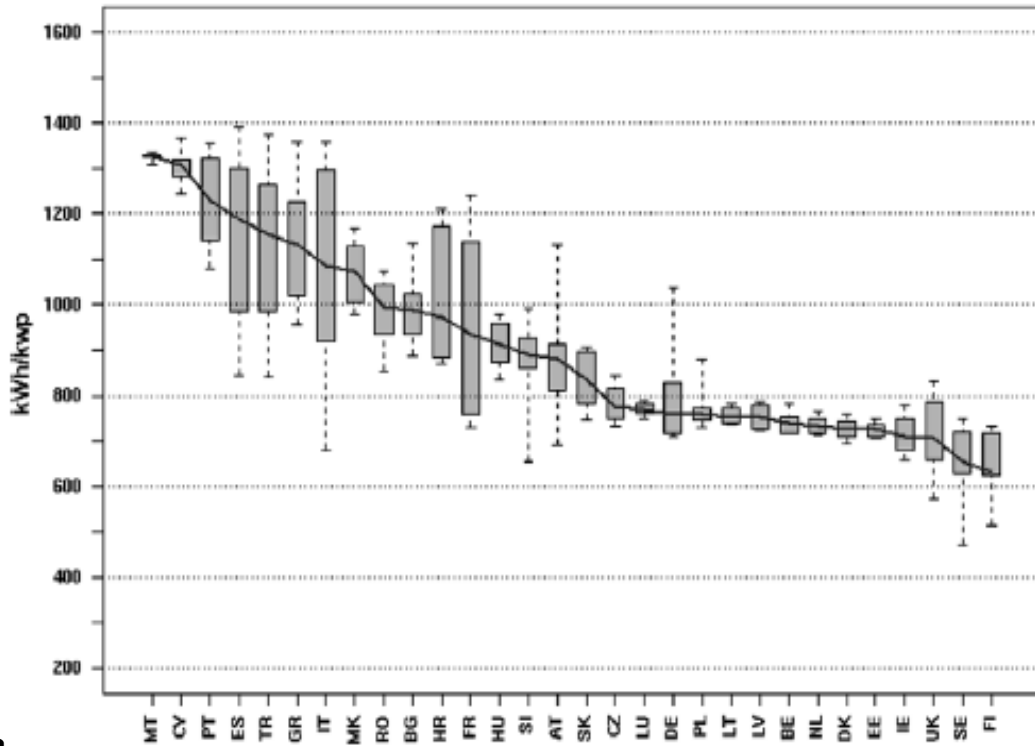
a
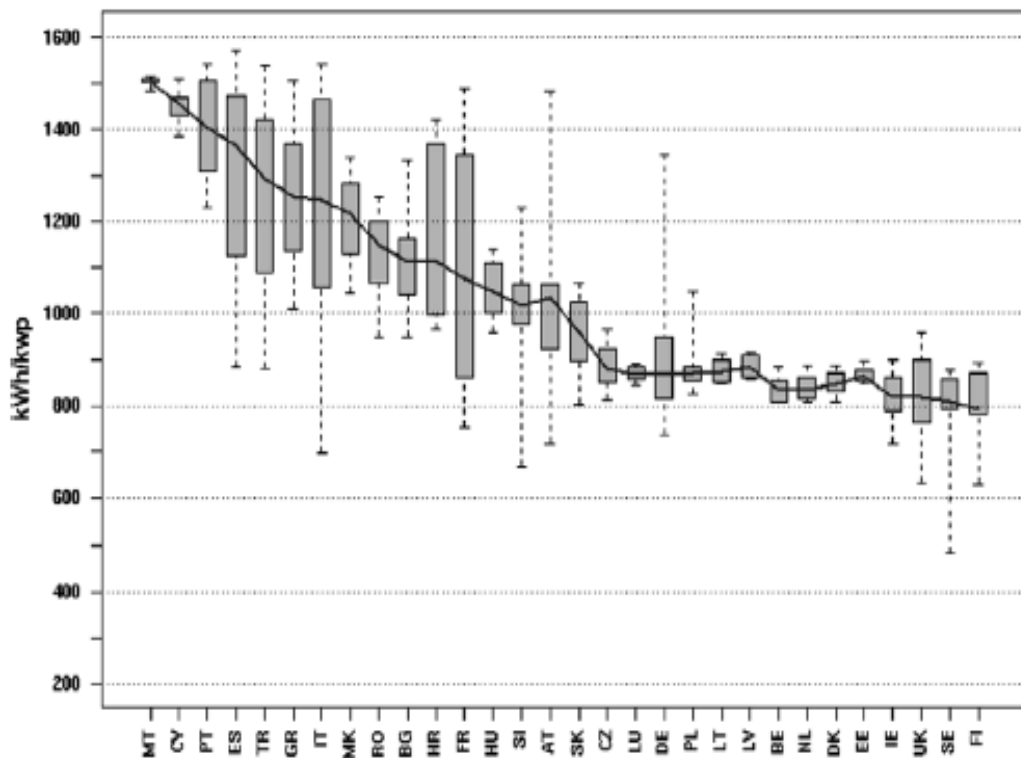
b

c

Figures 25: annual electricity generated by a typical 1 kWp system in the 25+5 EU States − modules mounted a: horizontally, b: optimally inclined, c: vertically (solid line: country's average value, dash lines: min /max values, box plot: 90% of value occurrence in urban residential areas) [38]

PV modules installed horizontally

The annual energy generated per kWp in this case varies between 470-1390 kWh where the lower limit is due to shadowing effects of mountain terrains, otherw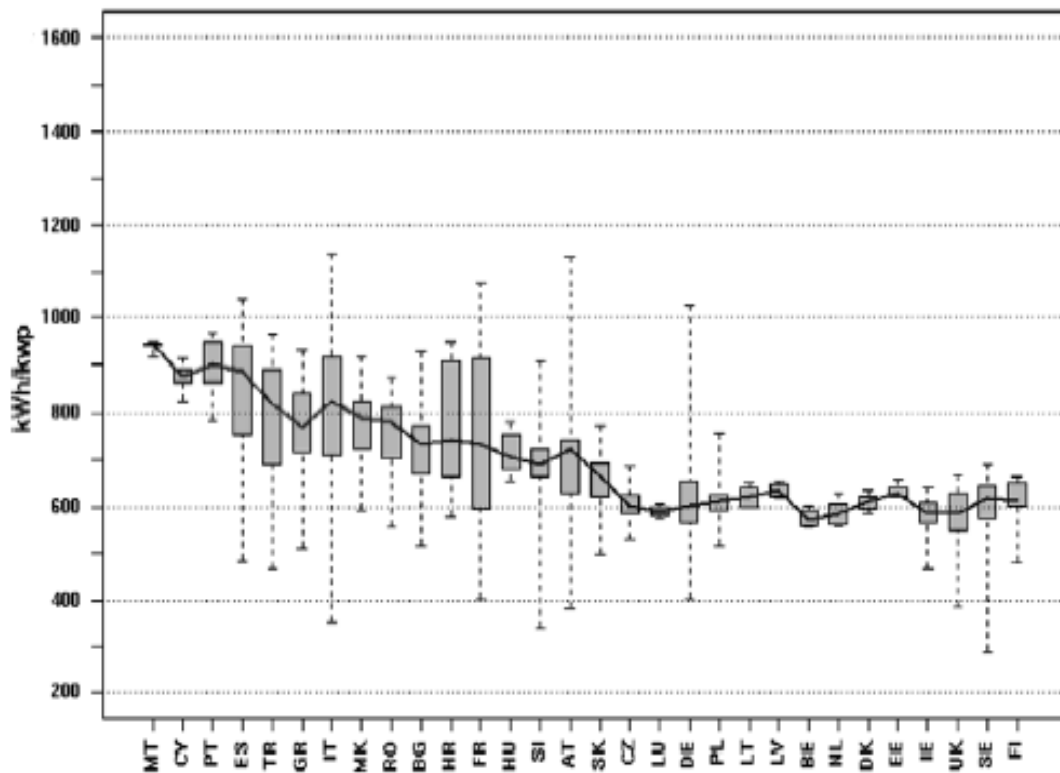ise not going below 530 kWh in northern Scandinavia. In populated areas the above value varies between 630-1330 kWh for northern Finland and Malta respectively.

Naturally the highest potential for solar energy generation, 1100-1330 kWh/kWp, is found in the Mediterranean region i.e. Malta, Cyprus, Spain, Greece etc. A second region with relevantly favourable climatic conditions of 1000-1100 kWh/kWp includes northern Spain, Italy, Croatia and countries surrounding the Black Sea (Turkey, Romania, and Bulgaria). Decent conditions of 800-1000 kWh/kWp are available in France (apart from the northern part) and most countries of central

Europe with more continental summers. Less favourable conditions of 700-800 kWh/kWp are observed in North West as well as northern central Europe with mostly in this case diffuse radiation having a greater share of incident global irradiation. Because of longer daytime in summer, the Baltic region has similar annual energy yields with Western Europe (it is quite humid due to the Atlantic Ocean). Poorest regions concerning solar energy yields are Scotland, northern Sweden and Finland with annual energy falling below 700 kWh /kWp.

PV modules installed in optimal inclination

Basic factors determining optimum array inclination:

- Geographical latitude

- Share of diffuse to direct radiation

- Shadowing due to local terrain (near by mountains)

In the case of populated locations, optimum inclination of PV modules varies from 28° in western Peloponnese (high aerosol concentration in ambient air) to 47° in northern Scandinavia. In latitudes between 45-55° the optimum angle increases modestly from 33-36°respectively.

Changing module plane from horizontally inclined to optimally may improve annual energy generated in urban locations between 9-26% i.e. 760 (Scotland, northern Scandinavia) up till 1510 kWh/kWp (Malta, Portugal). Lowest contribution is observed in Greece where the increase is only 9-10%.

When looking into absolute values, most energy is generated in Mediterranean islands, Spain, Portugal, southern France, southern Italy, Greece, Croatia, Turkey (over 1200 kWh/kWp). On the other hand Baltic region, Scandinavia, British Isles and partially central Europe annual yields are below 900 kWh/kWp. The rest of Europe varies between 900-1200 kWh/kWp.

PV modules installed vertically

When compared to optimally inclined, vertically installed PV modules deliver 42% - 33% less energy in the Mediterranean and Black Sea zone. In Central Europe

percentages drop to 28%. In northern Sweden and Finland these are further reduced to 20%.

The abundance of sun light is responsible for annual yields in the Mediterranean region remaining over 900 kWh/kWp (Malta, parts of southern Spain, France, Turkey and Portugal) and 650 -900 kWh/kWp in the rest of the Mediterranean and Black Sea. Values around 650 kWh/kWp are observed in Poland, Germany, Baltic States and Scandinavia.

PV installations with solar trackers

The cumulative solar energy incident on a PV system depends strongly on the modules' orientation and inclination as discussed above. Common practise is to mount modules on a structure facing due south and inclined on an angle equal to the local latitude. In some cases however PV cells may be mounted also on horizontal and vertical surfaces especially in the case of systems installed on buildings. Furthermore energy generation can be maximised by mounting PV modules on a single or double axis solar tracking device in order to keep cells pointing constantly towards the sun's direction.

King and Boyson [31] have presented data from 3 different locations (Buffalo, Sacramento and Albuquerque). Buffalo is 60% where as Sacramento is 85% of solar energy available in Albuquerque. They have compared all of the above mentioned orientation and inclination scenarios for a typical multi crystalline PV system as shown in the following table:

	Albuquerque	Sacramento	Buffalo
Laitude-Tilt	1.00	1.00	1.00
Horizontal	0.86	0.90	0.90
Vertical	0.73	0.71	0.83
1-Axis Tracking	1.21	1.23	1.15
2-Axis Tracking	1.32	1.31	1.23

Table 5: influence of inclination / orientation on annual DC energy generated by a typical mc-Si module [31]

Solar trackers were observed to be more efficient as expected in sites with more available direct solar radiation (Albuquerque).

Angle of incidence (AOI) effect

Optical losses related to a PV module's angle of incidence obviously have to do mainly with solar beam radiation. These losses are linked in the case of flat plate modules to solar radiation reflected from a module's glass surface. The amount reflected is observed to be quite significant when angles are over 60°. Annual energy yields are not considerably affected by these losses. However it is quite useful to observe the seasonal effects of solar angle of incidence - AOI (angle θ in chapter 3.1. General solar angles) on various module inclination scenarios [31].

The following table provides us with some insight on the effects of **AOI** on 3 different locations and 4 module inclination scenarios:

	2-Axis	Lat.Tilt	Horizontal	Vertical
Albuquerque	1	0.989	0.976	0.960
Sacramento	1	0.989	0.981	0.957
Buffalo	1	0.993	0.985	0.975

Table 6: effect of angle of incidence on various module inclinations [31]

The greatest noted annual loss was 4% in case of vertically inclined modules when optimally inclined resulted in a mere 1%. The following figure illustrates the AOI effect on various modules as measured:
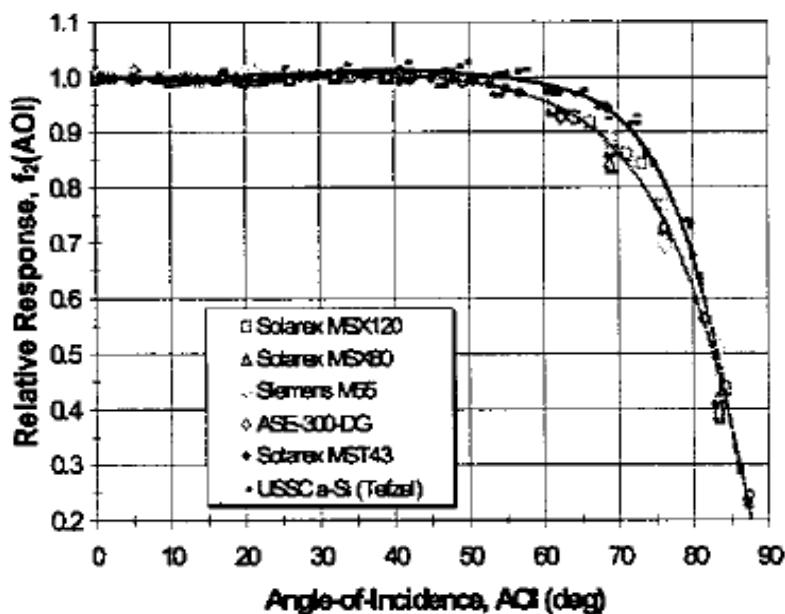

Figure 26: Isc response on angle of incidence of various cell types [31]

Furthermore it is useful to notice the responding differences between power yields of horizontally and vertically inclined modules in a per month comparison especially in the case of designing Building installations. The following figure shows the response of a mc-Si module installed horizontally and vertically in a site in Albuquerque.
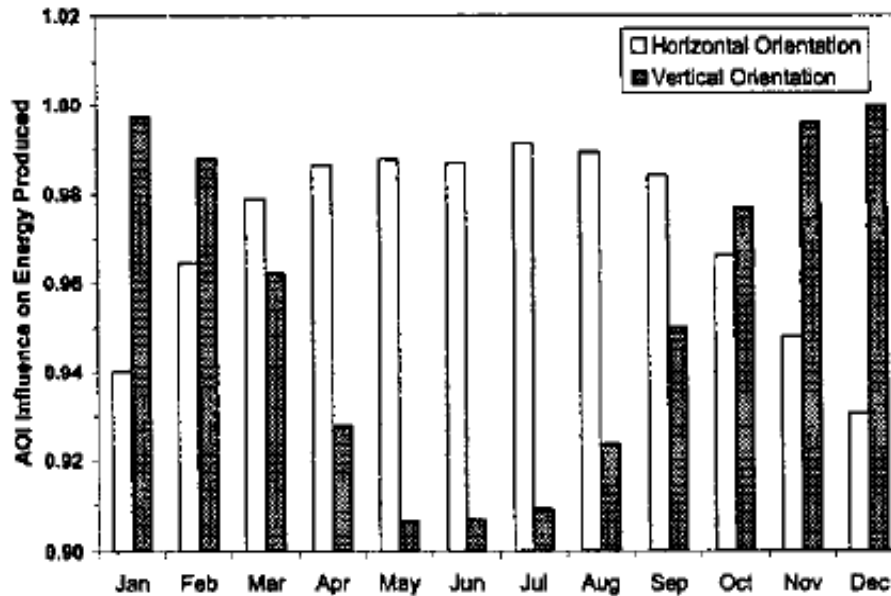

Figure 27: monthly effect of AOI on energy yield of a mc-Si module installed vertically and horizontally [31]

4.4.4 PV Temperature influence on cell performance

PV cells power rating, as it was mentioned previously, is based on them being tested in specified conditions (standard test conditions STD: incident insolation: 1000 W/m^2, air density: 1.5 kg/m^3, cell temperature: 25°C). Naturally these conditions never occur in reality. As far as temperature is concerned, there is a thermal coefficient used which varies considerably in relation to each type of PV technology.

Coefficients for mono crystalline cells are approximately -0.5% / °C whereas for example Unisolar's triple junction amorphous silicon is roughly -0.21% / °C when temperatures rise over operating levels of 25 °C (actually a non linear function) [40-42]. These moderate temperature conditions i.e. 60 °C on the panels would lead a 100kW array of triple junction amorphous or single crystalline cells to generate 92.65 and 82.5 kW respectively.

When going in more detail, it is useful to investigate how short circuit current Isc and open circuit voltage Voc are influenced by solar irradiance Φ and ambient temperature Ta. Isc is relatively proportional to incident solar irradiance when Voc increases insignificantly.
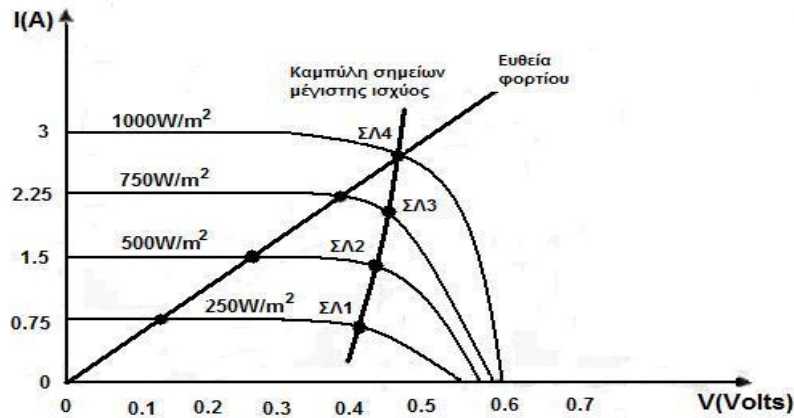
Figure 28: I – V curve regarding incident insolation [43]

On the other hand temperature increase leads to noticeable decrease of Voc and a small Isc increase. The V_{OC} decrease is about 0.5% / °C for crystalline PV cells and 0.20-0.30% / °C for the amorphous ones. The above changes are leading to a significant maximum Power decrease [44].
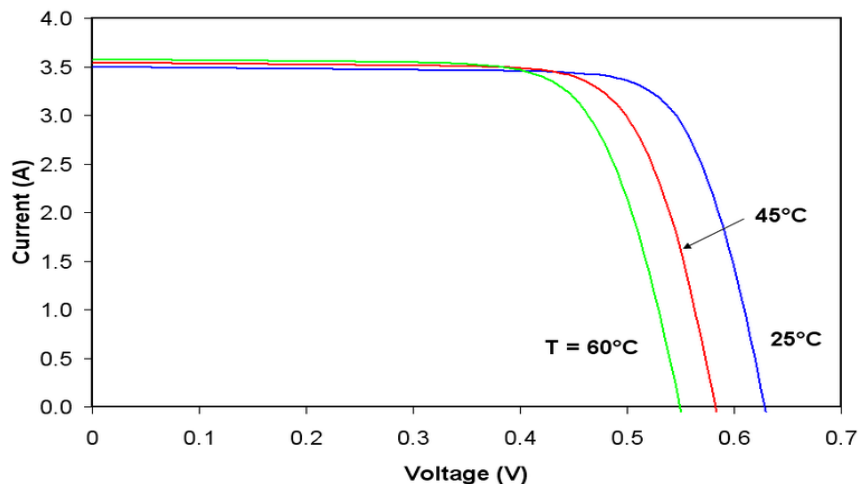
Figure 29: I – V curve regarding PV temperature [45]

Reports show that photocurrent I_L increases with temperature (0.065 - 0.1% /°C) due to the gap decrease of the solar cell. Voc drops at -2 mV °C^{-1} at temperatures 20-100°C due to gap reduction and increase of the saturation current. The latter leads to

maximum power decrease of 0.35% / °C [46]. Others estimate the same reduction to be equal to 0.5% /°C [47]. Most recent estimations vary between 0.3-0.5% / °C [48-51].

Del Cueto [52] studied performances of various technologies for a temperature change span of 30°C and came up with the following shown in the table below (data from various sources in literature are in good agreement):

| Module type	c-Si	c-Si	c-Si	pc-Si	pc-Si	CIS	CdTe
% °C^{-1}	−0.496	−0.388	−0.427	−0.401	−0.431	−0.484	−0.035

Table 7: temperature coefficients for several PC cell types [52]

For amorphous silicon cells, temperature coefficients are lower (0.1%) [53].

Bearing in mind the above, the most popular model concerning PV module efficiency is the following [54]:

$$n = n_r \left[1 - \beta\left(T_c - T_r\right) + \gamma Log\Phi \right] \quad \{38\}$$

η_r: reference cell efficiency at a temperature T_r=25°C and irradiation incident on a PV array per unit area Φ=1000W/m^2.

γ: radiation intensity coefficient regarding cell efficiency

β: temperature coefficients concerning cell efficiency

T_C: cell temperature dependent on environmental conditions

The parameters η_r, T_r, γ, β are usually provided by the manufacturer.

However researchers have suggested regarding γ and β for silicon/CIS modules 0.12/0 and 0.0048/0.006 °C^{-1} respectively [55], [56]. In the above equation solar irradiance might be partly neglected but still remains integrated in the cell temperature (cell temperature strongly depends on its values). The above equation was experimentally tested taking η_r = 0.125, T_r=25°C, β = 0.0044°C^{-1} on the 29th of April 2001. The results are presented in the following figure:
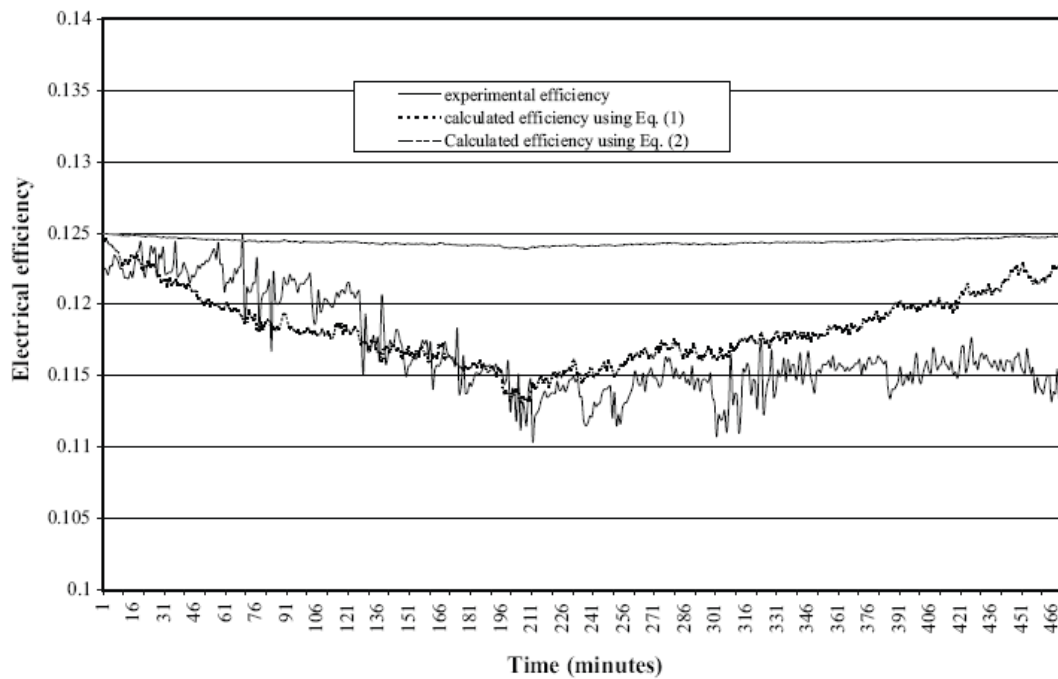
Figure 30: comparison of experimental data with two alternative efficiency models [54]

When comparing experimental electrical efficiency data acquired with results of the above equation we can observe an adequate agreement which is not the case when considering the results of the equation with γ = 0 as illustrated by the line introduced as equation 2.

Estimating cell temperature

Cell temperature T_C is most commonly determined by using Normal Operation Cell Temperature (NOCT) [57]. NOCT is estimated for $T_C = 20°C$, wind speed v = 1 m/s and hemispherical irradiance $\Phi = 800W/m^2$. This parameter is also provided by the manufacturer. T_C is related to ambient temperature T_a and solar irradiance Φ as shown in the following equation:

$$T_c = T_a + (NOCT - 20°C)\frac{\Phi}{800} \quad \text{\{39\}}$$

This equation has been proven to produce decent results in case of not fully roof integrated PV systems. Definitions and further reading regarding NOCT is available in references [58], [59].

An energy balance of a PV cell has been followed through by Mattei, Notton [54] considering the above with some further assumptions made:

- Temperature between PV cell and covering glass is neglected.

- Panel temperature is considered uniform.

- Radiative exchanges are considered negligible.

Energy absorbed by the cell is the product of solar irradiance $\mathbf{\Phi}$, a transmission coefficient $\mathbf{\tau}$ relevant to energy passing through the cover glass and an absorptivity coefficient $\mathbf{\alpha}$ relevant to energy absorbed by the cell ($\mathbf{\alpha\tau\Phi}$). This product should be then equal to the sum of energy converted in to electricity $\mathbf{\eta*\Phi}$ by the cell and heat losses from the panel to the surrounding environment $\mathbf{U_{PV}}$ ($\mathbf{T_C - T_a}$) where $\mathbf{U_{PV}}$ is the cell overall heat transfer coefficient.

$$\alpha\tau\Phi = n\Phi + U_{PV}(T_c - T_a) \quad \text{\{40\}}$$

This equation has been applied in Furler's [60], Sandnes's and Reskstad's [61] estimations. Considering $\gamma = 0$ in the previously introduced equations lead to the following:

$$T_c = \frac{U_{PV}T_a + \Phi\left[(\alpha\tau) - n_r - \beta n_r T_r\right]}{U_{PV} - \beta n_r\Phi} \quad \text{\{41\}}$$

According to Furler [60] ($\alpha\ \tau$)/ $\mathbf{U_{PV}}$ = 0.0325 °C/m^2/W and Sandnes and Redkstad [61] ($\alpha\ \tau$) = 0.9 $\mathbf{U_{PV}}$ = 28.8 W/ m^2 /°C are in agreement.

Wind related convection heat transfer coefficients

In order to increase the accuracy of $\mathbf{U_{PV}}$ it is important to consider the influence of the wind speed (m/s) and direction (deg) to which it is strongly related. Numerous correlations are available to estimate $\mathbf{U_{PV}}$ relative to wind speed $\mathbf{v}$. Jones and Underwood [62] reveal a considerable range of values regarding the forced convection coefficients. In the case of a value of v =1 m/s the surface heat transfer coefficient h$_c$ is equal to 1.2 W/m^{2}C [61], 5.8 W/m^{2}C [62], 9.1 W/m^{2}C [63], 9.6 W/m^{2}C [64].

Duffie and Beckman [65] suggest McAdams's [66] expression regarding flat plates to outdoor conditions.

$$h_c = 5.67 + 3.86v \quad \{42\}$$

Nolay [57] made use of the following:

$$h_c = 5.82 + 4.07v \quad \{43\}$$

Furthermore Cole and Sturrock [67] have focused on the importance of wind direction's effect to the heat transfer coefficient. Specifically they have considered two alternative directions as expressed from the following equations:

$$h_c = 11.4 + 5.7v \quad \{44\}$$

when subject is a windward surface and

$$h_c = 5.7 \quad \{45\}$$

when subject is a leeward surface.

Also another proposed used equation is [109]:

$$h_c = 5.7 + 3.8v_w \quad \{46\}$$

v_w is the corrected wind speed (m/s)

The wind speed is corrected by making use of the equations below:

For windward conditions, with wind speed greater than 2m/s, $v_w = 0.25v$ $\{47\}$

For windward conditions, with wind speed less than 2m/s, $v_w = 0.5$ $\{48\}$

For leeward conditions with wind speeds greater than 2m/s, $v_w = 0.3 + 0.05v$ $\{49\}$. v is the actual wind speed, as it is referred to all the previous equations

U_{PV} corresponds to the total surface area of a module meaning twice the area corresponding to h_C as heat is dissipated from both front and back surface (an air gap

exists also behind the PV's back surface). The resulting equations based on the above four mentioned cases are respectively the following:

$$U_{PV} = 11.34 + 7.72v \quad \text{\textcolor{red}{\{50\}}}$$

$$U_{PV} = 11.64 + 8.14v \quad \text{\textcolor{red}{\{51\}}}$$

$$U_{PV} = 17.1 + 5.7v \quad \text{\textcolor{red}{\{52\}}}$$

$$U_{PV} = 11.4 + 7.6v \quad \text{\textcolor{red}{\{53\}}}$$

Barker and Norton [68] recommended the use of a formula established by Ingersoll [69] including all heat transfers occurring in which heat transfer coefficients where differentiated according to panel surface area. Numerous coefficients are required as well as correlation tables in order to determine certain parameters.

Mattei and Notton [54] have researched and presented work supporting the fact that heat transfer coefficients related to wind speed provide models closer to actual experimental data.

After certain wind speed levels though, given a certain ambient temperature, their further increase does not seem to affect PV cell power output as illustrated in the following figure in relation with various temperatures (after 10 m/s wind speed impact seems to remain constant).
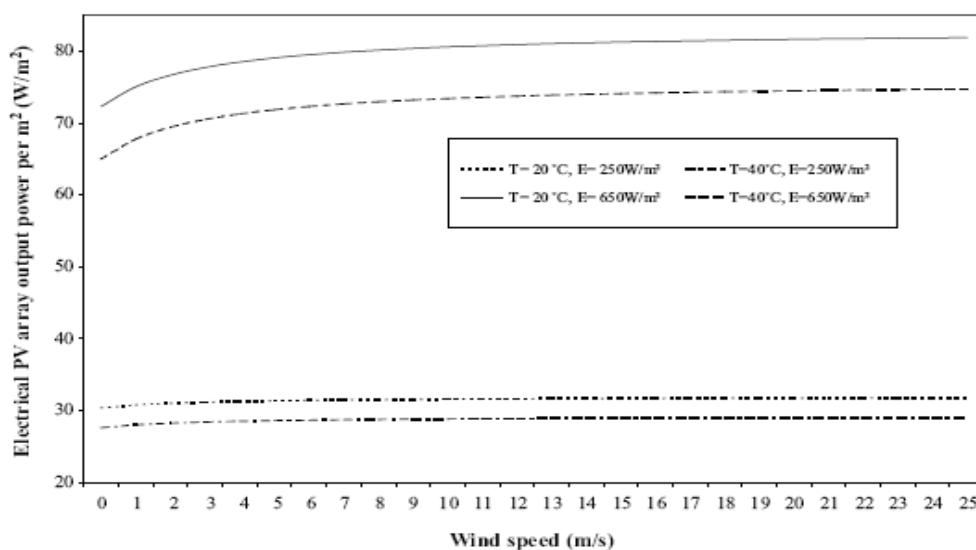

Figure 31: influence of the wind parameter to PV cell power output [54]

Heat radiation exchange

A thermal loss often neglected in formulas estimating panel temperature is radiated heat to the environment and especially to the sky. There are numerous available sky temperature models which usually require local dew point temperature T_d and relative humidity **r.h.** values in order to estimate the temperature of the sky dome T_{sky}. This dome tends to absorb a noticeable amount of thermal energy thus further reducing cell temperature (sky temperature may be often 10-20°C less than ambient temperature with which is strongly related). The energy exchanges between ambient and PV panels including radiated heat are illustrated in the following figure:
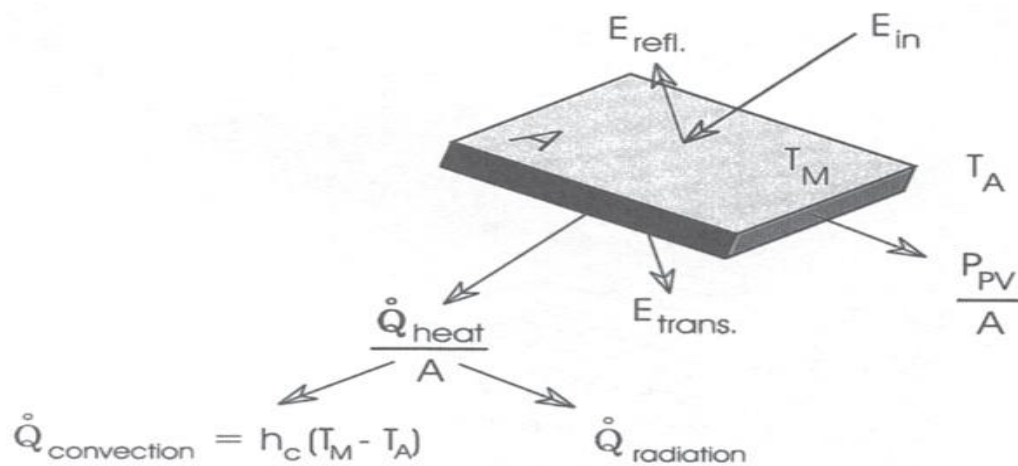
Figure 32: energy balance on a PV panel [70]

Total radiative heat flow from the panel to the neighboring environment and sky dome may be calculated based on the following equation [70]:

$$
\begin{aligned}
\dot{Q}_{rad} = \frac{1}{2}\sigma \Big[&A_F \epsilon_F\big(\epsilon_{sky}(T_F^4 - T_{sky}^4)(1 + \sin(90° - \gamma_M), \\
&+ \epsilon_G(T_F^4 - T_G^4)(1 - \sin(90° - \gamma_M)), \\
&+ A_R \epsilon_R\big(\epsilon_{sky}(T_R^4 - T_{sky}^4)(1 - \cos\gamma_M), \\
&+ \epsilon_G(T_R^4 - T_G^4)(1 + \cos\gamma_M))\Big].
\end{aligned}
$$

{54}

$\dot{Q}_{rad}$: total radiative heat flow of the PV surfaces with the environment and sky dome

σ: Stefan- Boltzman constant

γ_M: inclination of the module surface

ε_R: rear module surface emissivity

ε_G: ground emissivity

ε_{sky}: sky emissivity

ε_f: front module surface emissivity

T_F: front side PV module temperature

T_G: ground temperature

T_R: rear side PV module temperature

T_{sky}: sky temperature

A: PV module surface area

4.4.5 Effect of the urban microclimate on PV efficiency

PV projects in the urban environment, when evaluating potential energy yields, should consider some noticeable deviation of local actual climatic conditions to available climatic data from meteorological stations often positioned in neighbouring rural locations i.e. airports.

Big cities especially in warmer climatic regions may be responsible for reduced wind speeds of scattered directions, less direct solar gains and higher maintenance requirements due to pollution which may additionally increase soiling of PV modules considerably.
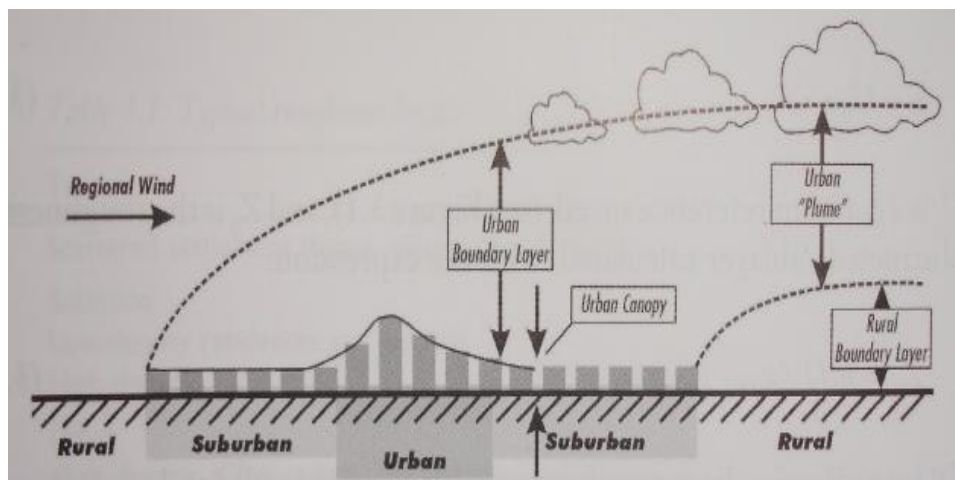

Figure 33: urban boundary and canopy layers [13]

Ambient-city canyon wind speed /direction

Analysed in the above section of this project is the importance of wind speed and direction concerning cell temperatures. Especially in case of BIPV greater overheating issues may occur due to their rear end being part of the building construction and thus heat not dissipated freely and directly to the environment.

Wind speed / direction and the effect of the built environment on urban canyons in which BIPVs may be installed have been studied thoroughly by Santamouris et al. [13].
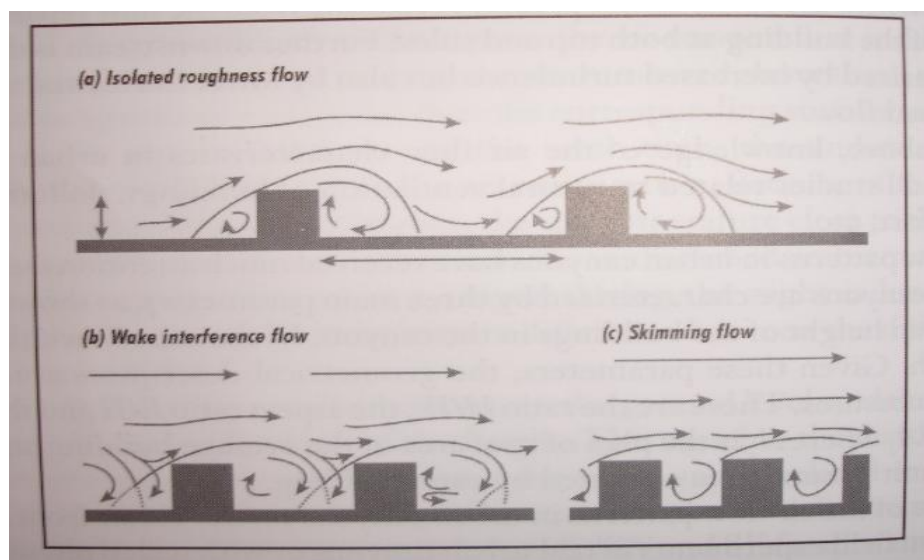
Figure 34: canyon flows relative to flows over building arrays of increasing height to width ratio (H/W) [13]

In more detail, wind speed estimations in urban canyons vary in relation to wind flow speed and direction above roof levels. Obviously, in contrast to parallel, vertical wind flows above a canyon can not influence as significantly magnitudes in it.

After conducting numerical studies researchers have reported that in case of a wind flow at an angle of 45° as well as perpendicular to a city canyon's axis [with an average building height (H) to canyon width (W) ratio of 1 and an ambient wind speed above 5 m/s], the developed vortex in the canyon was approximately an order less [13]. Naturally wind speeds closer to the top may obtain values slightly higher.

In case of parallel flows statistical analysis has shown that both median and quartiles in the canyon increase proportionally to ambient wind speed above it. However

outliers with high values in low ambient wind speeds do not allow firm conclusions to be drawn.
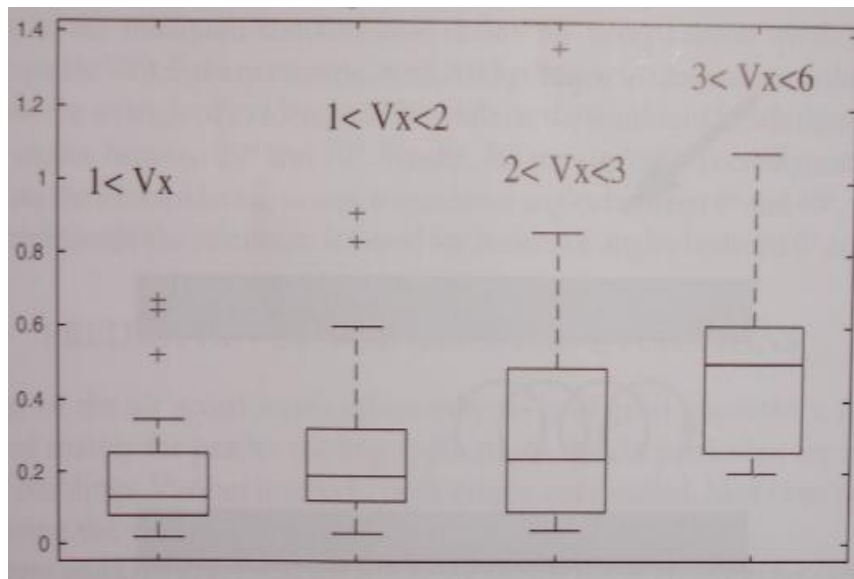
Figure 35: box plot concerning wind speed inside a canyon relative to varied wind speed values above for parallel wind direction (V_X: wind speed values) [13]

A specific case study in central Athens is illustrated in the following figure where airport measured values are compared to those of a centrally located canyon.
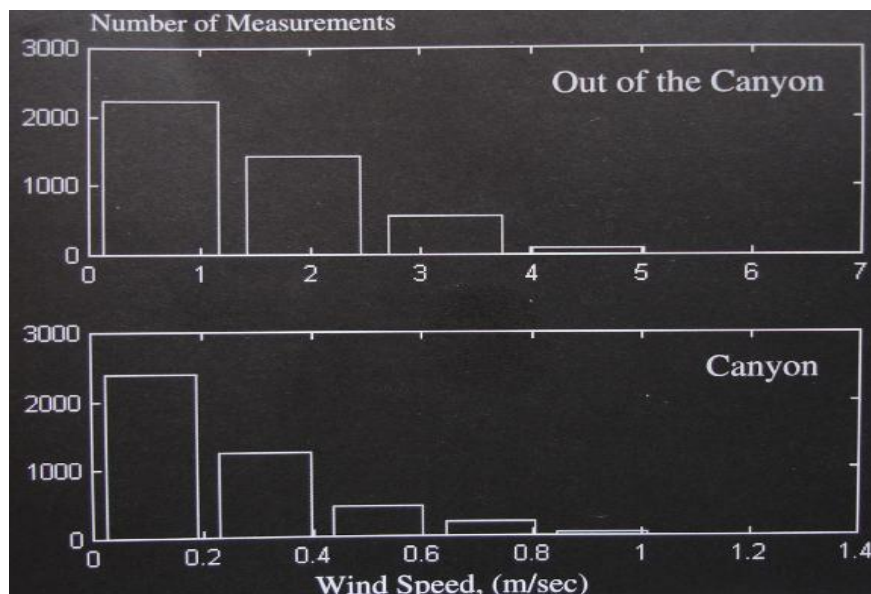
Figure 36: frequency wind speed distribution in and above a canyon in central Athens [13]

As far as wind speed estimations on roof tops are concerned, these may vary depending on various parameters not analysed in the present study. Values obtained

may be occasionally become higher than rural. Two conditions in which that may be the case are:

- high speed air layers either deflected downwards by high buildings or channelled i.e. 'jets' moving parallel with the wind flow
- low level flows from the country adequately strong to overcome frictional drag of canyon vertical surfaces

When considering PV installations on building facades it is important to bear in mind vertical and horizontal external surface overall heat transfer coefficients vary as a function of wind speed. Convection in case of wind speeds lower than 2 m/s (which seems to be often the case in city canyons) shall be mainly attributed to ambient – external surface temperature differences and buoyancy rather than wind speed. In the case of buildings highly exposed to ambient wind or PV systems installed on roof tops convection shall be related occasionally to all the previously mentioned parameters [13].
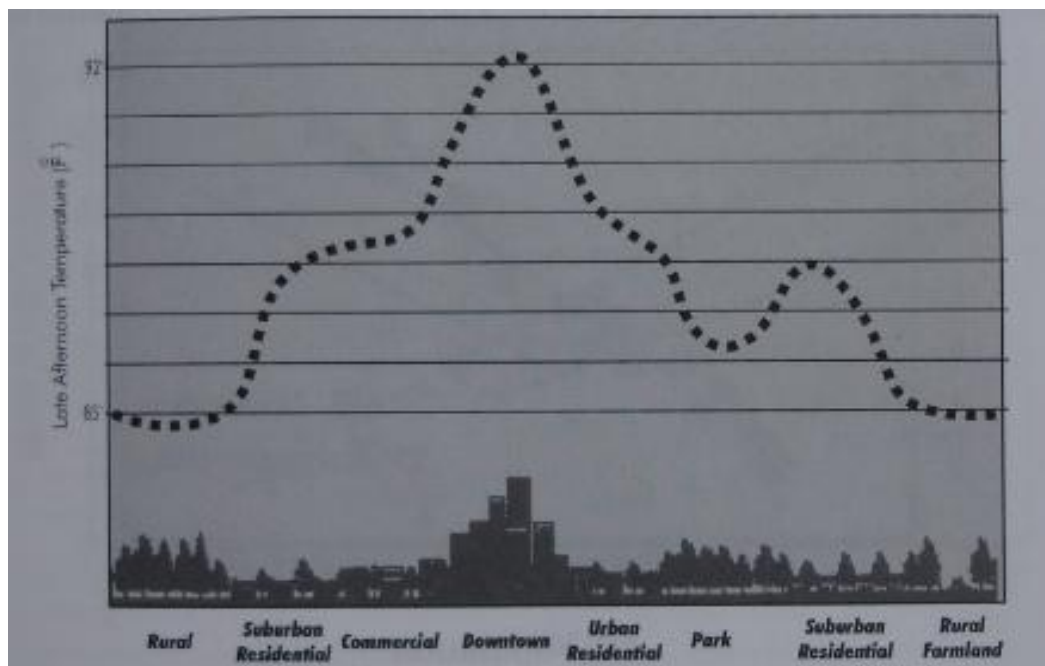
Local microclimate in cities

Figure 37: sketch of a heat island profile in late afternoon [13]

Ambient temperatures in densely built cities are always higher than neighbouring rural locations. This phenomenon otherwise known as the 'heat island' was first noticed by meteorologists more than a hundred years ago. The intensity of the heat

island is mainly determined by the urban thermal balance and may result to a temperature difference of up to 10°C [13]. The temperature increase in some overpopulated cities around the world is illustrated in the following table:

Table 5.1. Heat-island effects in some cities⁴

City	Temperature increase, (K)
30 US cities	1.1
New York	2.9
Moscow	3–3.5
Tokyo	3.0
Shanghai	6.5

Table 8: heat island effect in various cities [13]

Detailed research concerning heat island intensity (meaning temperature difference between maximum urban and rural area) measured values in Athens (1996-99) came up with average values of 12 K [13]. However this impressive value is a maximum and may occur rarely in summer afternoon hours. It would be interesting to acquire average day light hour values in order to further understand the potential effect of this temperature rise on PV systems.

Apart from reduced wind speed conditions and higher local temperature levels the urban environment is responsible for the increased density of certain air pollutants. Such particles i.e. smog (exhaust fumes-factory chemicals, dust etc) accumulated on PV modules which are installed in densely populated cities of warmer and sunnier climatic regions can reduce considerably PV module performance.

In addition researchers in urban environments have measured (as mentioned in former chapters) considerably decreased global, direct and increased diffuse solar radiation values. This could encourage more detailed research-experimenting on various cell technologies' response to the urban global solar radiation spectrum. A significant change in the available solar resources obtained especially in the summer period in a central city location might put less popular PV technologies in a more advantageous position.

4.4.6 Inverter efficiency – system matching

Inverter losses account for 6-10% system losses in general. In case of a 3 phase system the accompanying isolation transformer may add an extra 2.5-3% loss over that of the inverter. This could be reduced by a high efficiency transformer to 1.5-2% (more windings but a higher cost). Inverters incorporating contactors in the secondary winding circuit may further improve the efficiency through disconnecting the system from the AC line when the inverter is shut down. This way the night time load due to the isolation transformer's secondary winding is removed, which is a measurable portion drained from the load generated during daytime.

Inverter power ratio IPR (nominal power of the inverter / nominal PV system power) with values between 70-90% are conventionally considered for climatic regions similar to the UK. When inverters are oversized compared to an installation, operation efficiencies are usually lower especially in low insolation periods around the year with impaired system performance and reduced electricity yield.

Inverters may fail to track the maximum power point concerning an array which could result in a very poor PV output [71].

Inverter companies do not have adequate experience concerning grid connected amorphous silicon cells. The inverter used for instance in Omer's experiment [71] was designed for crystalline modules and therefore had adopted a MPPT algorithm focused on crystalline PV where operating voltage range is relatively short with varying insolation intensities in contrast to amorphous silicon cells (the inverter algorithm is also related to the ratio of peak power to open circuit voltage). Allowing a broader MPPT voltage range improved the efficiency of the system but specifications especially for amorphous cells need to be attributed by inverter companies in the immediate future.

As far as the operation of the inverter, the network operator can request specific voltage levels. For instance, an inverter can have a AC voltage range $V_{AC} = 196 - 253V$ (with input voltage range from the array $V_{DC}=125V-150V$), meaning that any voltage outside these limits would lead to arrays temporarily cut out from the grid. Inverters are designed to re-connect automatically (usually after a 3min delay) when the array voltage matches the specified limits which are related to the net work load.

4.4.7 Maximum Power Voltage V_{mp} related to Irradiance

This PV cell characteristic is not usually measured by manufactures. It may however influence annual energy yields. Specifically it describes the performance of a module relative to irradiance levels. The following figure illustrates V_{mp} relative to irradiance regarding two module types.
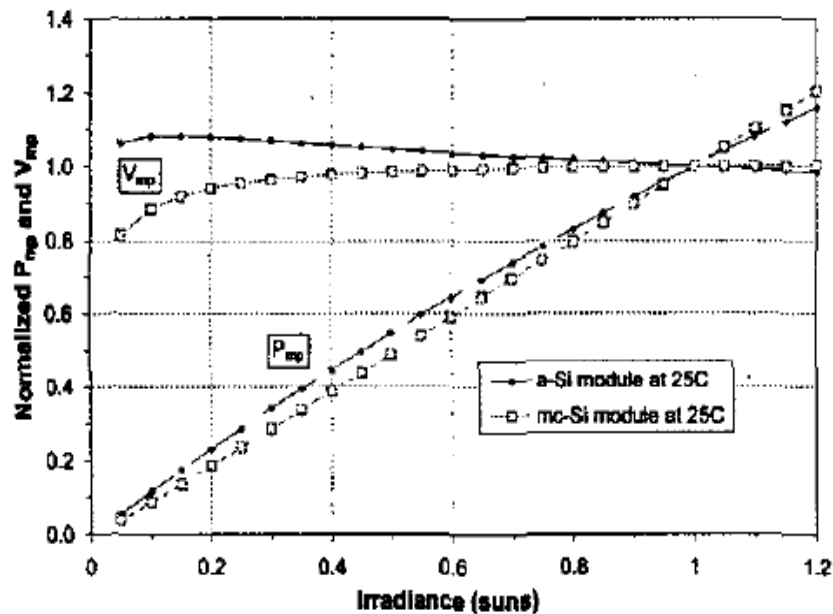
Figure 38: Vmp, Pmp measured values relative to irradiance for mc-Si, a-Si [31]

As far as a-Si is concerned, Vmp increases with irradiance decrease thus maintaining higher voltage values than the one-sun condition reference. This behaviour may result to a 10% increase of annual energy yield [31]. A further 2% increase in the annual energy yield is attributed to the relatively smaller temperature coefficients of a-Si compared to crystalline cells.

4.4.8 Shading issues

Shading due to neighbouring obstructions i.e. Buildings, trees may reduce considerably a module's efficiency. PR can be greatly affected by partial shading of a PV module especially in the case of crystalline technologies that luck bypass diodes. The a-Si modules are less affected by shading due to the existence of bypass diodes. In addition, shading can be caused by remaining dust or other substances. Therefore, maintenance plays a significant role and will be further analysed in 4.4.9 System aging – Maintenance.

4.4.9 System aging - Maintenance

When selecting a building surface for a PV installation it is important to maintain it clean of accumulated substances which would lead to shading of the actual cell material. Especially in the case of crystalline panels, any type of shading even partially of an array may cause significant decrease of its capacity. If for example even two cells of a crystalline cell are heavily shaded, that may result in the 36 cell series strings to generate amounts of energy close to zero (one cell in each of the series would be enough). It is also reported that 10% shading of a cell's surface area may lead to a power loss of 2.6% when 50% shading would result in a power reduction of 38% [72].

Triple junction panels on the other hand are manufactured by much bigger cells protected with bypass diodes and i.e. in the case of 22-cell Uni-solar the hard shading of two cells would only result in a panel output reduction of 9% [42].

Air quality in the urban environment is highly polluted due to car and building exhaust fumes, factory chemicals, toxic rain, dust etc. This leads to the acceleration of permanent module soiling which would reduce a cell's solar absorbtivity significantly and thus its efficiency.

Furthermore any potential damage to a system installation (usually concerning panels) during the installation process should be dealt with immediately as it could affect its whole lifespan. Even a small crack of the glass cover in the case of crystalline cells may result to its destruction. Specifically one cracked cell may lead to a module power loss of as little as 2% [73] naturally depending on the severity of the crack. However a cracked cell may heat up during dissipation of power and lead to irreversible damage. If in such cases no bypass diodes are included, hot spots may occur resulting to cell damage (Bypass diode are used for short circuiting to prevent power generation. Through these diodes it is possible to cover the one cell leading to its entire sub string to be short circuited when designed correctly [74]).

The sensitivity of crystalline cells may restrict access in case of horizontally roof mounted panels. On the other hand thin film PV cells can tolerate damage and would be seldom required to be replaced.

Aging in actual case studies

Reis and Coleman (Shatz Energy Research Center [75]) conducted a report (2002) on a PV system installed in 1990 and exposed to a cool marine environment. The system performance parameters investigated were short circuit current I_{sc}, open circuit voltage V_{oc}, parallel resistance R_p, series resistance R_S, a parameter related to the knee curvature '**ekt**', maximum power point P_{max}, maximum power point voltage V_{mp} and maximum power point current I_{mp}. The meaning of each parameter can be better understood through the following figure:
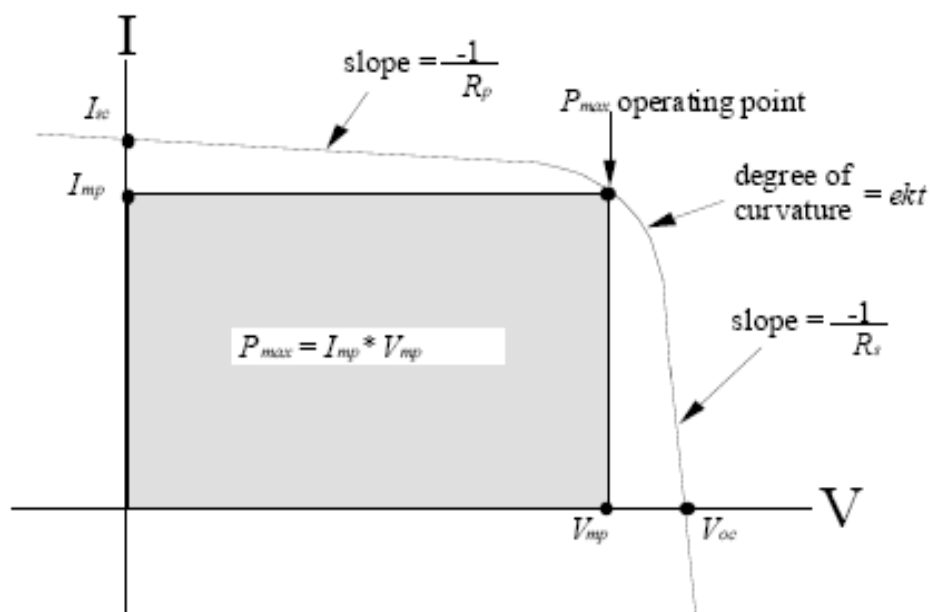
Figure 39: I-V curve demonstrating performance parameters [75]

Their findings concluded that in this 11 year period there was a 4.39% drop in average P_{max}. The majority of power loss was attributed to I_{sc} and I_{mp} decrease of 6%. They further noticed that P_{max} was shifted further down the I-V curve knee, R_S increased by 10.66% and R_p decreased by 32.75%.

The increased series resistance R_S led to a significant amount of energy converted to thermal losses. Parallel resistance R_p decrease on the other hand, indicated a current leak increase in the cell area further reducing the amount available.

In addition, variability of P_{max} has increased considerably as illustrated by the larger range of values in the following figure:

65
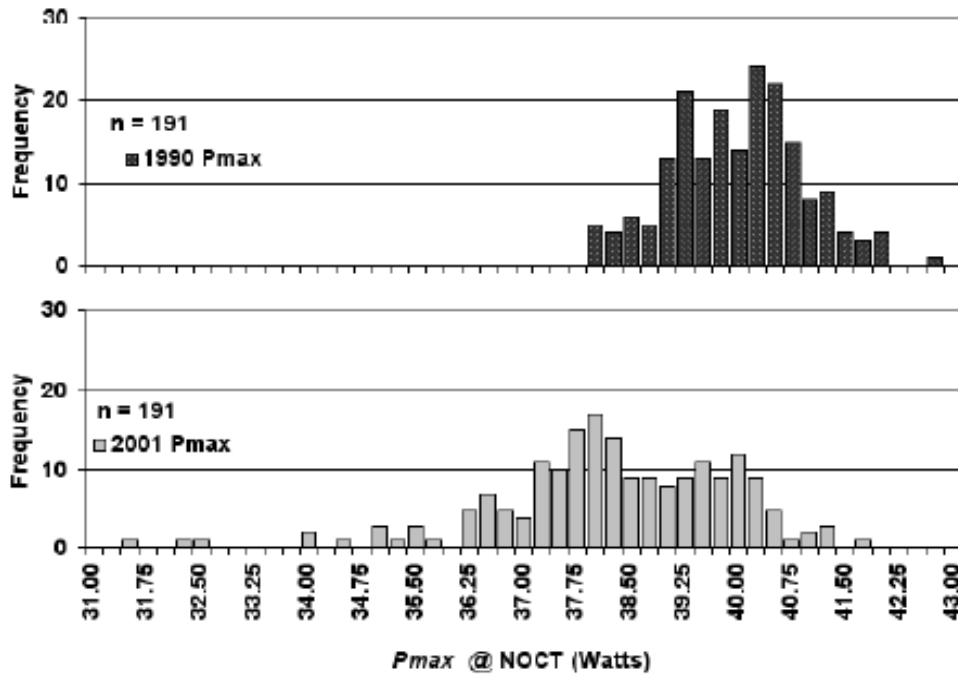
Figure 40: P_{max} distribution in 1990 and 2001 [75]

Current reduction was attributed partially to the following physical defects observed visually:

- Moderate discolouration of the EVA encapsulant [76]

- Encapsulant delamination at silicon cell − EVA interface [77]

- Localised hot spots leading to Intense browning of EVA over some cells [78]

Machida and Yamazaki [79] after investigating mono crystalline modules concluded that P_{max} decreased 4.8% in a five year exposure period. The lower degradation rates observed by SERC [75] were attributed to lower coastal temperatures in which the modules were exposed (it has been reported that higher ambient and system operating temperatures lead modules to degrade faster [76]).

4.4.10 Balance of system (BOS)

A PV system is made out of various components apart from the above mentioned PV cell, as it has been explained in 4.3 Photovoltaic systems. Regardless of a cell's technology the following factors may have a profound effect on the system's final performance

DC voltage selection

System voltage is mainly relevant to input DC voltage concerning the inverter in combination with the tendency of maximising its values (practically within NEC and UL limits) to reduce wiring losses. Most systems today have nominal DC voltages of 300-500 V_{DC}.

Panel voltage mismatch

PV panels are connected in series as to come up with the system operating voltage. Series strings are paralleled to increase system current values. The system voltage is generally a **V_{mp}** rating average of individual panels' voltage values. The difference between system voltage and individual panel **V_{mp}** is defined as mismatch. When the operating point is shifted regarding a panel's **V_{mp}** the power output shall be reduced. Obviously sharper 'knees' lead to greater effects /power reduction. Softer 'knees' observed in amorphous silicon cases lead to smaller mismatch losses which can be observed by the darker IV curve in the following figure [80].
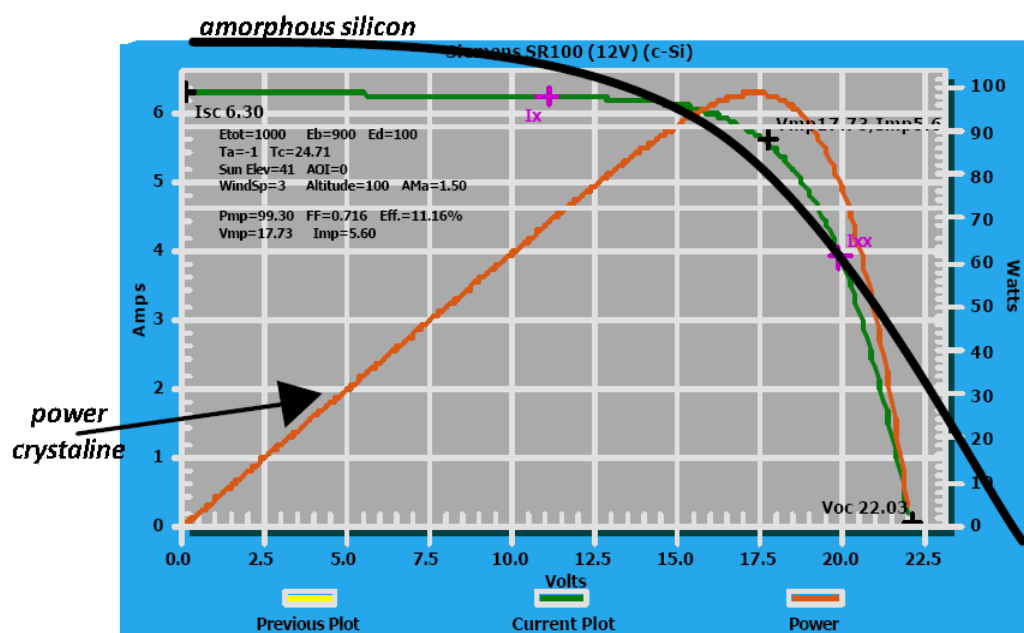

Figure 41: I-V curves for crystalline & amorphous silicon cells [80]

Shunt paths

In order to observe electrical current values in solar arrays, low resistance precision resistors are used which measure voltage drop across the resistance [73]. It has been

noticed that the light generated current may choose an alternative path of low resistance (if the shunt resistance is low) [72], thus reducing current flow through the solar cell junction and consequently reducing the voltage output. In this case this is caused by manufacturing defects rather than poor solar cell design. Low insolation levels further aggravate the problem since less light generated current is present. The impact of the current loss I_{SH} through the shunt resistance is in this case greater [81]. Low shunt resistance has been reported to result to a power loss of up to 63% [72].

Wire sizing

The size of wire used in a PV system should be chosen based on minimising I^2R heat losses instead of ampacity. Based on the expected currents through a system, wire dimensions need to result to a voltage drop not higher than 3%. Reducing wire diameter further than a specified minimum would keep the system safe. However the end to end system efficiency may drop up to 65% [80].

4.4.11 Parameter overview
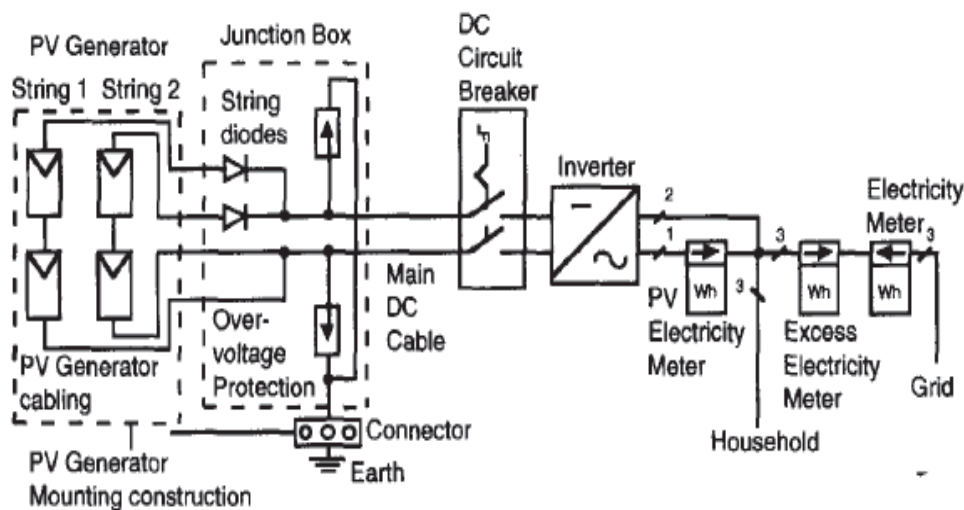
Figure 42: typical PV system [82]

For comparison reasons, normalised performance indicators are often quite useful [83]. It is possible to come up with reference yields through dividing the energy of interest by the nominal array power. **PR (Performance ratio)** presents the total effect of losses on an array's nominal power relevant to temperature, inadequate exploitation of irradiation and system failures or plain inefficiencies. Some of the most important performance parameters are shown in the following table:

Parameter	Symbol	Equation	Unit *
Array Yield	Y_A	E_A / P_0	h / d
Final Yield	Y_f	E_P / P_0	h / d
Reference Yield	Y_r	H_A / G_S	h / d
Array capture losses	L_C	$Y_r - Y_A$	h / d
System losses	L_S	$Y_A - Y_f$	h / d
Performance ratio	PR	Y_f / Y_r	-
Efficiency of the inverter	η_C	E_P / E_A	-
In-plane irradiation	H_A	$\int_\tau G_A d\tau$	kWh/d
Array output energy	E_A	$\int_\tau P_A d\tau$	kWh/d
Inverter output energy	E_P	$\int_\tau P_p d\tau$	kWh/d
Receiving power	E_U	$\int_\tau P_U d\tau$	kWh/d
Load power	E_L	$\int_\tau P_L d\tau$	kWh/d
PV array fraction	F_A	E_A / E_L	-
PV system fraction	F_f	E_p / E_L	-
Nominal array power	P_0	-	-
In-plane irradiance at STC	G_S	1	kW/m^2

Each parameter is often calculated as a daily-mean value.

Table 9: parameters overview concerning performance evaluation (symbols explained further in 4.4 parameters effecting PV performance when connected to the grid and building load) [84]

In further detail, system level factors may present yield losses due to module mismatch in an array, performance degradation of an array due to the age factor, module soiling, wiring, terminal resistance and incompatibility issues between system components.

As far as grid connected systems are concerned, further losses may occur due to inverter efficiency versus temperature and load, maximum power tracking (MPPT) efficiency, inverter tare loss, isolation transformer efficiency etc.

Stand alone systems may have increased DC losses as well as further system design constraints related to charge controller efficiency (optimum utilisation of DC current absorbed from the array), battery charging and discharging efficiency, battery capacity and correct sizing to obtain the best ratio between DC electricity available and AC demand anticipated.

Poorly designed systems which may be the result of any combination of the above factors' miscalculation could easily lead to 'system failures' due to inability of the system to deliver adequate energy amounts required by a building load.

King and Boyson [31] have made an attempt to categorise the different factors affecting a PV system's efficiency as illustrated in the following table. The effect of

charge controllers and inverters has been lumped into the 'power conversion AC to DC factor.

Factor	Range (%)
Module orientation	-25 to +30
Energy storage (batteries)	-30 to -5
Array utilization losses (MPPT)	-30 to -5
Power conditioning hardware	-20 to -5
Module power specification	-15 to 0
Module temperature coefficients	-10 to -2
Module (array) degradation (%/yr)	-7 to -0.5
Module V_{mp} vs. Irradiance	-5 to +5
Module soiling (annual average)	-10 to 0
Angle-of-incidence optical losses	-5 to 0
Module mismatch in array	-5 to 0
Solar spectral variation	-3 to +1

Table 10: factors' estimated ranges concerning PV systems' AC energy output [31]

However as time passes on ranges mentioned above are likely to become broader according to expected module mismatch increase. The selection of compatible hardware (namely the inverter) with the PV array's specifications has troubled researchers for a long time [85].

Researchers in Germany have summarised their results concerning system losses in 42 case studies in 1994:
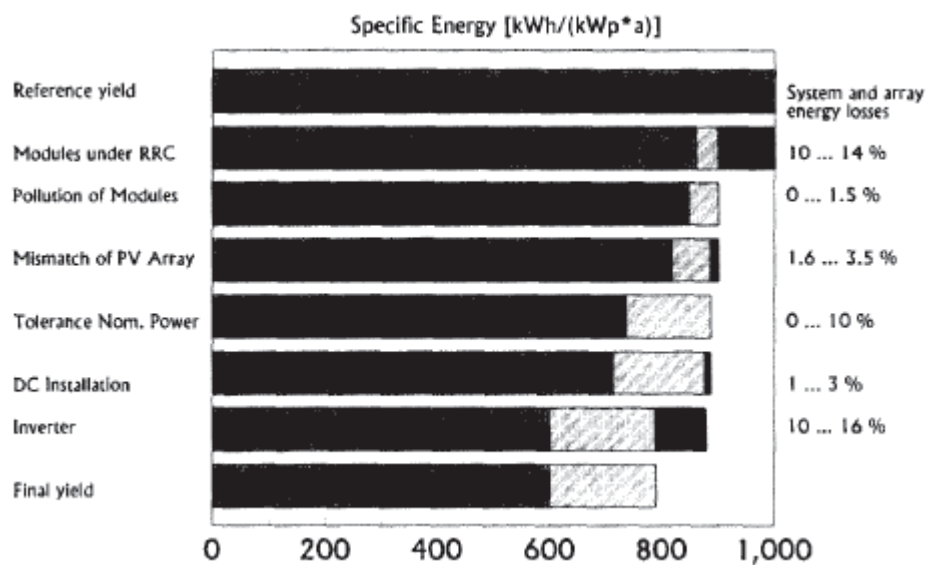

Figure 43: special weights on factors responsible for energy losses concerning grid connected PV installations [82]

Performance ratio (PR)

When comparing PV outputs it is easier to use values independent of specific size system thus dividing PV energy output EPV with nominal power PPV and so introducing the final yield Y_f:

$$Y_f = E_{PV} / PPV_{nom} \quad \{55\}$$

PPV_{nom} : nominal power - power on the PV data sheet

E_{PV} : annual, monthly or daily energy output

As far as the whole PV system is concerned, the final yield may be estimated based on the following equation:

$$n_{PV,STC} = PPV_{nom} / (G_{STC}*A_{MOD}) \quad \{56\}$$

$n_{PV,STC}$: efficiency at standard test conditions

G_{STC} : annual solar radiation under Standard Test Conditions ($1000W/m^2$)

A_{MOD} : Array surface area

In order to estimate PV power output at realistic operational conditions considering module temperature and actual local climatic data for a whole year the following equation is also introduced:

$$n_{PV,RRC} = E_{PVGEN} / (H_A *A_{MOD}) \quad \{57\}$$

$n_{PV,RRC}$: module efficiency under realistic annual conditions

H_A : in plane irradiation

A_{MOD} : Array surface area

E_{PVGEN} : module energy output

Module efficiency under realistic annual conditions ($n_{PV,RRC}$) is usually 10-14% less than standard efficiency ($n_{PV,STC}$). This is due to the occurrence of lower irradiation levels, higher panel temperatures, greater reflective losses at flat incident angles and thermal mass (AM) deviation from standard 1.5 value [86]. Additional losses from the

71

PV array are attributed to pollution and power mismatch. Manufacturers introduce in general a tolerance value 10% of the nominal power.

PR, having being mentioned also before, is a percentage describing the quality of a grid connected system. This way it is possible to compare systems with various nominal powers, orientations, system sizes, tilt angles etc using the following equation:

$$PR = (Y_f * G_{STC}) / H_A = (E_{PV} * G_{STC}) / (PPV_{nom} * H_A) \quad \{58\}$$

PR values have varied based on past projects from 60% to 79%. Any values toping these were usually due to unreliable data coming from the AC counter which may sometimes interact with the inverter's harmonics. Lower values can be attributed to long term failures of a system's components (i.e. inverter).

The better understanding of performance ratio required the introduction of the standard performance ratio **PR$_{ST}$**. This is the optimal performance of a PV system meaning that all PV plants refer to the module's peak power, inverters are operating on maximum efficiency with optimal power matching.

In this case the equation used for estimating PR was the following:

$$PR = n_{sys} / n_{PV,STC} = n_{PV,RRC} * n_{INV} * n_{residualsys} / n_{PV,STC} \quad \{59\}$$

n$_{sys}$: PV system efficiency

n$_{INV}$: inverter efficiency

n$_{residualsys}$: residual system efficiency (mismatch losses due to modules, cell soiling, ohmic losses regarding the DC installation)

PR$_{ST}$ is then calculated as shown below:

$$PR_{ST} = PR * (n_{PV,STC} / n_{PV,act}) * (n_{INV,opt} / n_{INV}) \rightarrow$$

$$PR_{ST} = n_{PV,RRC} * n_{INV,opt} * n_{residualsys} / n_{PV,act} \quad \{60\}$$

n$_{PV,act}$: actual efficiency based on mean actual peak power ratings,

n$_{INV,opt}$: highest annual inverter efficiency in case of optimal power matching between inverter & PV generator

$\mathbf{n_{INV}}$: efficiency of used inverter and power matching

Bad performance of a plant can be due to one or more of the following occurring problems:

- Constant partial shading

- Module strings in off circuit mode due to loose clamped connections in the junction box

- Bad maximum power voltage adaptation of inverter

On the other hand higher than usual efficiencies may be (over 79%) attributed to:

- unreliable data (electricity counters or from the solar integrators responsible)

- high quality series with unusually higher peak power than mean module type value

PR is strongly related to weather conditions. Low irradiance, low incidence angles and partial inverter loads in winter lead to low **PR** values. Higher values in March and October can be attributed to temperatures maintaining moderate values.
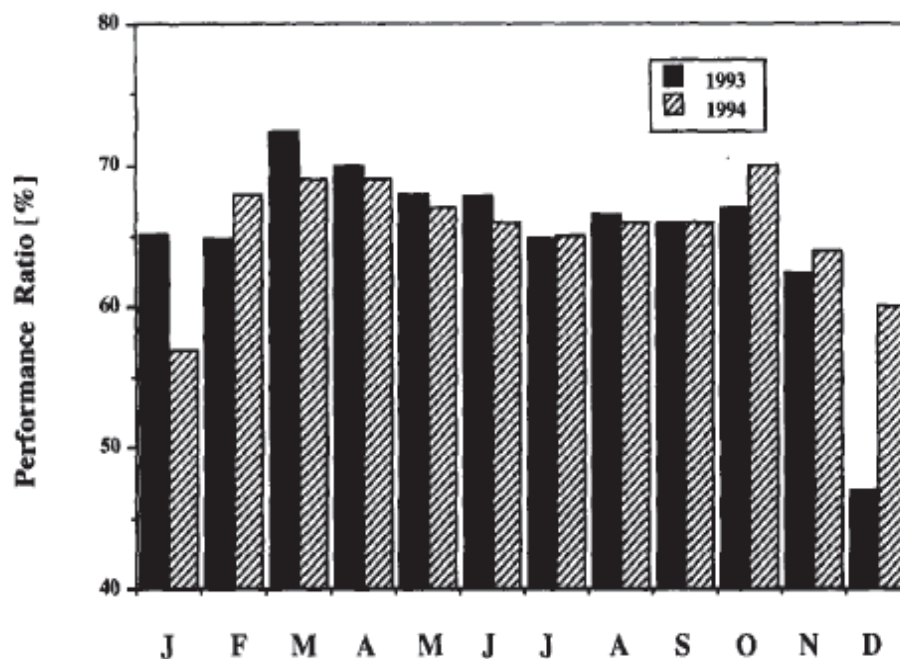

Figure 44: PR monthly average variation regarding systems in Germany for the year 1993 and 1994 [82]

4.5   Building integrated photovoltaic systems

Integrating photovoltaic systems in the building envelope seems to be one attractive method of reducing fossil fuel consumption in the building sector especially in sunnier climatic regions.

These systems are photovoltaic modules utilized additionally as construction materials. They can replace conventional roof tiles, wall materials, glazing membranes, skylights, shading devices or double façade external materials.

BIPVs have been increasingly incorporated into new buildings but constitute an effective alternative in case of retrofitting measures especially as far as building face lifting is concerned.

One main advantage is the fact that conventional materials are spared and no extra labor is required basically offsetting the cost of these installations. Apart from electricity generation BIPVs may support the heating and cooling demand of a building by utilizing the thermal gains of the panels.

Well-designed system architecture can make the best of the available solar energy. Thus electricity would be generated locally, hence avoiding distribution losses. Furthermore mounting photovoltaic cells on a building may reduce balance of system (BOS) costs. In this way roofs and other building construction surfaces could replace costs of ground mounting even if inclination angles may not always be ideal. PVs in fully integrated configurations could be part of the building structure (i.e. roof-wall tile). This would reduce construction costs apart from supporting a building's energy demand profile. This would challenge architects and building services engineers to develop know-how and techniques regarding building retrofits and new constructions.

However overheating of PV cells when installed on building surfaces is still an issue under consideration [71]. Furthermore building contractors are currently still confused regarding costing this newly introduced type of work resulting to PV suppliers having to introduce 'specialised' crews for fitting the systems which almost leads to double construction costs.

Most common forms of BIPV modules are:

Flat roofs

They are widely installed and are mainly constituted of flexible thin film cells.

BIPVs as pitched roofs

In this case modules function as roof tiles, or roofs constituted of solar shingles (incorporating flexible thin film technology) may replace Batten and seam metal roofing as well as 3-tab asphalt shingles. Roof lifespan is extended due to better protection of insulation from ultraviolet radiation and water degradation.

Facade construction materials

BIPVs can replace conventional materials or be installed as a second layer reinforcing a building cell. They are applicable in public buildings i.e. office complexes, production buildings, shopping centers, schools as well as private i.e. terraced houses.

Moderate temperatures can be maintained between the external PV and internal building façades in winter through wind protection and thermal exchanges between PV façade and air in the gap. On the other hand in summer the internal construction layers are protected from direct solar gains and excess heat can be dissipated through natural or mechanical ventilation from the gap to the environment. Systems integrated on building are consisted of various PV cell types, i.e. crystalline, micro-perforated amorphous transparent modules etc.

Glazing components

Image 1: PV skylight (NREL/ DOE)

Semitransparent or transparent modules may replace conventional glazings and expensive - sensitive reflective membranes in windows and skylights. Such systems with variable transparency levels may be applied in entrance halls, courtyards, parking plots and combine sun protection with financial gains.

Shading devices

BIPVs apart from protecting the building constructions from excess insolation (double facades) may be utilized as shading devices. These systems are now known as 'Shadow-voltaic systems'. They can be stationary or mobile programmed to track direct solar radiation for optimum energy yields or maintain comfort illumination levels in the building's interior (adequate daily insolation levels considering glare issues).

Image 2: BIPVs as shading devices on a commercial building in Athens (author's archive)

Past experience in Greece has stressed out the importance of choosing reliable companies when installing mobile systems. Software faults-incompatibilities-poor maintenance may result to these systems failing to deliver neither anticipated energy yields nor acceptable indoor luminance levels.

Image 3: Greek ministry of the environment-architect A. Tompazis (author's archive)

BIPVs as well as PV modules are manufactured using low iron tempered glass. Glazings can be constituted of simple glass /glass laminate or a complex isolation glass /glass laminate. Due to safety requirements concerning lamination PVB is usually preferred instead of EVA foil. Especially in case of transparent roofs PVB has been proven safe after decades of use in the automotive industry for laminated safety windscreen manufacturing.

4.6 Building integrated photovoltaic – Thermal systems

As already discussed PV cell efficiency is strongly related to temperature. Especially in cases of building integrated systems where heat is trapped into the structure (as modules rear is not exposed to ambient air) temperatures may rise to very high levels. This leads to considerable decrease of systems' performance (temperature rise decreases cell efficiency 0.2-0.5% / °C varying for different cell types as it is already mentioned).

Thus there has been considerable research delivered during the last decade concerning methods of cooling down cells and if possible utilizing the thermal energy for space heating. These systems' operation is based on passive or active heat exchange between air /liquid (circulated on the module's rear) and the module itself. These systems have been introduced as Building Integrated PhotoVoltaic – Thermal systems (BIPV-T).

Figure 45: actual BIPV-T system [87]

Typical PV collector efficiencies are roughly 4-7% regarding amorphous and 12-16% regarding crystalline PV cells. Apart from increasing PV efficiency by reducing cell temperatures PV-T /BIPV-T systems make use of the remaining 84-96% of incident solar energy thus providing additional thermal energy for water heating. Following are some methods of optimum utilisation of solar gains through conversion to electrical and thermal energy:

Several air-air systems have been researched:

- glass - glass photovoltaic modules with /without ducts for recovering heat (remaining solar radiation is absorbed by blackened surface after the air gap)

- glass - tedlar photovoltaic modules with /without ducts for recovering heat (remaining solar radiation is absorbed by the opaque tedlar leading to direct cell temperature increase)
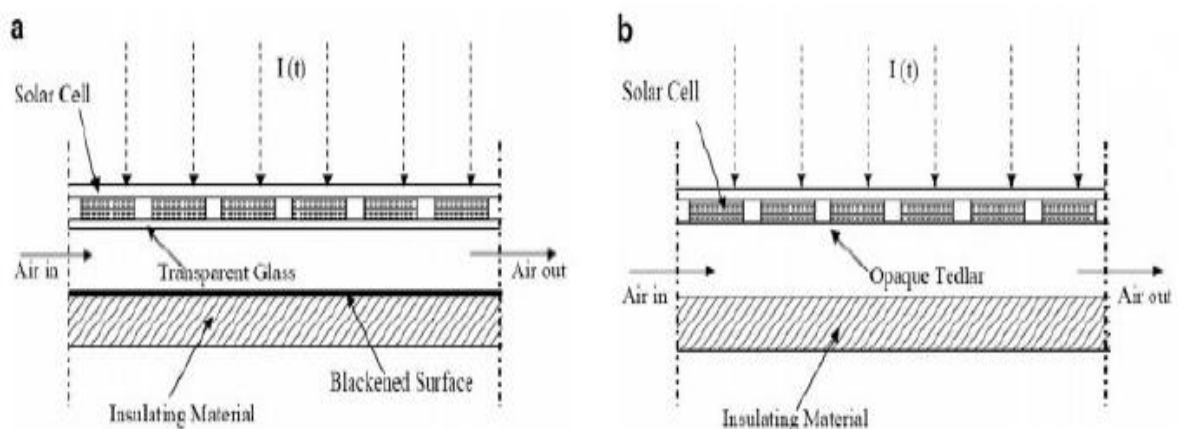
(a) Cut sectional view of glass to glass PV module with duct. (b) Cut sectional view of glass to tedlar PV module with duct.

Figure 46: 2 alternative PV-T technologies [88]

These systems can be installed on inclined roofs reducing considerably the heating demand in colder environments. BIPV-Ts can pre heat ambient air and work together with ventilated concrete slabs (thermal mass absorbing) for storing heat. This heat absorbed by thermal mass avoids overheating issues releasing heat gradually in evening hours. The whole configuration is illustrated in the following image:
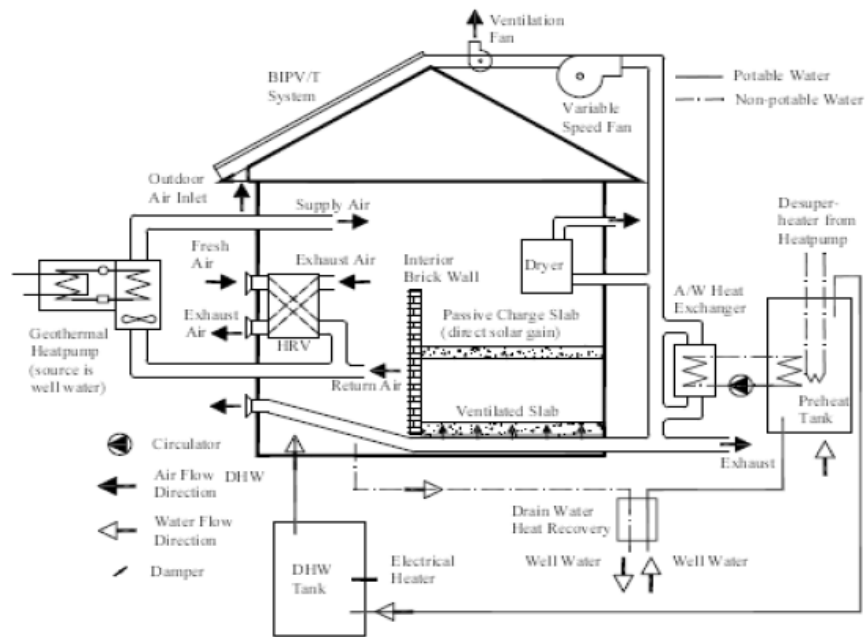

Figure 47: BIPV-T system transferring solar thermal gains to concrete slabs where it is stored for space heating [89]

· **Water systems**

Figure 48: PV-T alternative liquid cooling systems [90]

·

Although air cooled systems seem to be worth further research, liquids are generally more effective in absorbing surplus thermal loads.

Main advantages-disadvantages of PV-T systems

Concerning the main advantages of PV-T it is evident that such systems require less material in relation to PV and thermal collector systems when added up. Additionally, when fully integrated on rooftops or facades, PV-Ts lead to material reduction. Especially in the case of urban locations in highly populated areas (roof space is limited) such systems can exploit the available space most effectively. There is a significant increase of energy generated per m^2 as thermal is added to electrical supply.

However, PV-T thermal efficiency is lower compared to conventional solar collectors due to:

- part of the absorbed energy converted to electricity

- the absorption coefficient being smaller

- thermal losses becoming higher in order to maintain temperatures in which cell efficiency is at acceptable levels

If a glazed cover is attached to the structure, thermal efficiency would increase. That however would be on the expense of electricity generation due to higher cell temperatures and optical losses.

Furthermore there are some remaining issues i.e. reliability due to increased temperatures approaching stagnation levels. Cell efficiency decrease occurs especially when higher water temperatures are required (i.e. when connected to DHW systems).

Temperature inputs-outputs

The cooling effectiveness of water circulating and exchanging heat with PV cells is strongly related to its temperature. Systems operating in lower temperatures provide higher electricity outputs.

When considering conventional systems i.e. radiators there needs to be a golden line drawn between optimal operating PV and water output temperature levels. In this case a glazed PV-T is more appropriate including amorphous cells as their efficiencies are less temperature sensitive.

An interesting alternative regarding heat-electrical energy generation is BIPV-Ts connected to a Direct Solar Floor. This is a combined system ideal for optimum electrical generation as it operates at low temperatures (35°C). Controls function similarly as in conventional solar collector systems. Circulation is switched on or off according to temperatures of the collector output, floor loop return and domestic water tank.

In the case of combined systems a hybrid collector may be utilised for domestic hot water as well as for direct heating floor mass heating (no extra tank required).

BIPV-T systems considered can be exposed cells, cells covered with conventional glass or low-e glass. Refrigerant liquids are capable of reducing cell temperatures. However only exposed cells accomplish a higher efficiency (~10%) when compared to conventional systems with covered cell efficiency significantly reduced.
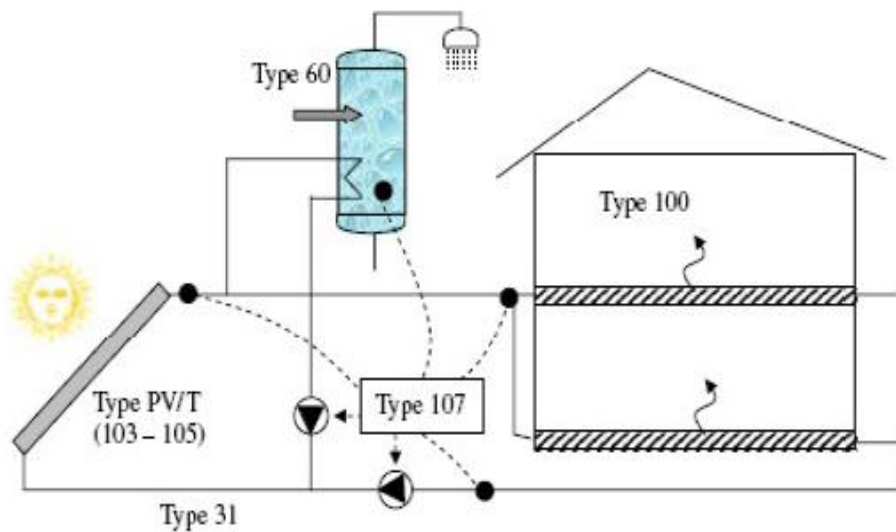
Figure 49: hybrid system incorporating PV-T connected with heated floor slabs [90]

4.7   Environmental performance - Carbon emissions savings

The use of PV as a replacement for fossil fuel – based electricity generation has serious environmental benefits. PV systems don't make noise and are friendly towards the environment. They don't produce greenhouse gases or any other kind of gases while they generate electricity. A typical PV installation will save about 350 kg/kWp of CO_2 emissions [26] helping alleviate global warming.

Figure 50: Greenshouse gases (grams per kWh of CO_2 equivalent)

There are also other key indicators of the environmental performance such as the enegy returned on energy invested (EROEI) and the energy payback time. The energy payback time can de determined from a life cycle analysis and is the time interval required in order to produce an amount of ener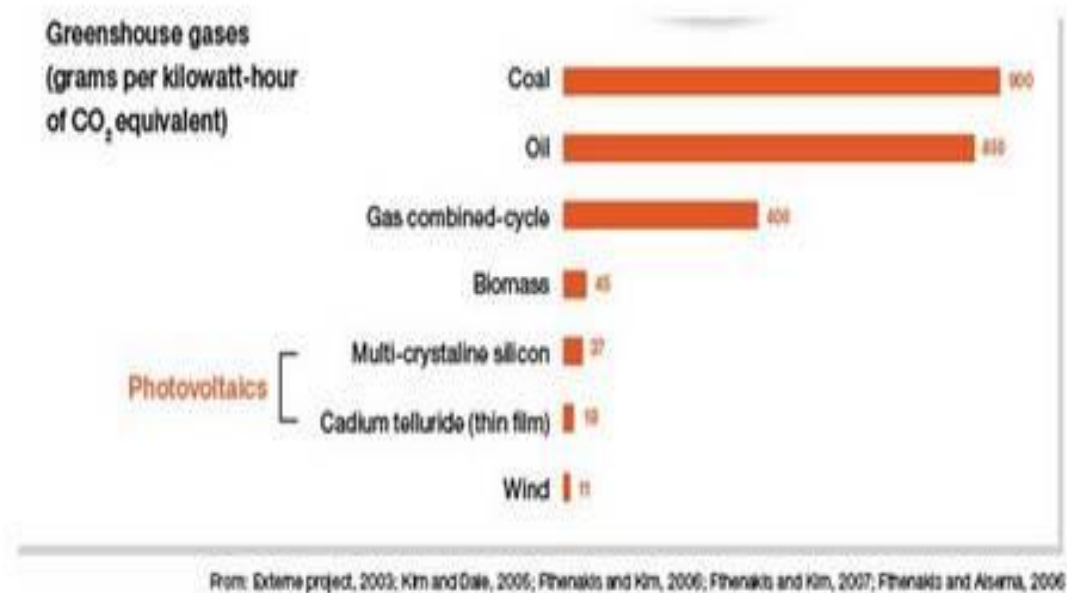gy equal to that consumed during the PV production procedure. EROEI is a quite similar indicator defined as the ratio of the PV generated electricity divided by the energy required in order to "build and maintain" PV. The energy payback time varies from 1.5 to 3.5 years depending upon the PV type – technology.

4.8   Financial aspects and the PV market

Energy generation from PV cells has started to penetrate the market especially in countries with clear and stable policy commitments. Three incentive mechanisms are designed and usually used in combination so as to encourage the adoption of renewable energy systems and provide the essential motivation for increasing the installed PV output;

- ✓ Investment subsidies: part of the installation cost of the PV system is refunded by the government

- ✓ Feed-In Tariffs (FIT): the regional/national electricity utility is obliged to buy the renewable electricity generated by PV at a specific fixed price through a

long-term contract (usually 15-25 years). The price/kWh under FIT is always higher than the price of the regional electricity utility.

✓ Renewable Energy Certificates (RES)

Germany is a good example of the perspectives of PV technology expanding even in a climatic region with very moderate solar energy resources. Other European countries have introduced similar policies (i.e. Greece, Spain, the Czech Republic and Italy) which have been less popular in spite of the more promising climatic conditions. This can only be due to the lack of adequate and clear knowledge /understanding of PV potential.

In 2010, new feed-in tariffs (which are substantially higher than the ones of 2009) have been introduced in **France**. The tariff for fully integrated BIPVs (constituting part of the roof construction) is now 0.58 €/kWh regarding occupied dwellings and health care buildings and 0.50 €/kWh for other buildings. Feed-in tariffs for partially integrated "simplified BIPV systems" (PV mounted on top of the roof) was decreased by 24%, to 0.42€/kWh from 0.55€/kWh [91].

In UK, grants presented by the government for small scale PV system (0.5 kWp – 5kWp) are [92]:

✓ top of roof installed PV systems → smallest scenario between 50% of the total eligible costs or £3000/kWp

✓ for roof-integrated systems → smallest scenario between 50% of the total eligible costs or £4250/kWp

In addition to the grants, the feed-in tariffs for PV systems (contract for 25 years) in the UK (20th of October 2010) are [93]:

✓ new, up to 4kW → 36.1 p/kWh

✓ retrofit, up to 4kW → 41.3 p/KWh

An additional 3p per kWh is paid for each unit exported back to the electricity grid. These feet-in tariffs will be reviewed in 2013 [93].

In Greece, the feed-in tariffs are one of the larger all around Europe, equal to 0.55€/kWh concerning PV installed in dwellings guaranteed for 25 years. However, in

August 2010, the Greek Parliament modified the feed-in tariff laws. For systems less than 100 kW the new feed-in tariffs for the mainland and the Greek islands are 0.45€/kWh and 0.50€/kWh respectively. These feed-in tariffs are now guaranteed for 20 years. In addition to the feed in tariffs, there are grants up to 40% of the cost for installations that are up to 100,000€, but roof-top projects won't be eligible for a grant [94].

The main factors which determine the financial performance of a PV system are the cost per unit of installed peak power, the operational cost (including the capital cost), the estimated lifetime and solar energy reaching the earth's surface.

System costs

It is very interesting to understand the cost distribution between system components and decide on design aspects' special weights regarding expenditure. The annual energy cost for a system is related to installation costs, maintenance costs, a presumed lifespan (usually a very modest 20 year) and interest rate (UK: 6%). As far as the total capital installation cost, this could be split between PV modules, array framework, inverters, balance of system (BOS), design/ installation costs, meter and value added Tax (VAT UK: 17.5%). The presumed lifespan of 20 years is quite moderate; usually PV systems are expected to last about 30 years, being very reliable and requiring minimal maintenance as there are no moving parts. However, the replacement costs should also be considered, since the power electronics - inverter and the storage system – batteries may have to be replaced during the period of 25-30 years, usually every 10 years. The thin film solar cells require higher maintenance costs than crystalline because they are more sensitive concerning degradation.

PV modules costs constitute 50% to 60% of those of the whole installation. As a result, the higher the installed power is, the lower the cost/kWp. A 1kWp PV system has an indicative cost of 6,000 to 7,000 £/kWp, whereas a 5kWp one has almost 5,000£/kWp. When our system consists of fully integrated BIPVs the cost augments to 8,000-9,000 £/kWp [95] or even more, but this increase can be outweighed by the cost of the building materials which are replaced. In addition, a 1kWp to 5kWp installed PV system, depending upon its nominal power output and the location, covers between 25% - 100% of the 3,000-4,000 kWh required by a typical household [96].

The PV market has expanded dramatically these last years due to the augmenting demand of RES (Renewable Energy Systems). The crystalline PV share almost the 90% of the existing market. The remaining 10% corresponds to the thin film ones, as you can notice from the following figure.
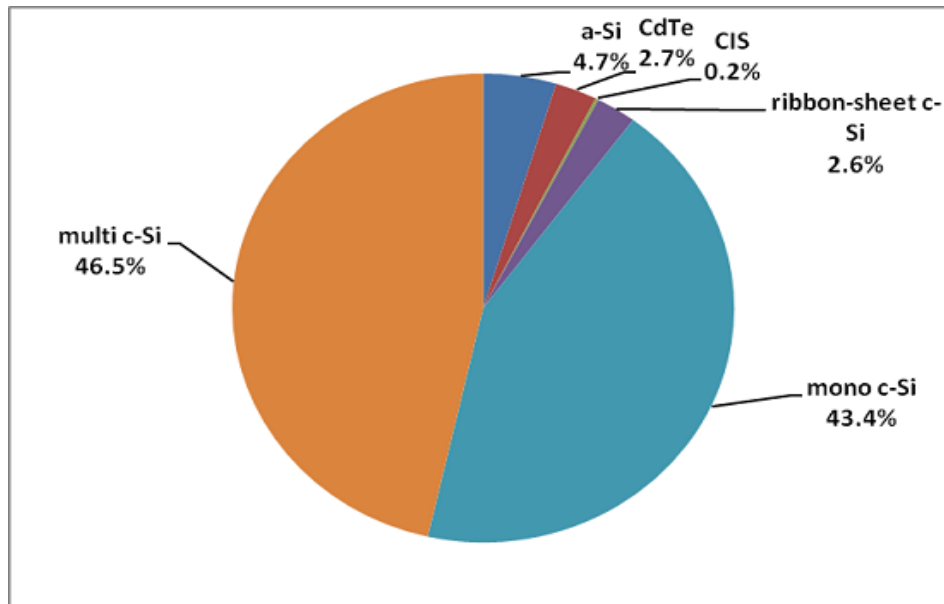

Figure 51: distribution of the PV market among the different technologies [97]

PV are seen as an expensive solution compared to other types of RES. The PV manufacturers aim to decrease their cost and improve their efficiency. Generally the higher the PV demand, the bigger the decrease in their retail price. Nowadays, the lowest prices, not including taxes, are; 1.68 €/Wp for monocrystalline PV, 1.39 €/Wp for polycrystalline and 1.25 €/Wp for a 130Wp thin-film solar panel. Therefore, the specified target of 1 €/Wp concerning thin-film and polycrystalline PV has become quite realistic [98]. The biggest driver of the lower costs is the better efficiency.

Unfortunately it seems that in practise until this day house contractors seem to be reluctant in trading new types of work as may be the case of a fully building integrated photovoltaic installation in a conventional roof structure (meaning PV suppliers might be still required to make the installation and so roof labour costs may be paid twice) [71]. Even so, costs of such systems tend to be significantly less than those of PV systems installed on top of the roof where no material savings occur.

5 Simulation Tools

5.1 General – former methods in literature

A generally accepted equation which has been introduced in chapter 4.4.3 Array inclination regarding energy generated by PV systems in an annual basis is the following:

$$E = P_k * PR * G$$

(in case neither PV conversion efficiency nor module surface area are available)

Based on the SV (sophisticated verification) method (group in TUAT), PV system operation was cut down to several types of loss factors i.e. shading, maximum power point (MPP) mismatches etc [99]. Otani and Sakuta [34] have made some estimations based on statistical processing of such factor values from a large number of systems installed on residential buildings in Japan. Their method is indicated by the following equation:

$$Y_f = K * Y_r \quad \{56\}$$

- ➢ Y_r : reference yield

- ➢ Y_f : final yield

- ➢ K: product of several efficiency factors relative to the following loss factors

$$K = K_{low} * K_{const} * K_H * K_{PT} * K_C \quad \{57\}$$

- ✓ K_{low} : Low irradiance loss factor (non linear),

$$K_{low} = 1 - e^{-Y_r/\beta}, \beta=0.01 \quad \{58\}$$

- ✓ K_H : Shading loss factor (usually set at 1.0 apart from when the SV method detects shading in which case must be altered accordingly)

- ✓ K_{PT} : Temperature loss factor

$$K_{PT} = 1 - \alpha_{pmax} * (T_c - T_s) \quad \{59\}$$

α_{pmax} : Temperature coefficient, typically 0.0020 for amorphous and 0.0041 for crystalline silicon cells

T_c: module temperature in reality

T_s: module temperature at STC

✓ K_C: Conversion loss factor (determined by averaged monitored data-for shorter time periods conversion efficiency curves can be applied by following a Box Lucas 2-exponential function model $n_c = b/(b-\alpha)*(e^{-\alpha EA} - e^{-bEA})$)

✓ K_{const}: Constant other loss factor (product of factors shown in the following table)

Type of loss factor	Value
Contamination loss factor	0.90
Spectral mismatch loss factor	0.97
Array unbalance loss factor	0.997
Wiring loss factor	0.98
Load mismatch loss factor.	0.94
Constant other loss factor K_{const}	0.75

Table 11: Factors based on JQA systems (crystalline cells) [34]

5.2 Merit

There are numerous software programs involved with predicting PV output energy generation. One considered by Omer for the comparison of the effectiveness of such an investment in a domestic and an educational building in Nottingham is PVSYST3. (This program estimated the PV output to be 3-6 times more than the actual which was explained partially due to the over sizing of the inverter in the one examined case study and the fact that the inverter was failing to track the maximum power point concerning the array) [71].

Another software tool is Merit. It has been created in order to investigate the demand and supply matching. Matching the demand for and supply of energy provides the opportunity to identify the strategies for the integration of Renewable Energy Systems into the generation portfolio. It can be used by a wide range of users for various applications, since it isn't designed only for specialists. It is friendly towards

individuals without prior knowledge of the available different technologies. Therefore, the potential users include engineers, private power developers, energy managers and consultants, architects etc.

Merit enables the selection of climate files together with the days of interest. The applied demand profile can be specified, either by choosing from a profile database or by importing a demand profile from an external source. Having thus defined the demand, the renewable supply technology parameters can be specified based upon manufacturers' data. Supply simulation is then undertaken according to these parameters. Also, a variety of RE supply technologies could be selected from the available databases and if desired a range of auxiliary technologies. It supports PV data (apart from others) and therefore can evaluate PV performance under specific conditions - parameters. Furthermore, Merit contains a supply search engine in order to identify the optimum combination in terms of the selected criteria.
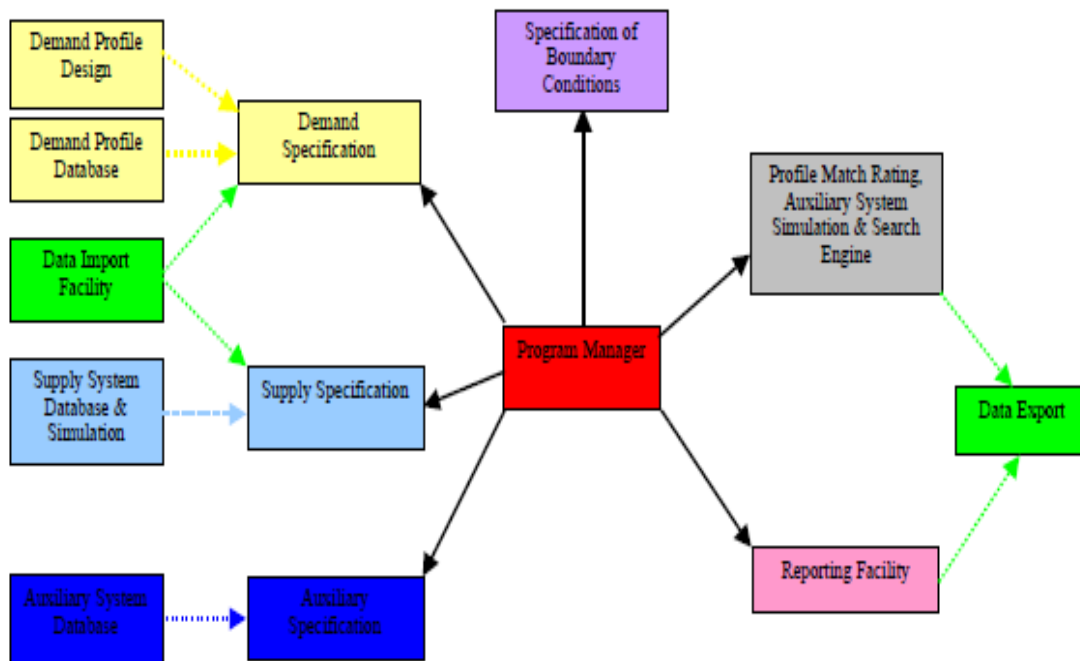

Figure 52: principal components of Merit [100]

5.3   Project method - model description (Excel)

The key performance parameters concerning a PV system model are:

- Insolation

- Cell temperature

- Array DC output current & voltage

- Inverter AC output current & voltage

- Power – energy delivered to AC lines

Quantities estimated through such an excel tool can be:

- PV array yield under specified site conditions

- Inverter efficiency

- System efficiency

- Energy conversion efficiency

The accuracy of such a model is based on the specified variables introduced:

- Climate data files (solar, ambient temperature, wind etc)

- Soiling factors

- Shading factors (trees, neighbouring structures, etc)

- PV Specifications

- Inclination – orientation of PV cells

- Snow cover

- Ground reflectance

- Array mismatch

- Inverter efficiency

- Distribution losses (wiring losses)

6   Case study – Developed tool

Part of the purpose of this project is the evaluation and comparison of the developed excel tool as well as Merit with actual climatic and PV system output data from an actual case study.

The case study used was a project named "Bradan Road Sheltered Housing Complex, Troon". The aims and objectives of this project were the following:

- Design and install a 28.8 kWp PV system and monitoring equipment

- Monitor PV systems

- Ensure quality of installation and deal with any faults of the systems during monitoring period

- Undertake project work in line with the objectives of the field trial

- Provide a highly visible demonstration of sustainable energy production

- Reduce fuel bills and achieve a target of affordable warmth for a vulnerable group

6.1   Residential buildings

6.1.1 Location

The installation is located at Bradan road sheltered housing complex in the sea side town of Troon, South Ayrshire (Grid location NS 315 310). The site is fairly exposed, meaning it could be a decent testing location for the panels.

Image 4: case study roof tops (Google earth)

6.1.2 Building description

The case study constitutes of 31 flats spread out in 7 residential semi detached and one detached blocks. The blocks are two storey and contain 4 flats each. The flats are all single bedroom flats, built in the 60s, with electric night storage heating systems. The roofs are oriented between approximately 17°-34° east of south.

PV cells were retrofitted onto the existing roofs. At the same time with the PV installation there was ongoing energy efficiency refurbishment work within the properties. The majority already were insulated with 200mm in the loft as well as the wall cavities.

Image 5: PV system installed in Troon (author's archive)

Flat Demand profiles

The council was keen in to provide affordable warmth for all tenants. Single bedroom properties with one occupant were the hardest to achieve this in. Heating these flats with electricity or alternative means could make the difference between a single occupant living with affordable warmth or living in fuel poverty.

The expected generated electricity from the PV system was 750 kWh/annum for each flat. This generated electricity covered first the flat's energy demand and then sold the surplus to the grid.

The dwelling's actual energy demand profile can be estimated by data acquired from the sum of energy input from the grid and the inverter energy output from the PV system not absorbed by the grid in order to create a similar profile required by Merit to produce most accurate results for comparison.
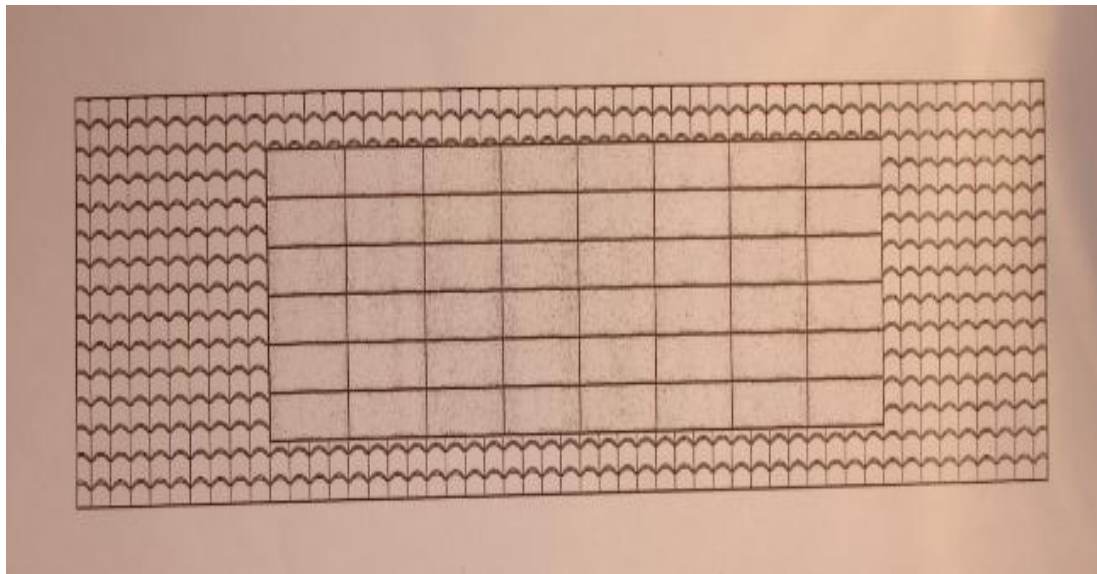
6.2   PV system

Image 6: draft deployment for each 4 flat block (PV array comprises 48*80W modules mounted as one single array at the roof centre split to 4 sub arrays of 12 module with 960Wp each)

Beginning with the panels applied, these were BP380. BP 380 modules consist of 36 multi crystalline silicon cells in series with a nominal power of 80W. The BP 380 module uses cells with antireflective SiN coating. The cells are laminated between sheets of ethylene vinyl acetate (EVA) and high-transmissivity low-iron 3mm

tempered glass. The characteristics of the applied used module are shown in the table below.

Nominal Power (P_{nom})	80W
Tolerance	+/- 5%
Module Efficiency	12.6%
Nominal Voltage	12V
Voltage at MPP (V_{mpp})	17.6V
Current at MPP (I_{mpp})	4.6A
Short circuit current (I_{sc})	4.8A
Open circuit voltage (V_{oc})	22.1V
Temperature coefficient of I_{sc}	(0.065 ± 0.015)%/K
Temperature coefficient of V_{oc}	$-(80\pm10)$mV/K
Temperature coefficient of P	$-(0.5\pm0.05)$%/K
NOCT (Air 20°C, Sun 800W/m², wind	47±2°C
Maximum series fuse rating	15A
Weight (kg)	7.7
Warranty	90% power output over 12 years
	80% power output over 25 years

Table 12: characteristics of the BP 380 PV module

Each flat is supplied 12 PV modules, thus the nominal array power is 960Wp. As already mentioned, the total capacity for the project was 28.8 kWp.

The modules were mounted above the roof on a steel / aluminium support frame at an angle of 45° from horizontal. Each array was connected to an SMA AWR850 inverter mounted in the loft space right behind or adjacent to the PV array. The technical characteristics of the inverter are

Input voltage range V_{PV}	125V – 250V
Output voltage range V_{AC}	196V – 253V
Maximum input current I_{PVmax}	8.0 A
Nominal output power P_{Acnom}	850W
Frequency range f_{AC}	49.8 – 50.2Hz
Weight	approx. 18kg

Table 13: characteristics of the SMA AWR850 inverter

The Inverter Power Ratio **IPRT** is equal to 850W / 960W=0.8854=**88.54%,** thus it is well designed since it is between the limits of 70% - 90% for the UK regions (chapter 4.4.6 Inverter efficiency – system matching).The inverter was then connected to an MCB in each flat's consumer unit. A kW/kWh meter was installed in each property to display the PV array output as per DTI specifications.

Monitoring would be managed through SMA Sunny control plus data loggers. Eight were utilised, one for each block of four flats. Data collection from the SBC loggers was managed directly via a PC link or remotely via a modem. Each house was equipped with separate import and export meters, connected to the local logger.
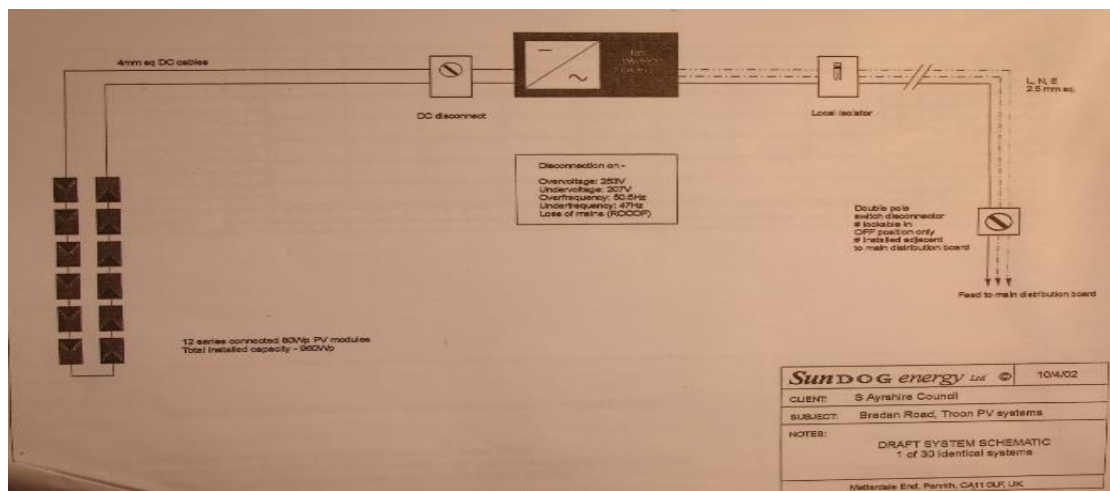

Image 7: Amended single line schematic of the format

Process of the installation

The installation involved removing a number of existing roof tiles and anchoring the roofing system in the existing roof structure. A risk assessment has been followed through regarding the roof loading by the structural engineer in order to be eligible for a design certificate.

Key issues dealt with during installation

The first issue arisen was the condition of the existing roofs where the PV arrays where to be installed. Whilst the overall roof condition was acceptable and adequate for the installation the contractor highlighted some other areas that required repair. The repairs were dealt with by a specialist roofing contractor whilst the scaffolding was around the building. This avoided roofing contractors having to access the roof in the near future and endangering the newly installed PV panels. Minor repairs were also performed by the contractor mostly replacing cracked or broken tiles.

The second issue was lack of availability of metering equipment. After meetings with all parties involved, tariff costs, meter locations, timescale etc were determined.

Monitoring system

- External sensors were fitted during the roofing works while scaffolding was in place. Specifically this included array temperature sensor fitted to the rear of a module, while array fitting was progressing.

- Internal sensors were limited to the import / export meters.

- Data loggers were installed and connected to the sensors and inverters during the installation process.

- Data cabling was installed in the same time with other AC / DC cables were laid.

- Eight BT lines were installed, one in each loft space. These were linked to the eight loggers via modem.

Project Financing

Funding of the PV modules for the first 25 flats was requested from the DTI with the remaining 5 to be paid for by the council.

The total cost of the project was £7.55/Watt.

6.3 Actual data output - Statistical analysis

Data have been generated by pyranometers, thermometers regarding climate data. Power ratings are also available regarding energy generated and utilised or exported to the grid as explained bellow beginning from 1st August 2003 for a 2 year period:

Climatic data

- total horizontal solar radiation

- total solar radiation on inclined surface (array)

via a calibrated silicon photocell pyranometer (one horizontal and three array plane sensor).

- ambient temperature via a PRT probe fitted with a radiation shield (two sensors on the site)

- PV module temperature via PRT probes (one sensor per block)

Power ratings

- array power DC output

- inverter power AC output inverter via a data signal from the SMA SWR850 inverters

- Electricity import / export was measured via pulse output kWh meters (NB additional to any electricity company meter – 60 total)

- AC output of each inverter was displayed via a kW/kWh meter mounted so as to be visible to the house occupant just to keep him informed.

Data processing with excel

The measured data, from August 2004 until July 2005 with 5min time step intervals for the 31 flats, were provided to the university as CSV (Comma Separated Values) files. The aim was to compare power output results between calculated and on site measurements. Thus it was essential to convert the input data into a format compatible with MERIT or any other estimation method.

First of all, the comma separated values were placed into columns. The horizontal and the array plane solar radiation measurements from the pyranometer had some negative values especially during night time. In reality, it is impossible to measure negative values related to solar radiation, thus a zero value was introduced whenever there was a negative. Merit requires hourly input data, thus the 5min data was converted into hourly. Then hourly output data were produced through averaging or summing the related 5min logged parameters. Meaning that the average was calculated for; the horizontal and the array plane solar radiation since these parameters are related to power (W/m^2) as well as for the ambient and the array temperature. Finally the rest of the parameters representing energy in Wh (DC output from the PV array, AC output from the inverter, electricity import from the grid, electricity export to the grid) were summed up. The above procedure was executed for all the 31 flats.

6.4 Graphical comparison of measured – calculated parameters

Data was provided concerning all 31 flats of the "Bradan Road Sheltered Housing Complex, Troon" project. Due to the volume of this data, the results from the Excel tool and Merit were compared only for the flat A in the 54, Bradan road. The assumption was that the conclusions from these comparisons would be indicative also regarding the rest of the flats. In addition, despite the fact that an analysis for the whole year was undertaken, the results only for a winter and summer week are demonstrated. This was done in order to achieve a higher resolution demonstration, taking also into account that PV perform differently in winter and in summer because of the different climatic conditions.

The site coordinates for Troon are; longitude l = 55°32'36" North and latitude L = 4°39'50" West. The measured provided data concerning solar radiation were; total horizontal solar radiation and total solar radiation on the inclined array surface. The PV for the flat A, 54 Bradan Road, were installed at an angle of 45° from the horizontal and the roof is orientated 17° east of south. In order to introduce the solar radiation data into MERIT and also apply the appropriate equations for evaluating the PV performance, the solar radiation should be divided into direct and diffuse horizontal. Also direct normal should be calculated.

For achieving that, the clearness index K_t should be identified through the equations in the chapter 3.3 Sky clearance index that make also use of the equations for the solar angles from the chapter 3.1 General solar angles. Having estimated the clearness index K_t, the ratio of the diffuse to the global horizontal equation can be calculated via either the Orgils and Holland correlation {21} or the Erbs et al. correlation {22}. Both the {21} and the {22} were estimated, but the decision was to utilize the Erbs et al. from now on. Having evaluated the diffuse horizontal radiation, the direct solar horizontal was calculated simply by deducting the diffuse component from the measured total solar radiation. Since the diffuse and the direct components for the total horizontal were known, the equations from the chapter 3.2 Diffuse – Direct radiation (that make use of the solar angles from the chapter 3.1 General solar angles) were applied in order to calculate the global solar radiation at the tilt angle of 45° with surface azimuth angle γ=-17° and the direct normal. The following graphs show the

measured and the calculated solar radiation (through the excel tool) on the inclined solar array for a winter and a summer week.
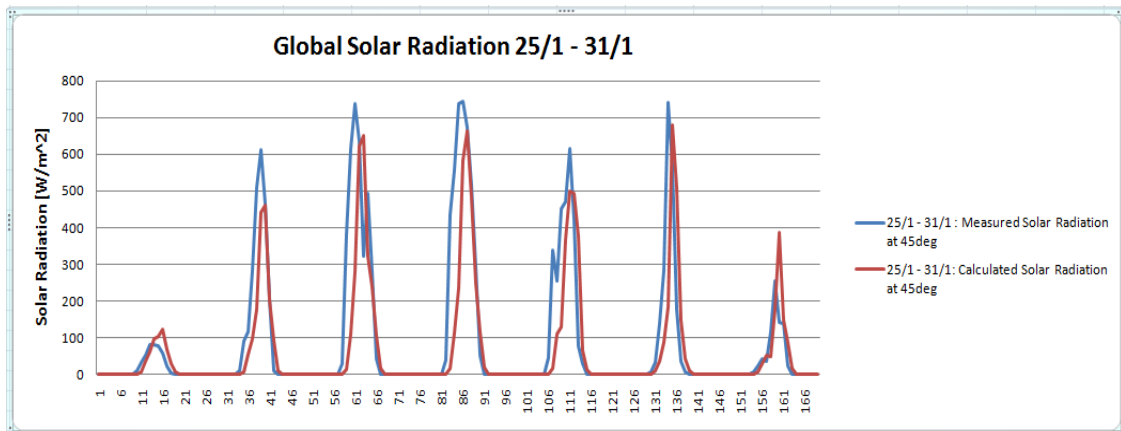

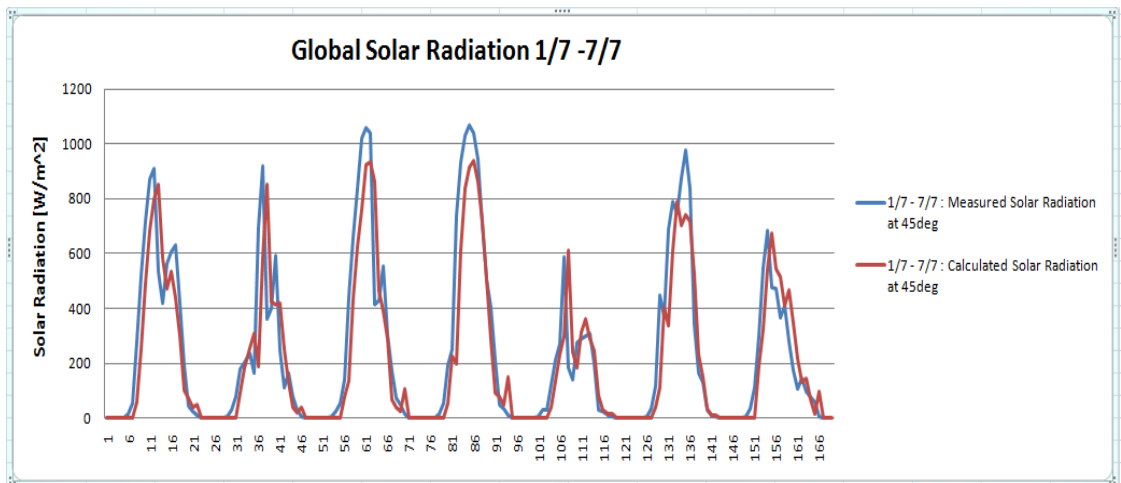**Figure 53**: measured and calculated global solar radiation for a winter week

Figure 54: measured and calculated global solar radiation for a summer week

The difference between the calculated and the measured solar radiation is quite acceptable both during the winter and the summer week. The calculated is lower than the measured especially regarding the peak values, but its shape follows well the measured one. During the winter week, solar radiation takes shorter values than during summer, while the peaks are observed at noon both in winter and summer. Also solar radiation is noticed for a shorter time interval (between 7a.m and 5p.m) during winter, while in the summer solar radiation was incident on the PV array from about 6a.m until 9p.m. Therefore, the amount of solar radiation is much higher in summer than in winter

Then, the target was to compare the measured T_{array} with 2 equations that can evaluate the temperature of a PV array. These two equations are the {39} and the {41} that

were analysed in the chapter 4.4.4 PV temperature influence on cell performance and more specifically in the sub-chapter Estimating cell temperature. The equation {39} will be referred from now on as the simple and the {41} as the complex. In order to calculate the T_{array} through the complex equation {41} the heat exchange coefficient U_{PV} must be estimated. The equations for estimating U_{PV} ({50}, {52}, {53}) were presented in the same chapter 4.4.4 in the sub-chapter Wind related convection heat transfer coefficient. These equations assume convection at both front and rear surfaces of the panels, since an air gap between the PV's rear surface and the dwelling's roof exists. The following graphs show these equations for the heat exchange coefficient for a winter and a summer week.
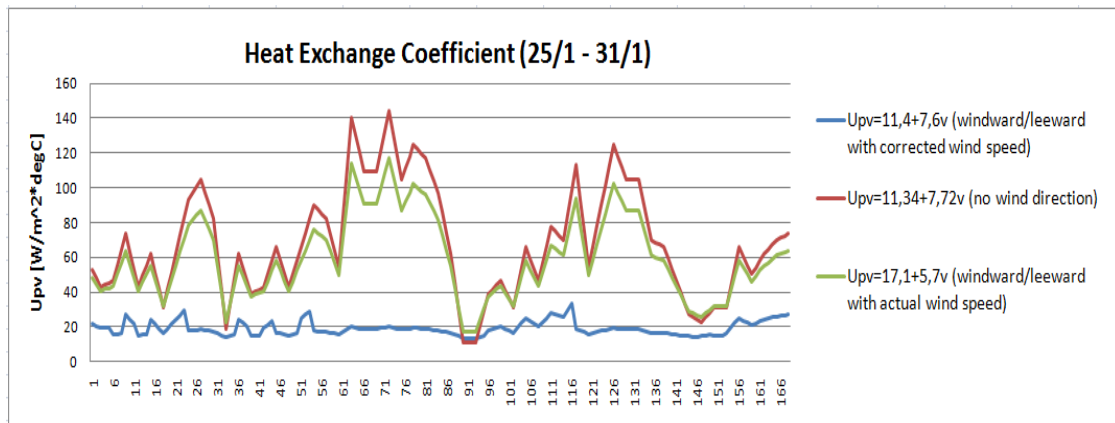

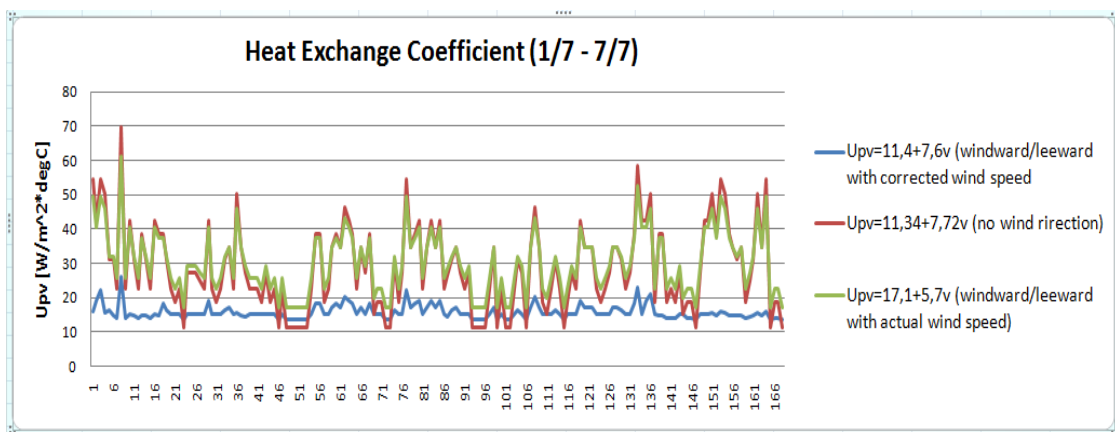**Figure 55**: Heat exchange coefficient U_{PV} for a winter week

Figure 56: Heat exchange coefficient U_{PV} for a summer week

From the above graphs, we notice that equation {53} (using corrected wind speed) - blue colour in the graphs- gives a U_{PV} that remains almost constant, thus equations {50} – red colour in the graphs - and {52} – green colour in the graph- are better because they represent a fluctuation which is logical for the U_{PV}. From the equations {50} and {52}, the {52} was selected since it takes into consideration also the wind

direction apart from the wind speed. Therefore, the {52} will be used in order to estimate the T_{array} from the complex equation {41}.

Having estimated the U_{PV}, the temperature of the PV array (T_{array}) can be calculated through the complex equation {41}. In order to estimate the Tarray either by the simple equation {39} or the complex equation {41} the solar radiation must be used. We have either the measured solar radiation on the inclined PV array or the calculated. Therefore, there were 4 different T_{array} regarding the different used parameters:

- T_{array} using the complex equation {41} and the measured solar radiation

- T_{array} using the simple equation {39} and the measured solar radiation

- T_{array} using the complex equation {41} and the calculated solar radiation

- T_{array} using the simple equation {39} and the calculated solar radiation

These 4 different T_{array} were plotted in the following graphs also with the:

- Ambient temperature

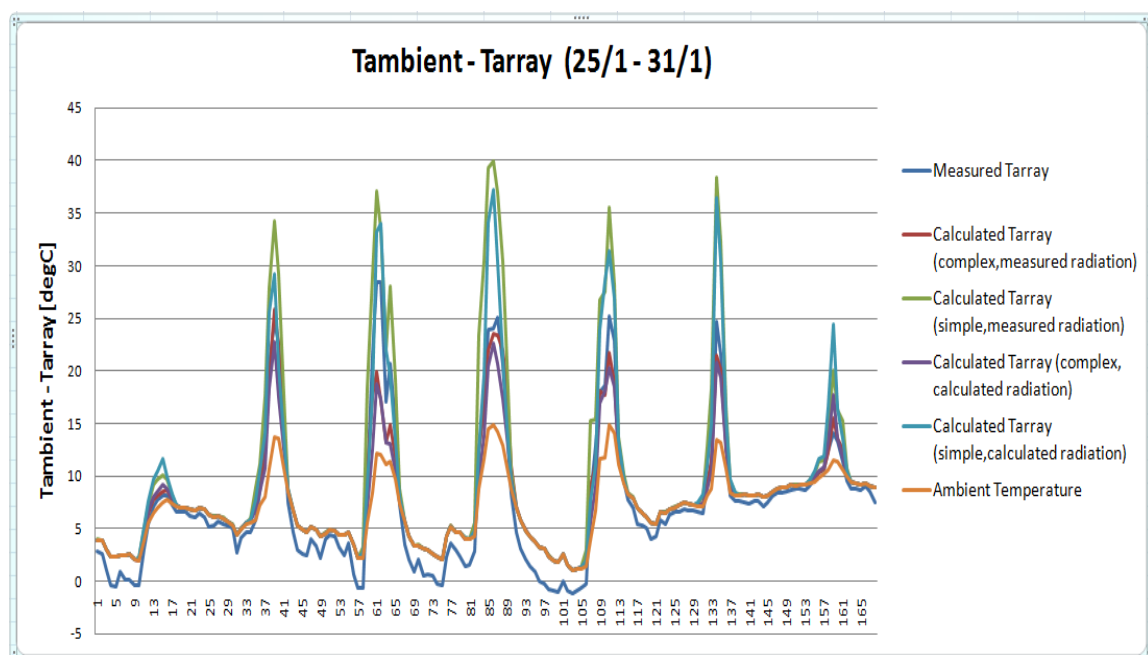- Measured T_{array} by the installed instrument

for a winter and a summer week.

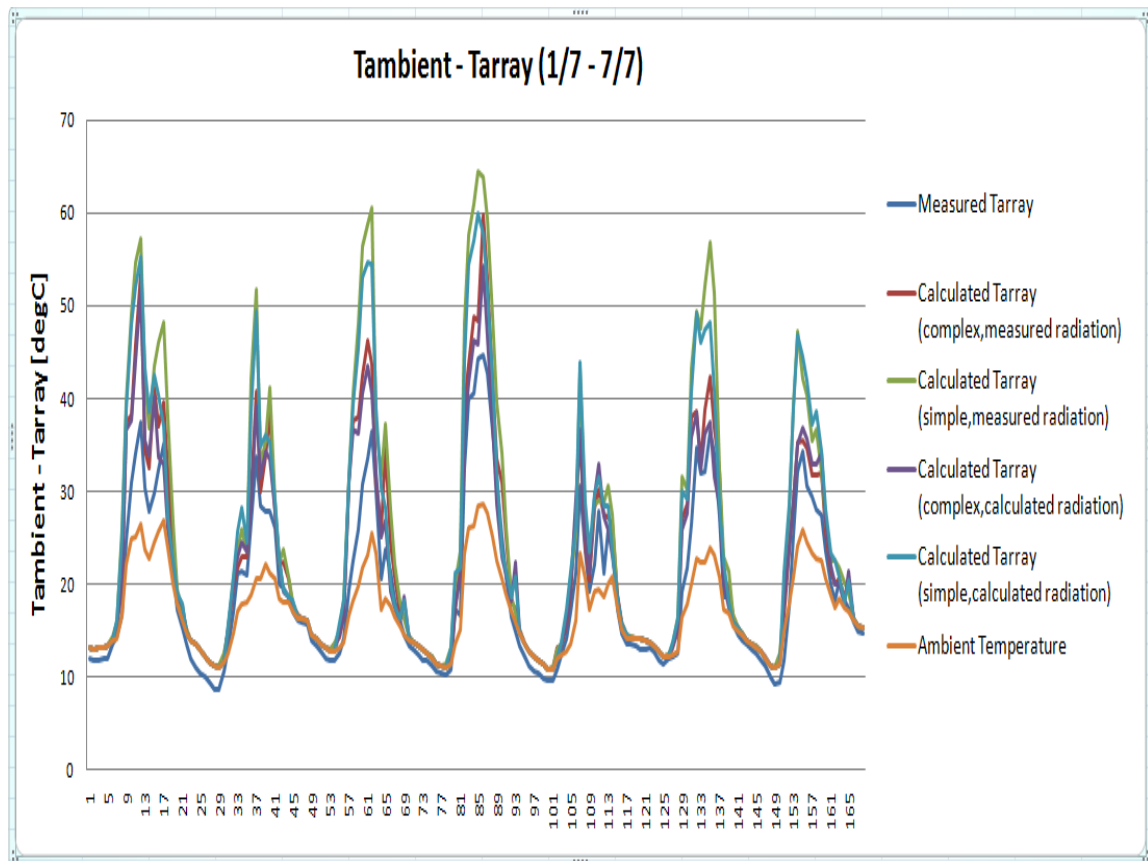**Figure 57**: $T_{ambient}$ and T_{array} for a winter week

Figure 58: $T_{ambient}$ and T_{array} for a summer week

Taking a closer look in the above graphs it seems evident that:

- During daytime the measured T_{array} is about 10°C greater than the ambient temperature during the winter week and about 15°C during the summer week. This difference is very logical and expected.

- During night, both during winter and summer the measured T_{array} is slightly less than the ambient temperature T_a by 1-2°C.

- The calculated Tarray based upon the simple equation {39} and either the measured or the calculated solar radiation takes values that are much greater than the measured Tarray especially at noon (peak value).

- In contrast, the calculated T_{array} using the complex equation and either the measured or the calculated radiation, provides results that are very similar or even sometimes the same with the measured T_{array}, especially for the winter week.

- However, during the summer week, the T_{array} using the complex equation provides values that were sometimes about 5°C greater than the measured, especially at noon peaks but still the results were much better than using the simple equation.

- There is a noticeable deviation (1-2°C higher during summer and 2-3°C higher during winter) between estimated and measured T_{array} during night. This may be attributed to the fact that radiated exchanges related to the neighbour surfaces and the sky dome were neglected.

Then, the efficiency of the applied PV array was estimated through the equation {38} from the chapter 4.4.4 PV temperature on cell performance taking into consideration the above mentioned T_{array} and the incident solar radiation. The absorbed energy by the PV array due to the incident solar radiation is converted into electricity and thermal losses from the array to the surrounding environment.

In order to estimate the power output from the PV array we made used of the equation {40}, $\mathbf{n_{array}*A_{array}*I_{array}}$. Thus the PV array output was estimated by multiplying the calculated array's efficiency with its surface area and the total solar radiation incident on its surface. It was mentioned that efficiency depends upon the array's temperature and that the complex equation {41} was chosen in order to evaluate this temperature. Therefore, 4 different PV array output exist concerning the different used parameters:

- PV array output estimated by using the measured radiation and the complex calculated Tarray

- PV array output estimated by using the calculated radiation and the complex calculated Tarray

- PV array output estimated by using the measured radiation and the measured Tarray

- Measured PV array output by the installed instrument

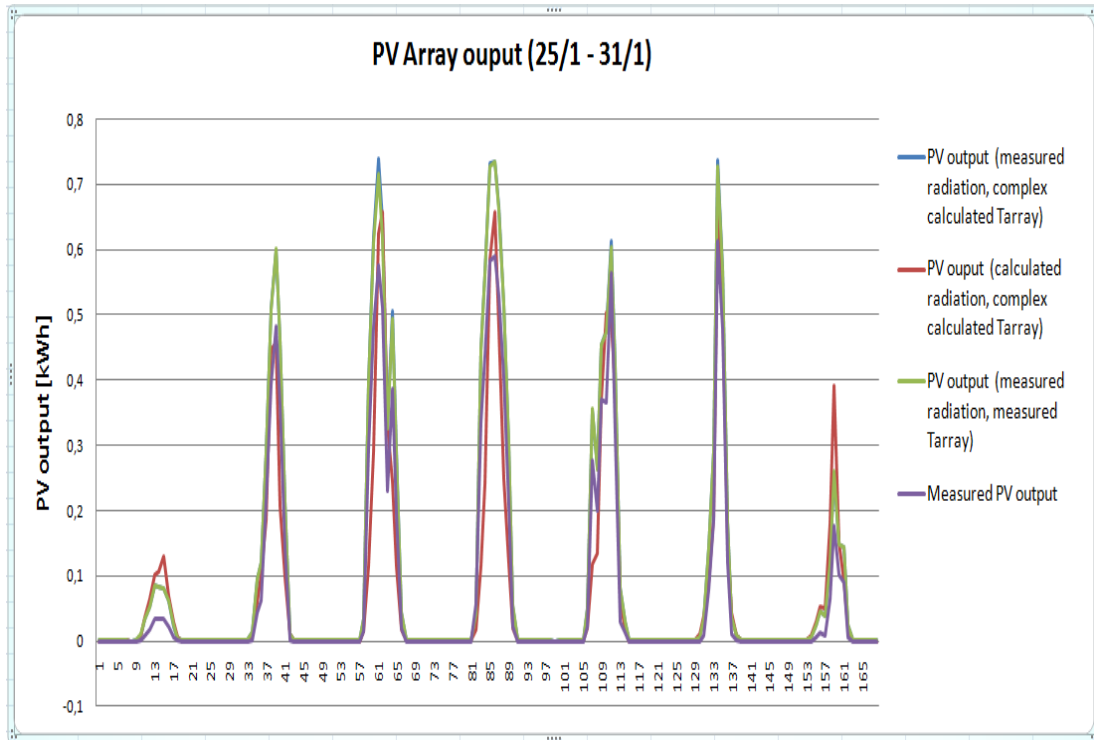These 4 PV outputs were plotted for a winter and a summer week in the following graphs.

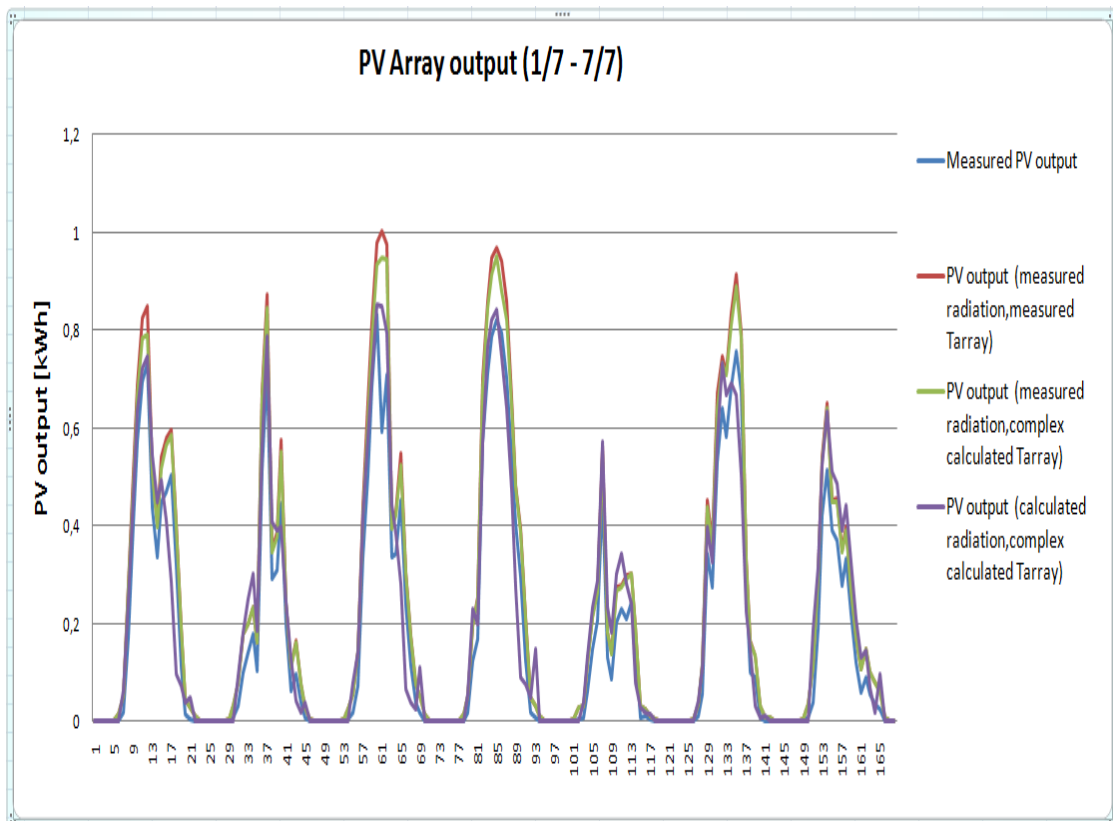**Figure 59**: PV array output for a winter week

Figure 60: PV array output for a summer week

The observations concerning the above graphs are:

- All the PV array outputs are equal to zero during the night as it is anticipated.

- The PV array generates electricity during daytime and the maximum output is remarked at noon when also the solar radiation is maximised

- All the different previously mentioned PV array outputs have the same fluctuation.

- The peak value for the summer week is about 30% larger than the one for the winter week.

- The areas below the plotted graphs represent the generated electricity and this area is much larger during summer than during winter. Roughly it is about 2.5 times larger.

- The measured PV array output (blue colour) seems to be closer to the estimated PV array output by using the calculated radiation and the complex calculated T_{array} (purple colour). There are even moments that these PV array outputs coincide. Therefore, this estimated PV array output provides results that are closer to the reality.

- The other 2 PV array output take values that are considerably higher than the measured PV array output, especially regarding the peak value when the difference can reach even the 20%.

Furthermore, the thermal losses from the PV array to the surrounding environment were estimated through the equation $U_{PV}*A_{array}*(T_{array} - T_{ambient})$. Thus, the selected U_{PV} and the five previously mentioned T_{array} were used. The following graphs demonstrate the various thermal losses concerning the different parameters for a winter and a summer week.
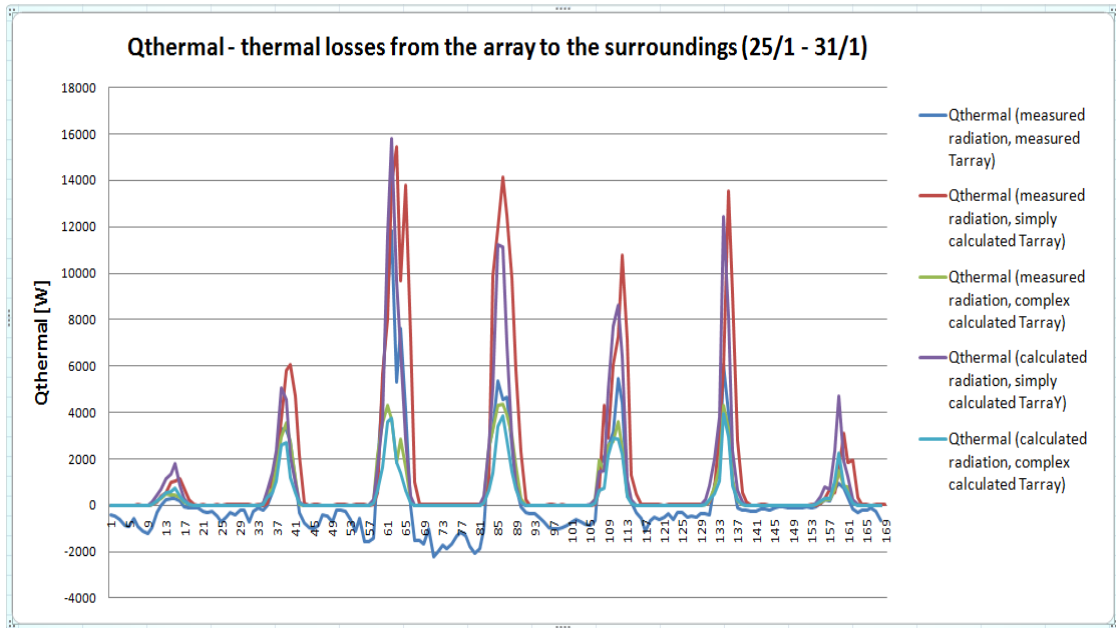
Figure 61: Thermal losses for a winter week
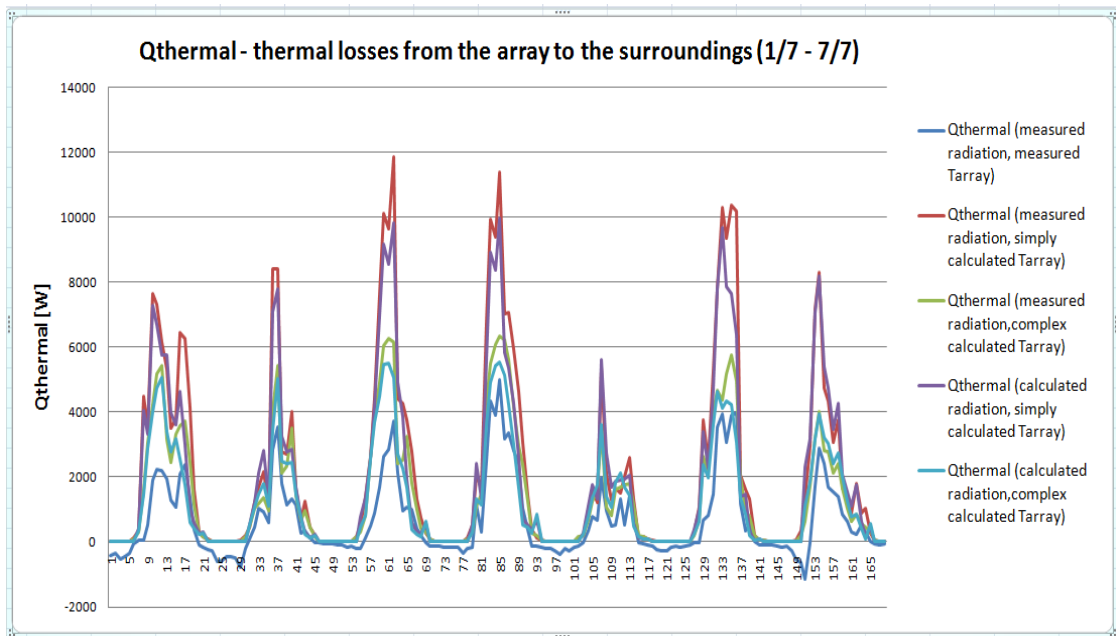
Figure 62: Thermal losses for a summer week

The thermal losses emerging from the measured radiation and the measured T_{array} are the more realistic. Then, the thermal losses emanating from the complex calculated T_{array} are closer to the one emerging from the measured radiation and the measured T_{array}. The thermal losses arising from the simply calculated Tarray are almost the double compared to the thermal losses from the complex. These results are quite logical and expected since the T_{array} is much better estimated through the complex equation and the thermal losses are proportional to the temperature difference between the array and the ambient environment.

The inverter constitutes an important part of the whole PV system. The inverter's efficiency and operation issues can influence the whole performance of the examined PV system. Thus, the aim was to evaluate and observe the fluctuations of the inverter's performance. The following two graphs illustrate the measured inverter's output in comparison to the measured PV array's output.
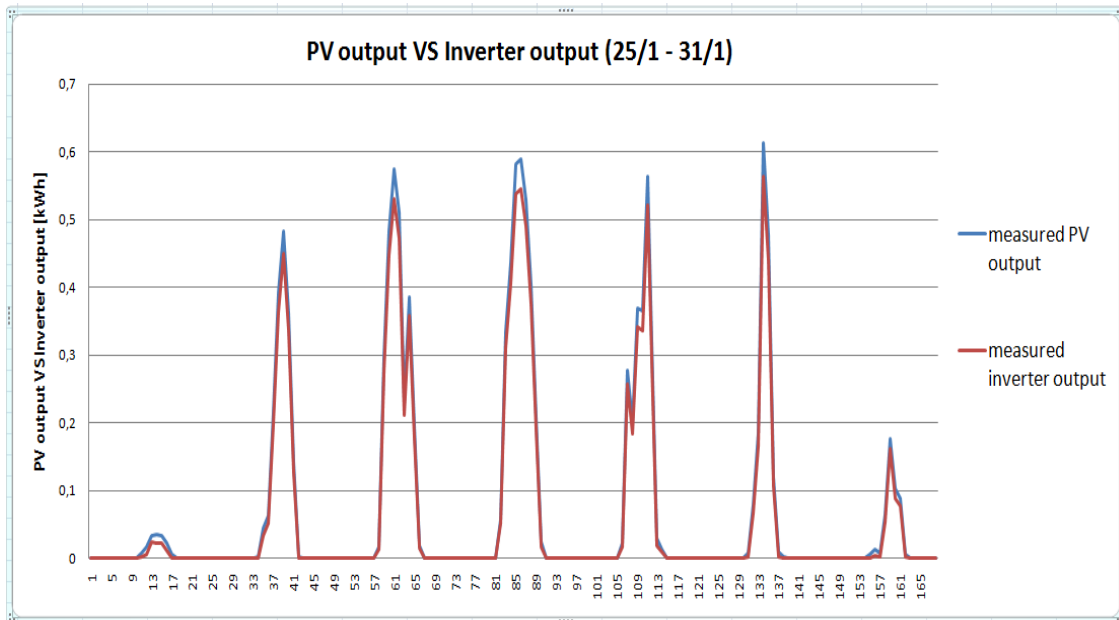

Figure 63: Inverter output in comparison with the PV array output for a winter week
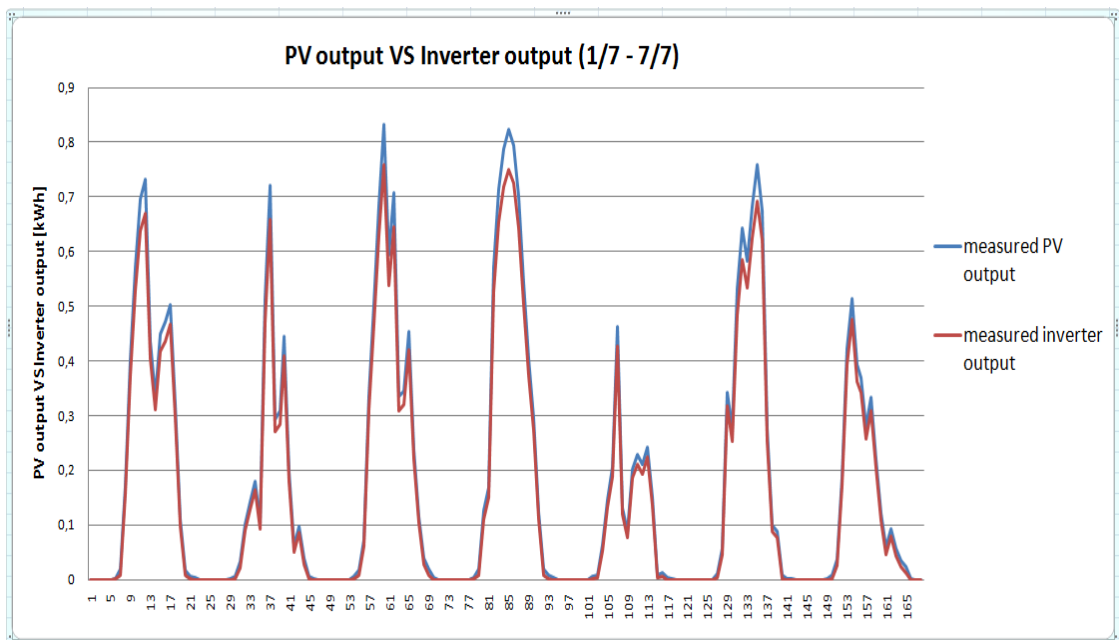
Figure 64: Inverter output in comparison with the PV array output for a summer week

The inverter's output is very close to the PV array's output both in winter and in summer. The 2 lines seem to be in considerably good agreement.

According to the manufacturer, the inverter's efficiency was supposed to be 93%. However, this wasn't always the case in the Troon's project and the graphs below demonstrate how this efficiency varied during time for a winter and a summer week.

Figure 65: Inverter's efficiency during a winter week

Figure 66: Inverter's efficiency during a summer week

The inverter's efficiency was always almost equal to 93% apart from minimal time intervals when it fell under 90%. Also, in extremely few cases its efficiency fell in considerably low levels. This could be attributed to momentary poor inverter operation.

6.5   Discussion – tool development

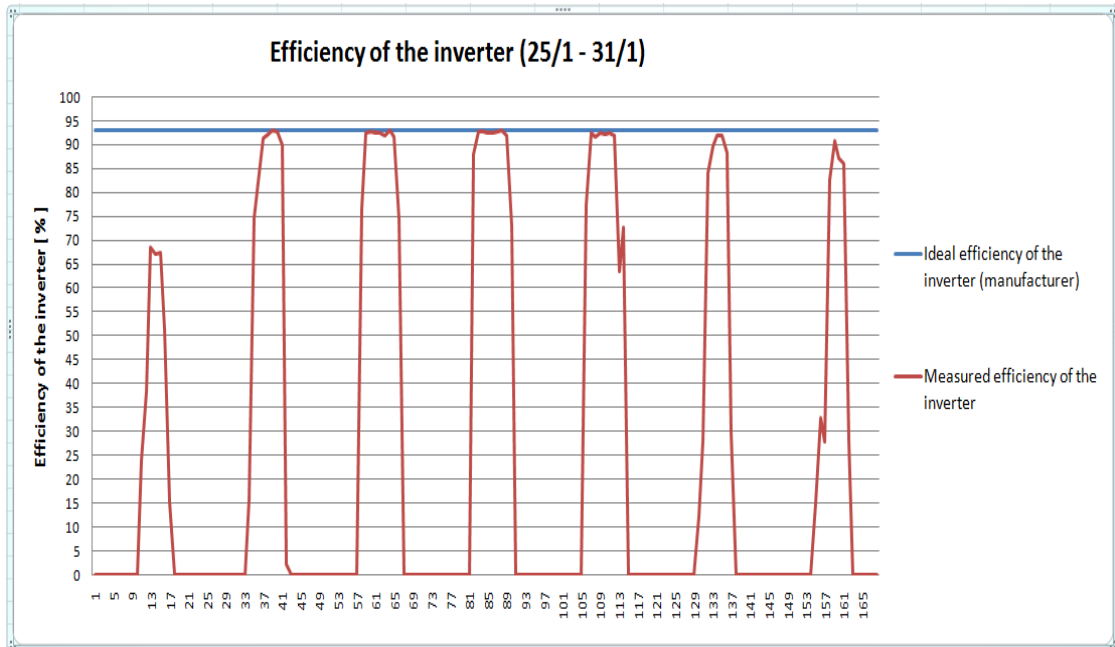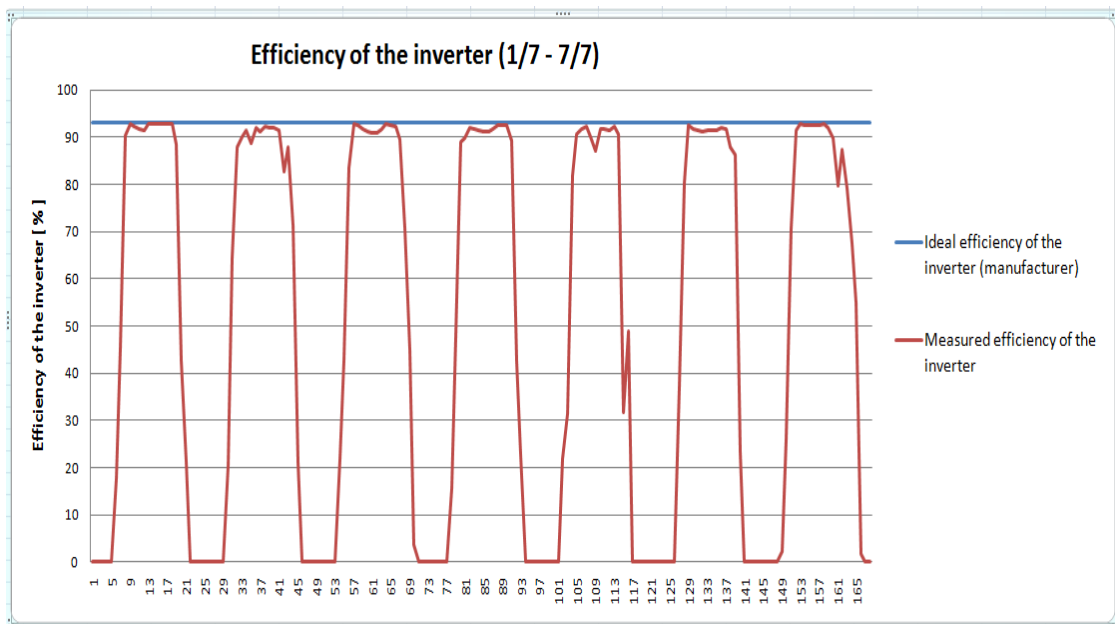In the chapter 6.4 Graphical comparison of measured – calculated parameters, the graphs concerning the PV array output were provided. These graphs lead to the following tables which include values regarding the generated electricity from the PV array (related to the different parameters mentioned in 6.4).

WINTER WEEK (25/1 – 31/1)	
Measured PV array output	11.858 kWh
PV array output (measured radiation, measured Tarray)	15.942 kWh
PV array output (measured radiation, simply calculated Tarray)	15.416 kWh
PV array output (calculated radiation, simple calculated Tarray)	11.448 kWh
PV array output (measured radiation, complex calculated Tarray)	16.049 kWh
PV array output (calculated radiation, complex calculated Tarray)	11.836 kWh

Table 14: PV outputs for a winter week

SUMMER WEEK (1/7 – 7/7)	
Measured PV array output	30.246 kWh
PV array output (measured radiation, measured Tarray)	39.295 kWh
PV array output (measured radiation, simply calculated Tarray)	37.104 kWh
PV array output (calculated radiation, simple calculated Tarray)	32.873 kWh
PV array output (measured radiation, complex calculated Tarray)	38.267 kWh
PV array output (calculated radiation, complex calculated Tarray)	33.77 kWh

Table 15: PV outputs for a summer week

The PV array electricity output estimated by using the calculated radiation and the complex calculated T_{array} is very close to measured generated electricity both in winter (11.836kWh compared to the measured 11.858kWh) and in summer (33.77kWh in comparison with the measured 30.246kWh). In addition, if the simply equation for estimating the T_{array} is applied (using the calculated radiation), the results are also quite satisfactory, 11.448kWh instead of 11.858kWh in the winter week and 32.873kWh instead of 30.246kWh in the summer week. However, the complex equation {41} for estimating the array temperature and consequently the array efficiency and the PV array output is selected since its shape in the relative graph (as it mentioned before) follows much more accurately the measured one.

From the chapter 6.4 Graphical comparisons of measured – evaluated data, it is obvious that the following equations perform quiet well:

- Equations for separating the total – global radiation into its direct and diffuse components (Erbs et al. correlation is chosen)

- Equations for calculating the solar radiation on an inclined surface taking into account that the measured direct and diffuse radiation falling on a horizontal surface are known.

- Equation for estimating the heat transfer coefficient U_{PV} taking into account the wind speed as well as the wind direction (equation {52}).

- Equation for evaluating the temperature of the installed PV array, Tarray {equation {41}).

- Equation for estimating the efficiency of the PV, depending upon the Tarray and the Tambient as well as the incident solar radiation.

- Equation for estimating the power output from the PV modules, taking into account the calculated efficiency n, the incident solar radiation and the array's surface area

- Equation for calculating the thermal – heat losses from the PV panel to surrounding environment, using the heat transfer coefficient UPV, the array temperature and the ambient temperature

- Taking into consideration the PV array output and the inverter's efficiency, an equation for estimating the inverter's power output.

- An equation regarding the performance ratio PR so as to estimate the PV system output

All the above equations can be incorporated and create a very useful and applicable excel tool in order to evaluate the performance of a PV system. This excel tool was used during this thesis.

6.6   Tool comparison to MERIT

One of the aims of this thesis was the evaluation and comparison of the developed Excel tool as well as Merit with the actual measured PV array output data from the case study in Troon. Therefore, the climatic data file, the demand profile and the used BP380 PV module were introduced into the Merit's database. More specifically, the total amount of the provided measured global horizontal radiation was divided into its direct and diffuse components through the developed Excel tool (as it was mentioned previously). The direct and diffuse components were then introduced into Merit enabling the evaluation of incident solar radiation on the inclined PV array. The PV array consists again of 12 PV modules that have a power output of 0.96kWp. It is tilted at an angle of 45° from the horizontal plane and it is orientated 17° east of south. As far as for the demand profile, it was estimated by adding the energy input from the grid with the inverter energy output from the PV array not absorbed by the grid. The obtained results from Merit for the same winter and summer week and their comparison in tables are presented in this chapter.

Winter week (25/1 -31/1)

Figure 67: Merit demand – supply profile for a winter week

This graph shows the demand and supply profile for the winter week. The total demand during this week is 34.8kWh, while the PV array generates 14.42kWh. One important feature of Merit is the fact that investigates the demand and supply matching. The match rate for this specific week is only 33.09%, meaning actually poor matching. This can be noticed also by the 2 represented lines in the graph.

WINTER WEEK (25/1 – 31/1)	
Measured PV array output	11.858 kWh
Excel tool - PV array output (calculated radiation, complex calculated Tarray)	11.836 kWh
MERIT PV array output	14.42 kWh

Table 16: Comparison of Merit results with the excel tool and the measured data for a winter week

The table proves that during winter the results from Merit are higher than the measurements and the estimations from the developed Excel tool, but the amount of divergence is in a way acceptable. The deviation may be attributed to the neglect of radiant exchange between the PV array and the sky as well as to the relative inaccuracy in the division of global radiation to its diffuse and direct normal components. Thus, the results obtained by either Merit or Excel tool are in acceptable agreement with the provided data.
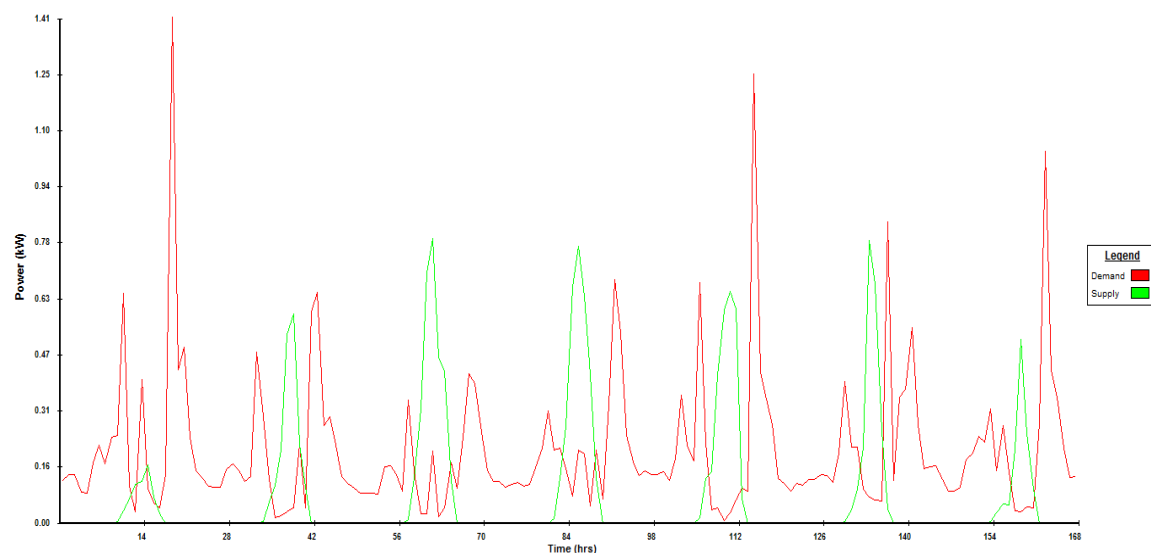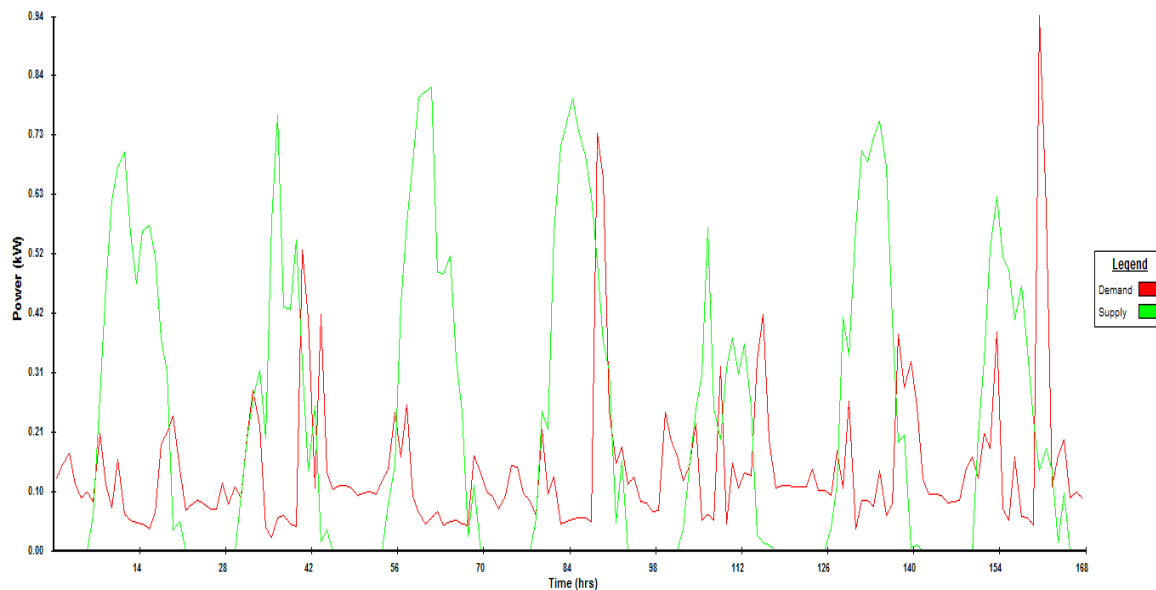
Summer week (1/7 – 7/7)

Figure 68: Merit demand – supply profile for a summer week

The graph illustrates the demand and supply profile for a summer week. The total demand during this week is 24.45kWh, while the PV array generates 38.41kWh. The match rate is now 42.29%.

The remarks obtained by comparing the summer and the winter week are:

- The demand is lower in summer than in winter. This is logical since Troon is in Scotland and the weather is quite cold especially during winter.

- The PV array as it is expected generates more electricity in the summer due to the fact that there is more incident solar radiation on the inclined array and the daytime is longer

- The matching rate is better in summer than in winter.

SUMMER WEEK (1/7 – 7/7)	
Measured PV array output	30.246 kWh
Excel tool - PV array output (calculated radiation, complex calculated Tarray)	33.77 kWh
MERIT PV output	38.41 kWh

Table 17: Comparison of Merit results with the excel tool and the measured data for a summer week

As it was previously noticed for the winter week, Merit results are also higher compared to both the estimated results via the Excel tool and the provided measurements during the summer week (due to the previously mentioned reasons). Nevertheless, the different values are into acceptable limits and not far away from the reality. Therefore, the conclusion is that the developed Excel tool performs again quite well.

6.7 Array orientation / inclination effect evaluation based on project tool

As it was presented in chapter 4.4, there are various parameters that affect the PV performance. Two important parameters are the array inclination (chapter 4.4.3) and the array orientation (chapter 4.4.2). The developed excel tool can evaluate and determine the significance of these parameters.

Array inclination

The PV array was orientated 17° east of south. It was installed at an angle of 45° from the horizontal surface. This slope was then varied from 30° to 60° with 5° step intervals, while the array's orientation remained constant. The following graphs show

how the PV array output responds regarding the tilt angle φ from the horizontal plane during a winter and a summer week.
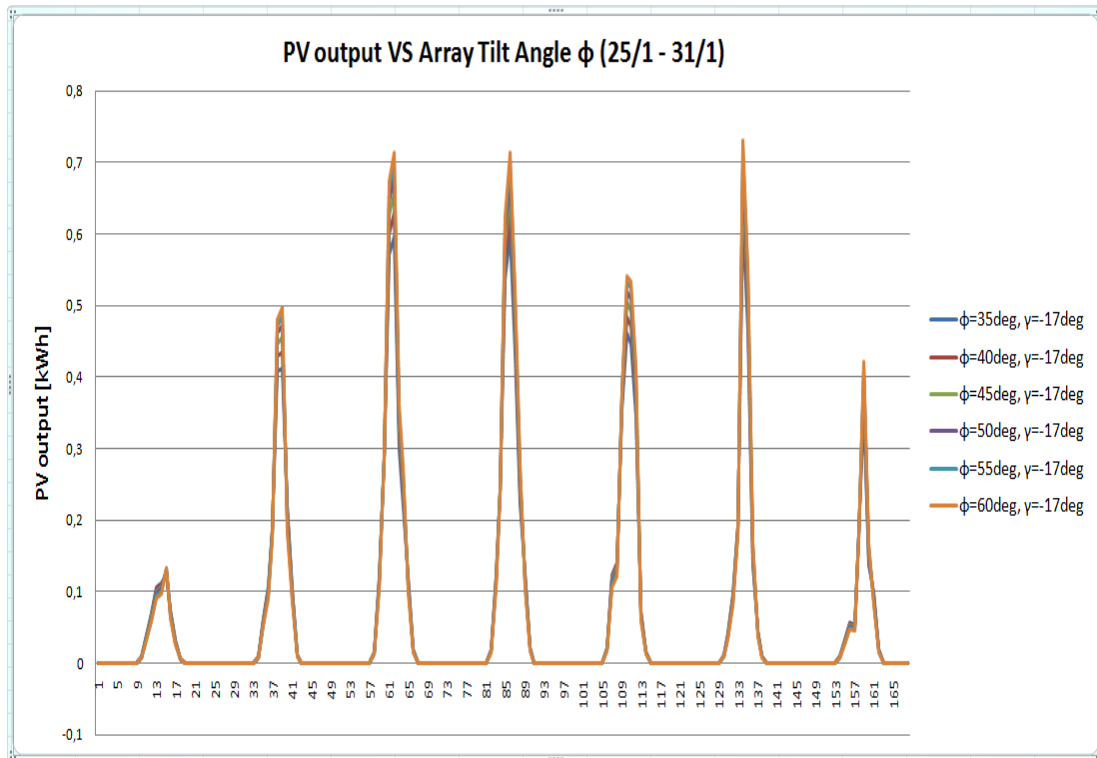

Figure 69 : PV array output regarding array inclination from the horizontal plane for a winter week
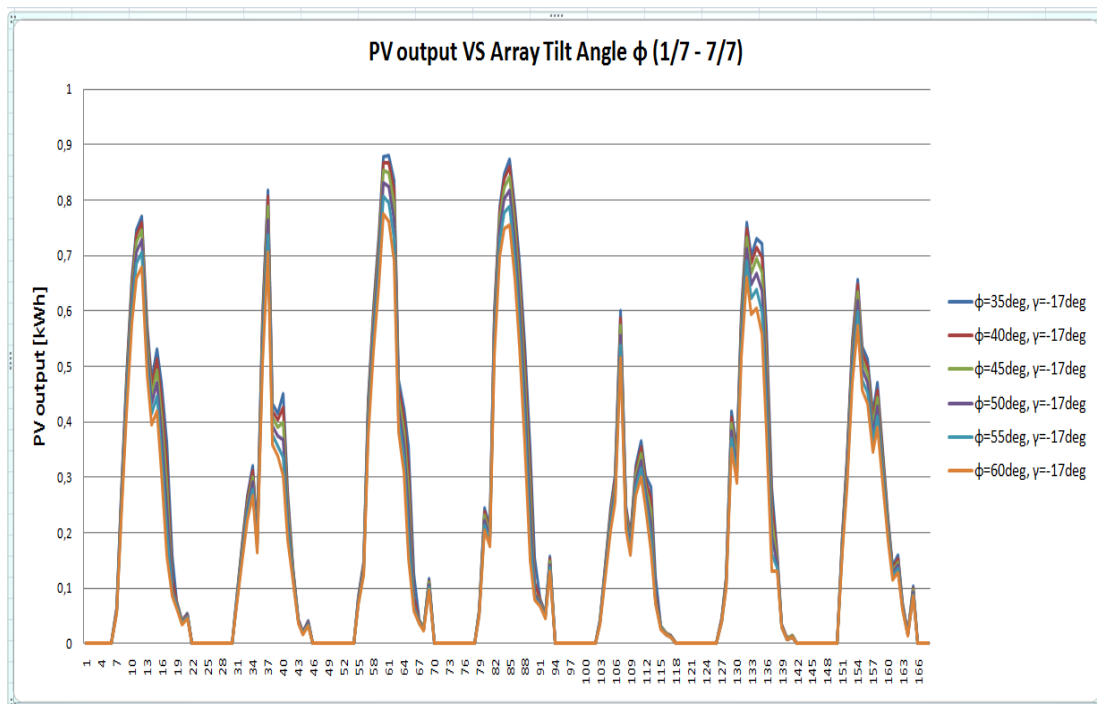

Figure 70: PV array output regarding array inclination from the horizontal plane for a summer week

113

Taking a closer look in the above graphs it seems evident that:

- during winter, steeper inclination angles from the horizontal surface lead to greater PV array output. Therefore 60° provides the highest energy yield.

- during summer, shallower inclination angles would lead to greater outputs with 35° offering the optimum.

These results are anticipated as PV performance is directly correlated to maximum solar gains which occur when solar radiation is vertically incident to the module plane. In winter the low solar elevation angle is thus responsible for higher planar inclination angles delivering higher yields, when as in summer higher solar elevation angles require modules installed in shallower angles.

The above graphs don't have the necessary high resolution in order to provide safe and accurate estimations and also illustrate only one winter and summer week. Thus the following table that includes the annual total solar radiation incident on the PV array as well as the annual PV array output based upon the Excel tool seems to be essential.

$\gamma=-17°$ φ [degrees]	Annual Global Solar Radiation on Surface [kWh/m^2]	Annual PV array output [kWh]
35	1032.3	996.2
40	1013.7	978.7
41	1009.5	974.8
42	1005.2	970.8
43	1000.8	966.7
44	996.1	962.4
45	991.3	957.9
46	986.3	953.2
47	981	948.3
48	975.6	943.3
49	970	938
50	964.1	932.6
55	931.7	902.5
60	894.6	867.9
90	604.2	594.6

Table 18: annual global solar radiation incident on the PV array and its relevant output concerning the inclination from the horizontal plane

The table provides accurate results and it is noticeable even the effect that 1° difference in the inclination angle has regarding the PV array output. Since PV array is installed at a tilt angle of 45°, the obtained results in the table are from 40° to 50° with 1° step. Also the table includes results for a vertically inclined PV array as well as for 35° tilt angle (from the horizontal plane). The 35° is very close to the 37° which is the optimum inclination according to the PVGIS. If the PV array was installed at 35° instead of 45°, its potential energy yield could have been increased by 3.85%.
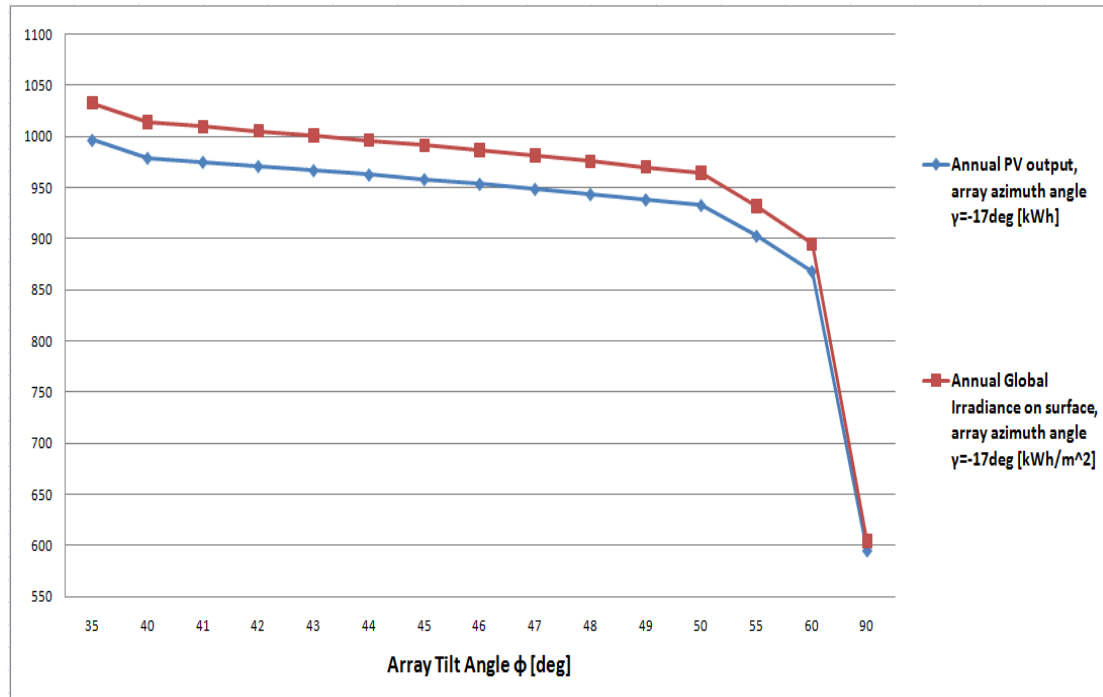
Figure 71: annual global solar radiation incident on the PV array and its relevant output regarding the inclination angle from the horizontal plane

The results from the table are graphically illustrated through the above graph. The 35° leads to the possible energy yield. Then, this yield decreases as the inclination angle augments and becomes significantly small for a vertically inclined PV array.

According to PVGIS the optimal inclination angle for a PV installation in Troon (55°32'36" North, 4°39'50" West) is 37° as it has been already mentioned [101]. This optimal angle varies during the year according to the following table:

Month	JAN	FEB	MAR	APR	MAY	JUNE	JUL	AUG	SEPT	OCT	NOV	DEC
Optimal inclination [deg]	70	63	49	36	24	16	19	29	44	57	69	72

Table 19: optimal PV array inclination in Troon

The following graph is a graphical presentation of the above table.
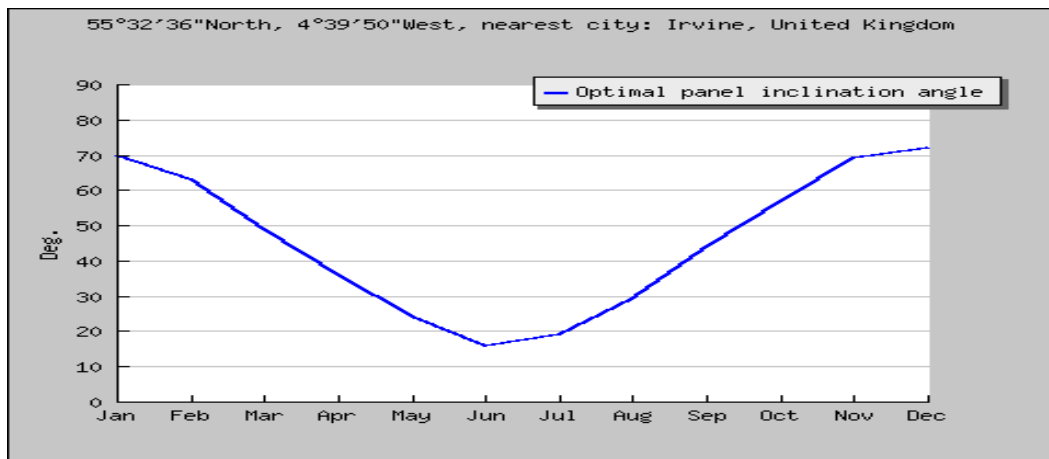
Figure 72: optimal PV array inclination in Troon [101]

Array orientation

Since Troon is in the northern hemisphere, the PV array should have been installed due south. However, the PV array was installed 17° east of south mounted on top of the roof, meaning that the surface azimuth angle γ is equal to -17°. The angle γ was then varied from 0° (due south) to -90° (due east) with -10° steps. The array's inclination remained fixed at 45°. The results regarding the variation of the array azimuth angle are shown in the graphs below for a winter and a summer week.
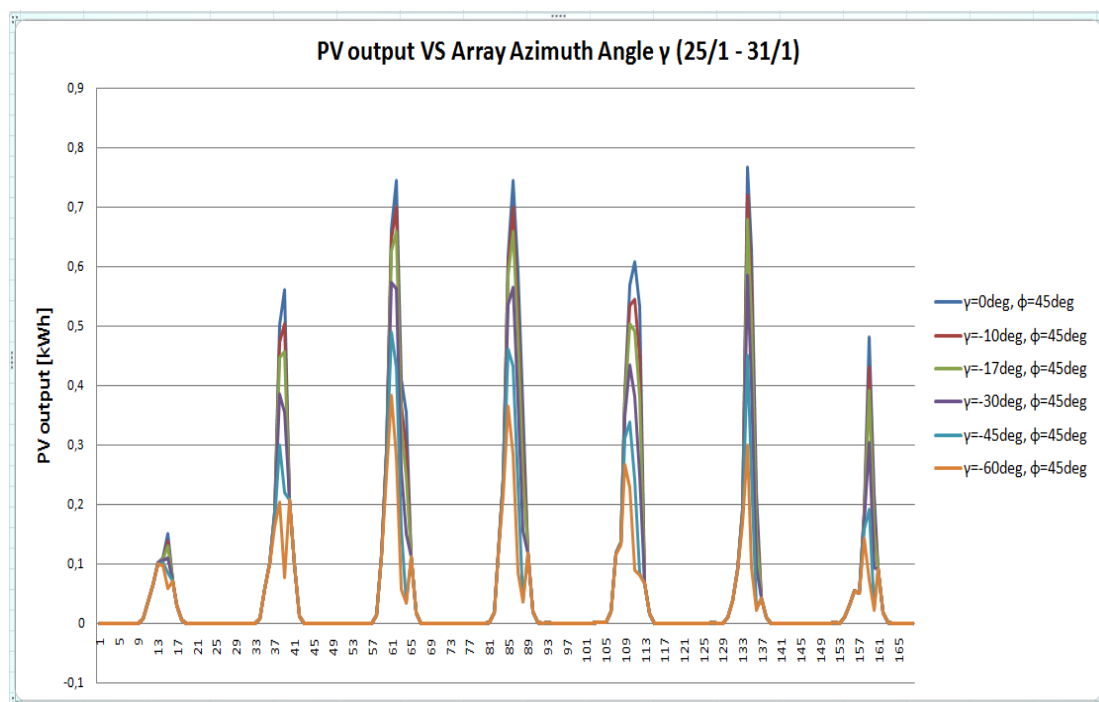
Figure 73: PV array output regarding array orientation for a winter week
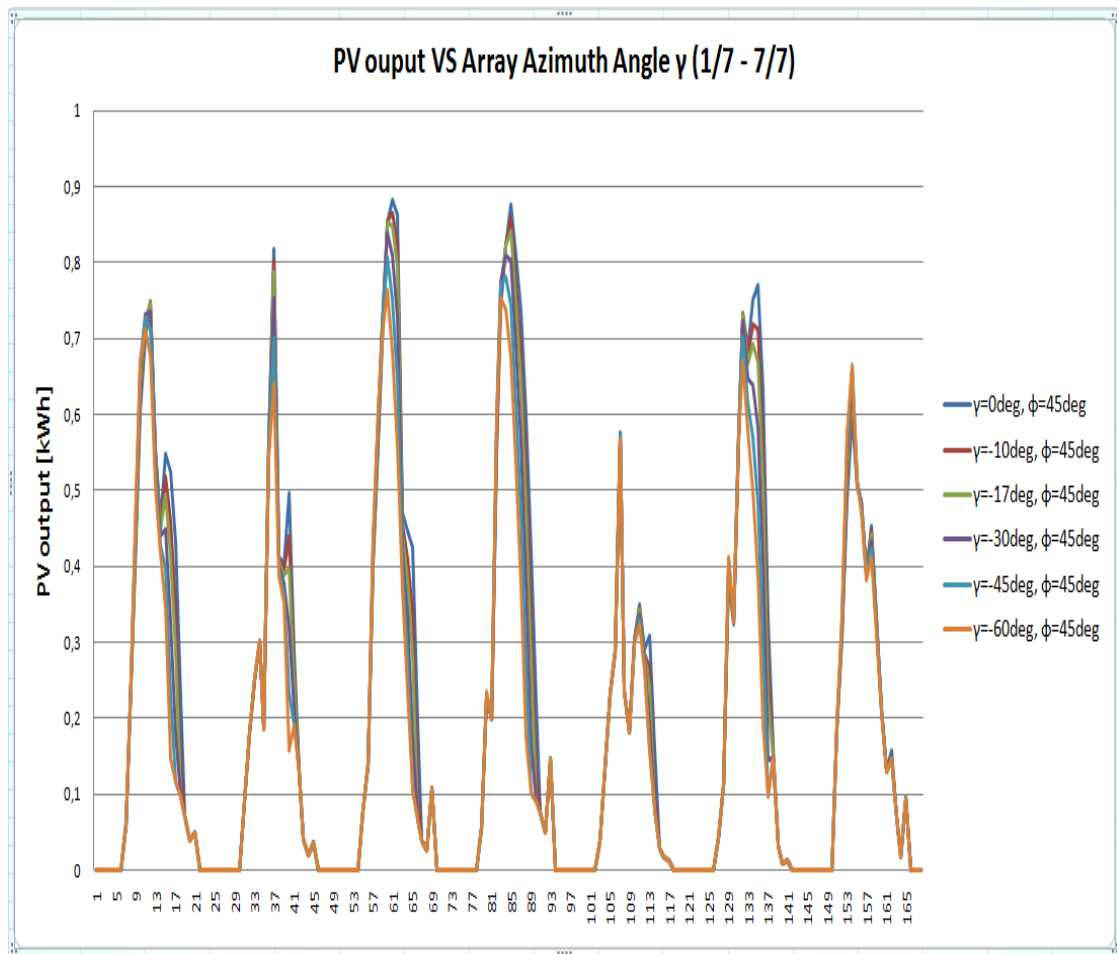
Figure 74: PV array output regarding array orientation for a summer week

As the array's orientation further deviates from due south the potential energy yield reduces both in winter and in summer. This result is absolutely logical. The higher the deviation (γ = -60°), the larger the decrease in the PV array output. Additionally, in winter, this decrease is significantly larger than in summer. During winter, PV array oriented 60° east of south generates almost half the electricity compared to due south (always at the same tilt angle). The same comparison in summer provides roughly a 15% decrease in contrast to the winter 50%. This may be attributed to the different sun's orbit between summer and winter. In summer the solar azimuth angle γ_s has a larger daily variation.

In order to acquire a broader understanding regarding the effect of array azimuth angle on the PV array output annual results have been generated and presented in the following table.

φ=45° γ [degrees]	Yearly Global Solar Radiation on Surface [kWh/m^2]	Yearly PV output [kWh]
0	1089.4	1049.1
-10	1030.7	994.5
-17	991.3	957.9
-20	974.2	942
-30	914.4	886.1
-40	858.8	834.1
-50	805.8	784.5
-60	757.6	739.3
-70	715.9	700.2
-80	680.2	666.9
-90	649.4	638.2

Table 20: annual global solar radiation incident on the PV array and its relevant output concerning the orientation
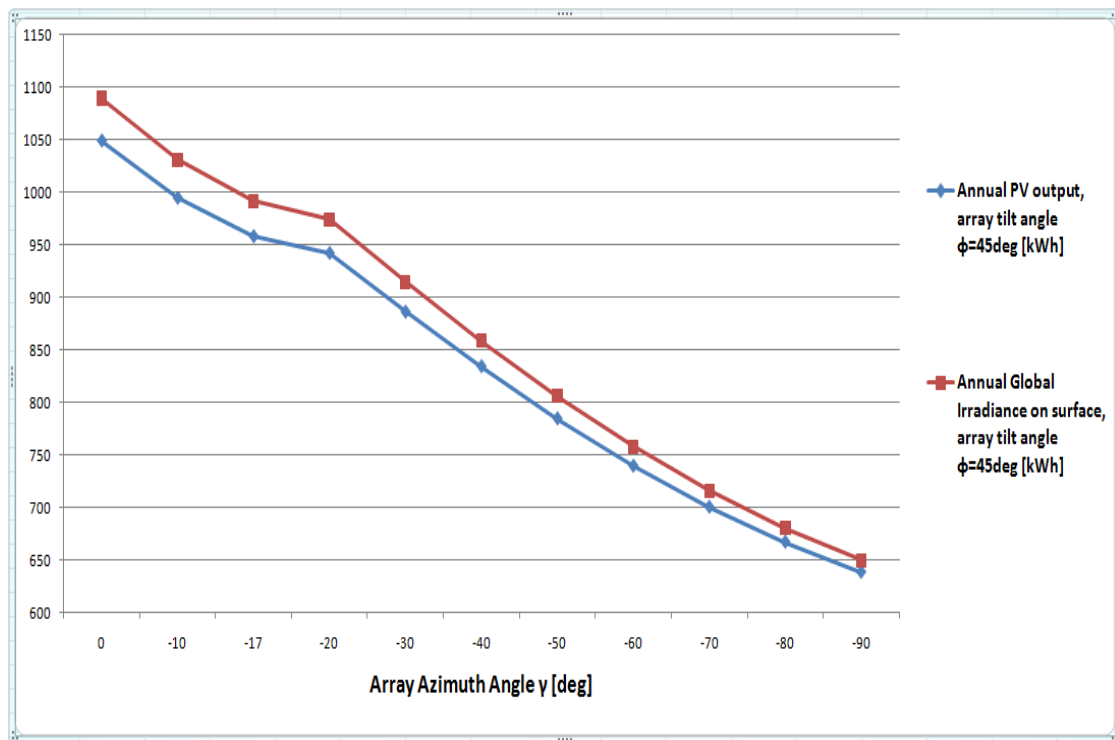
Figure 75: annual global solar radiation incident on the PV array and its relevant output concerning the orientation

If the PV array faced due south instead of 17° east of south it would have produded 8.67% more electricity. The above graph shows graphically the annual global solar radiation that leads to the PV array output for the specific inclination angle of 45° and different orientation angles. It is noticeable that PV array output responds almost linearly to the array azimuth angle.

118

7   Comparison of 4 European locations PV electricity yield

Apart from evaluation of actual case study data, aim of this project is the analysis of regional differences regarding the potential energy yield (generated by PV systems). Specifically in order to further understand these differences 4 climatic regions have been selected. These are 2 northern European regions represented by Glasgow and Oban (Scotland) climatic data, a more central European region represented by Jersey (a sunny island in southern UK with latitude similar to northern France) and a southern European region represented by Athens climatic data. The following maps show the annual global irradiation [kWh/m^2] and the annual electricity generated by 1kWp system with a performance ratio of 0.75 for both horizontally and optimally inclined PV modules in United Kingdom, France and Greece.

[102]

[103]

[104]

[105]
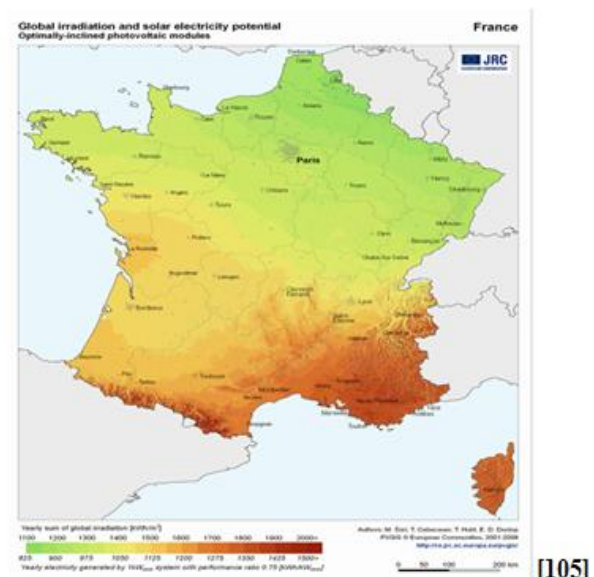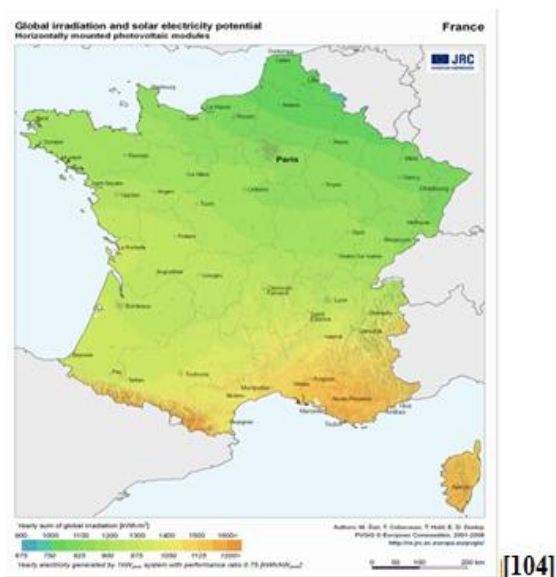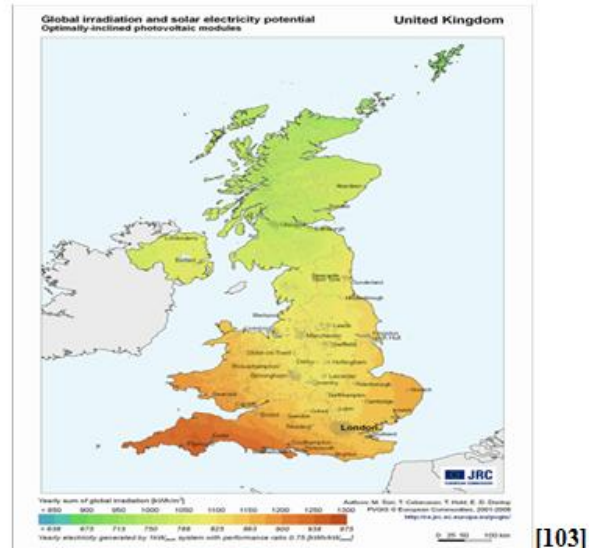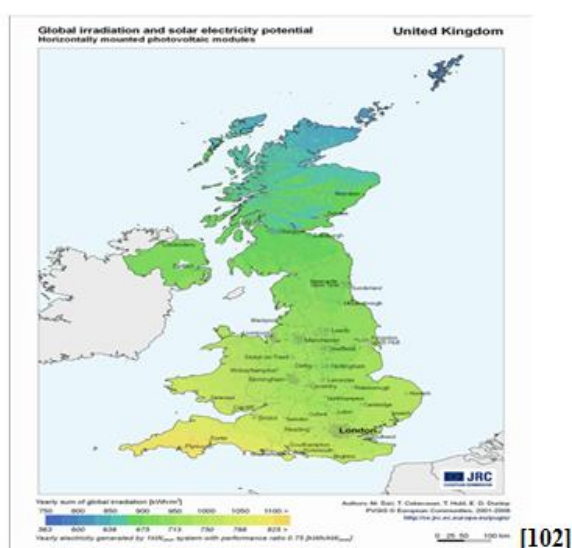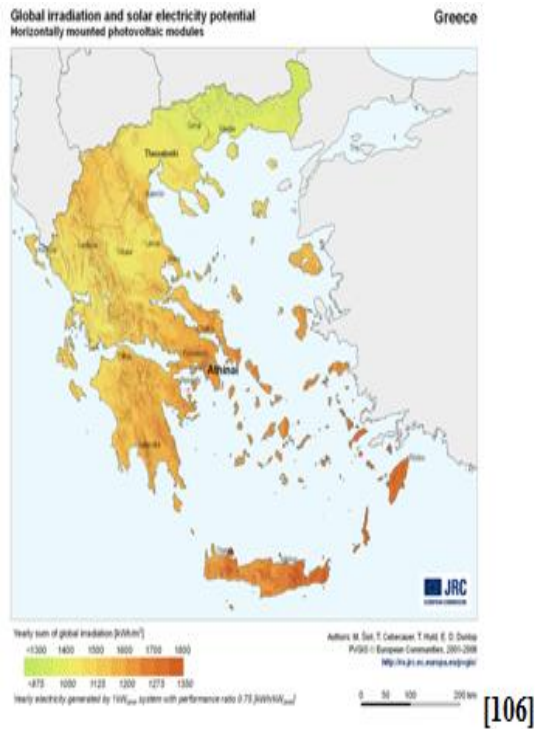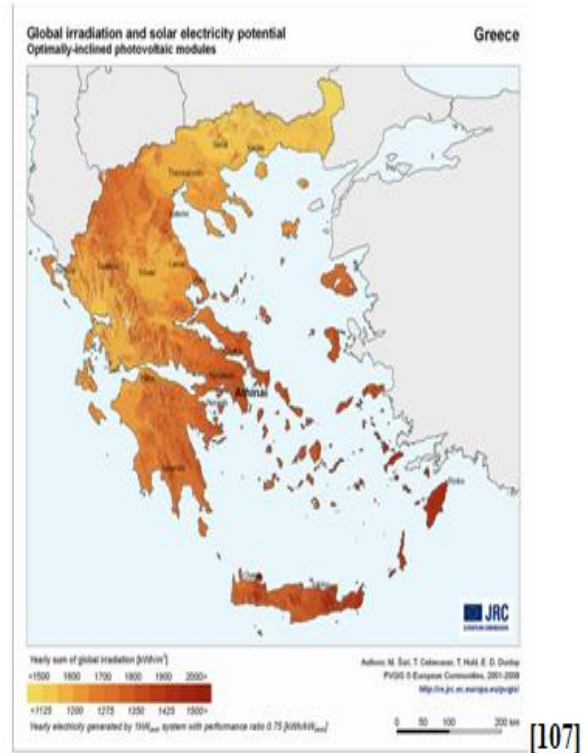
Furthermore, multi crystalline PV modules have been considered and compared concerning orientation as well as inclination of the PV installation. The BP380 PV module was used throughout chapter 7. The orientation has been modified from south to east with 10° intervals. The various inclinations of the PV installation which are taken into consideration are; horizontal, vertical, optimally inclined and small deviations of the optimum inclination. The results have been obtained by using either the Excel tool or Merit and were in a yearly basis. The estimated results from the Excel tool referred to; the output of a 0.96kWp PV array, the PV array output for a 1kWp PV array (kWh/kWp) and to the electricity generated by 1kWp PV system with performance ratio PR=0.75 (for comparison PVGIS site), while the Merit results referred only to a 0.96kWp PV array output.

In reality horizontal mounting is not very common apart from special cases of building integrated systems. However such calculations are useful as a baseline estimate since many sources of radiation data provide only values regarding a horizontal plane. Through the comparison of horizontal to inclined and vertical mounting results it is possible to make better predictions for the latter based only on horizontal irradiation data.

7.1 Glasgow

The geographical coordinates of Glasgow are; latitude=55°51'56" North and longitude= 4°15'26" West. According to PVGIS the optimal inclination angle for a PV installation is 37° [101]. This optimal angle is modified during the year according to the following table.

Month	JAN	FEB	MAR	APR	MAY	JUNE	JUL	AUG	SEPT	OCT	NOV	DEC
Optimal inclination [deg]	70	63	50	36	23	17	19	29	45	57	69	72

Table 21: optimal PV array inclination in Glasgow
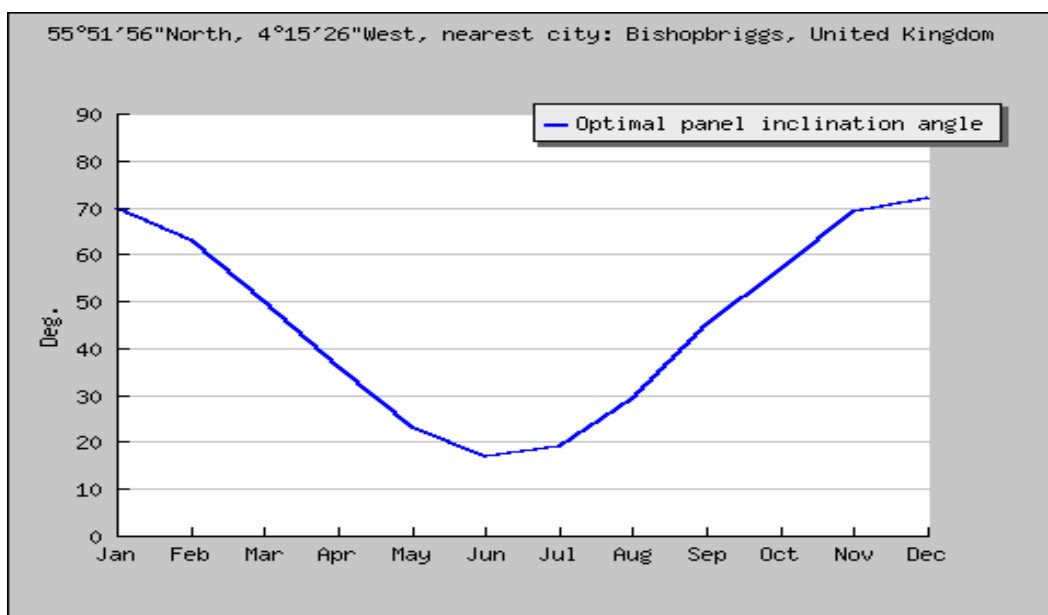
Figure 76: optimal PV array inclination in Glasgow [101]

➤ **Excel tool**

Array inclination φ from the horizontal plane

The array inclination plays a significant role regarding the PV performance. In order to evaluate the effect of the inclination angle the PV system was installed due south, meaning the best possible orientation, and the array inclination was varied from horizontal to vertical with certain degree steps. Around the optimal inclination the undertaken degree steps (of the array tilt angle φ from the horizontal surface) were only 1° in order to increase the resolution of the undertaken analysis. The results are presented in the following table and graph.

γ=0° φ [degrees]	Annual Global Solar Radiation on Surface [kWh/m^2]	Annual output for a 0.96kWp PV array [kWh]	Annual PV array output [kWh/kWp]	Annual PV System Output with PR=0.75 [kWh/KWp]
0	887.4	883.4	920.2	690.1
35	978.2	970	1010.4	757.8
36	976.8	968.5	1008.9	756.7
37	975.1	966.9	1007.2	755.4
38	973.1	965	1005.2	754
39	971	963	1003.1	752.3
40	968.6	960.7	1000.7	750.5
41	966	958.1	998.1	748.6
42	963.2	955.4	995.2	746.4
43	960.1	952.5	992.2	744.1
44	956.9	949.4	989	741.7
45	953.4	946	985.5	739.1
60	876	871.7	908	681
90	599.7	603.3	628.4	471.3

Table 22: Annual total radiation and PV performance in Glasgow regarding tilt angle φ from the horizontal plane

Figure 77: Annual total radiation and PV system output in Glasgow regarding tilt angle φ from the horizontal plane

According to the Excel tool, the generated electricity by a horizontal inclined PV system is 690.1kWh and by a vertical 471.3kWh. The value of 471.3 seems to be

significant smaller than the 570kWh found in literature. An optimally inclined PV system generates 757.8kWh which is almost in complete agreement with the 7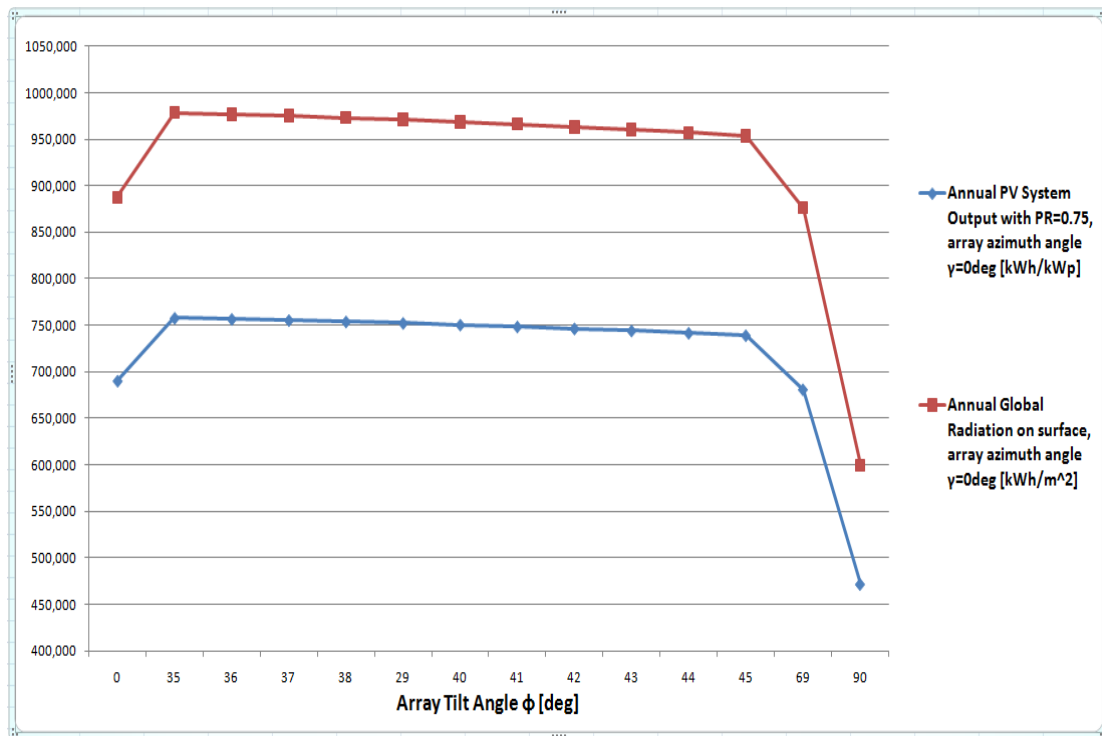60kWh mentioned in chapter 4.4.3 Array inclination and more specifically in the sub-chapter PV modules installed in optimal inclination. . It is noticeable also from the graph that the generated electricity remains almost stable around the optimal angle. For instance, a PV system installed at a tilt angle of 40° produces 750.5kWh instead of the optimal 757.8kWh. Moreover, the tool results imply that the PV system installed at an optimum inclination generates 8.93% and 37.8% more electricity than a horizontal and a vertical respectively. The table below presents a comparison between the developed Excel tool and the PVGIS site.

Annual PV System Output with PR=0.75 [kWh/kWp]			
Inclination	**Horizontal**	**Vertical**	**Optimal**
PVGIS site	667	557	767
Excel tool	690.1	471.3	757.8

Table 23: Comparison of PVGIS and Excel tool for Glasgow

Therefore, it seems that the Excel sheet performs quite well and accurately for a wide variety of inclination angles. An optimal inclined PV system generates about 9% more electricity than a horizontal inclined according to the excel tool and 12% according to PVGIS. However, an important divergence of about 100kWh exists when the PV system is inclined vertically (a possible factor for that deviation is the varying ground reflectance).

Array orientation

The array orientation is another factor that affects significantly the PV system performance. In order to estimate this effect, the PV system was installed at a fixed 35° tilt angle from the horizontal and the orientation varied from due south to south-east and east. Thus, the array azimuth angle was modified from 0° to -90° with -10° intervals. The results are shown in the following table and graph.

φ=35° γ [degrees]	Annual Global Solar Radiation on Surface [kWh/m^2]	Annual output for a 0.96kWp PV array [kWh]	Annual PV array output [kWh/kWp]	Annual PV System Output with PR=0.75 [kWh/KWp]
0	978.2	970	1010.4	757.8
-10	977.9	969.6	1009.9	757.4
-20	971.1	963	1003.2	752.4
-30	959	951.2	990.9	743.2
-40	941.1	934.1	973	729.7
-50	918.3	912	950	712.5
-60	891.4	886.1	923	692.3
-70	861.4	857.1	892.9	669.6
-80	828.5	825.4	859.8	644.8
-90	794.1	792.1	825.1	618.8

Table 24: Annual total radiation and PV performance in Glasgow regarding orientation
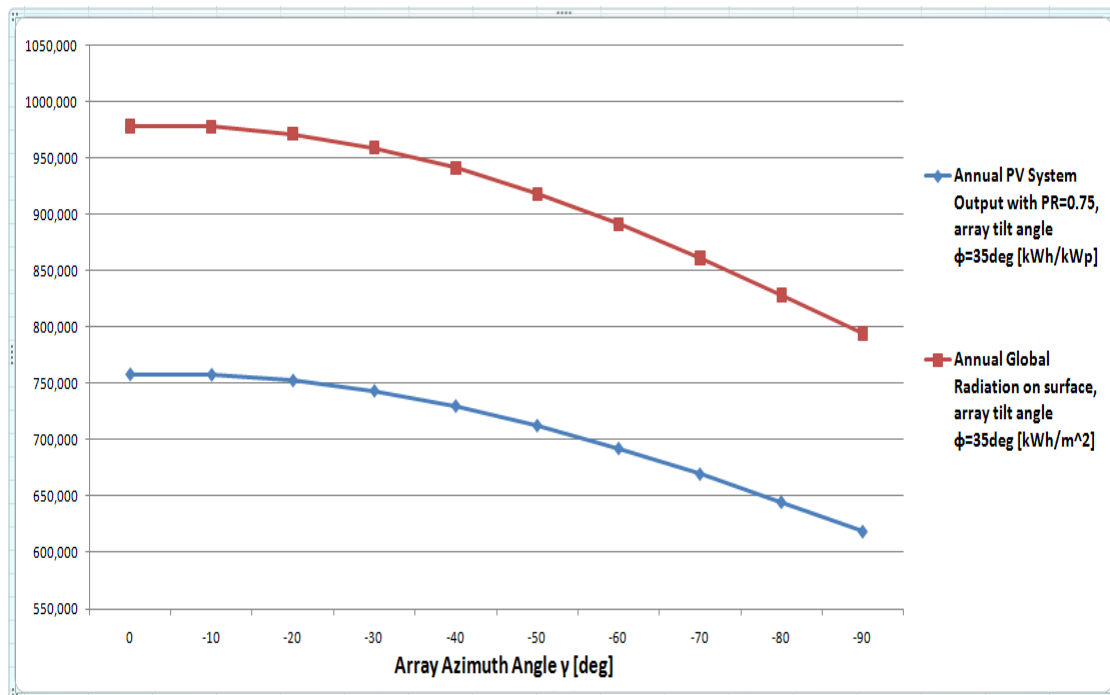
Figure 78: Annual total radiation and PV system performance in Glasgow regarding orientation

As it is anticipated, the higher the deviation for the south is, the larger the decrease in the generated electricity by the PV system. The PV system orientated due east (surface azimuth angle γ=-90°) produces 618.8kWh compared to the generated 757.8kWh by a due south (surface azimuth angle γ=0°) PV system, a decrease of approximately 18%. The shape of the line demonstrating the decrease of the PV system output as the array azimuth angle increases is a slight curve.

The target was also to compare the Excel tool results with Merit. Therefore, Glasgow climatic data was introduced into the Merit database. The following graphs show; the direct normal and the diffuse solar radiation, the ambient temperature and the wind speed in Glasgow.
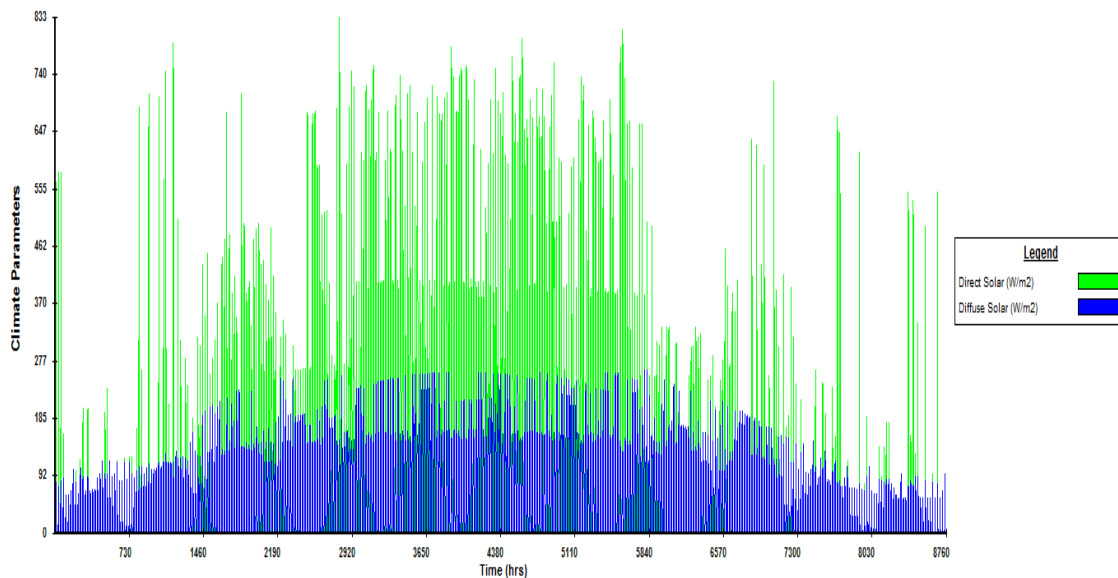
Figure 79: Direct normal and diffuse horizontal solar radiation in Glasgow
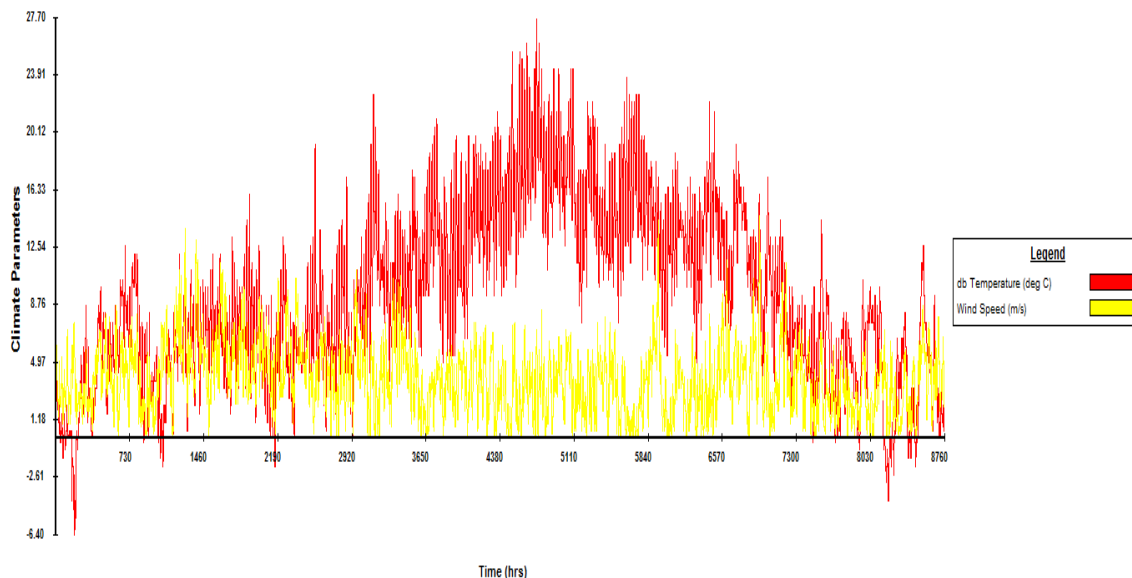
Figure 80: Ambient temperature and wind speed in Glasgow

In order to evaluate the Excel tool regarding Merit even one comparison may be adequate. Therefore, the annual output of a 0.96kWp PV array inclined 35° from the horizontal ($\varphi=35°$) and facing south ($\gamma=0°$) is presented in the graph below.
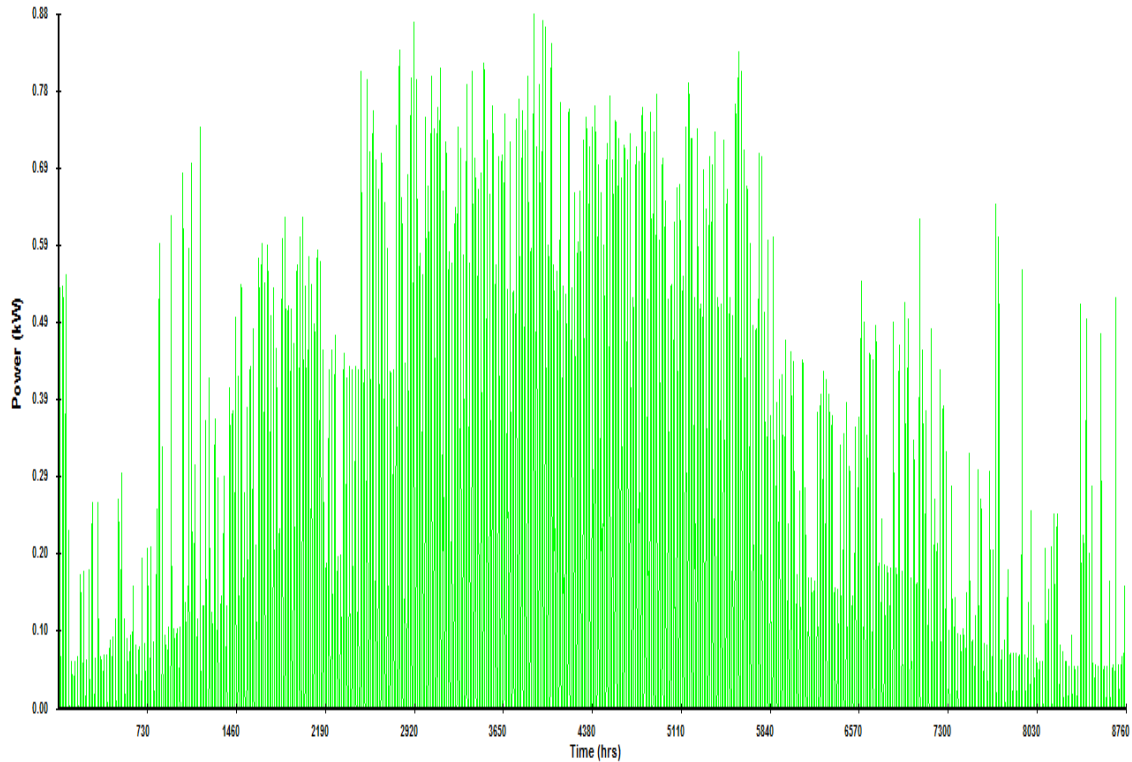
Figure 81: Annual output for a PV array of 0.96kWp in Glasgow (φ=35° & γ=0°)

The maximum power output of the previously specified PV array is 0.9kW and its annual energy yield is **1.01MWh**. This value is **3.97% higher** compared to the 970kWh emerging from the deveolped Excel tool.

7.2 Oban

Oban is selected due to the fact that is a coastal region placed even northern than Glasgow.

Its latitude is 56°24'37" North and the longitude 5°28'10" West. According to PVGIS, the optimal inclination angle for a PV installation is 36° [101]. The following table and graph shows how this optimal angle varies during the year.

Month	JAN	FEB	MAR	APR	MAY	JUNE	JUL	AUG	SEPT	OCT	NOV	DEC
Optimal inclination [deg]	67	62	50	38	25	17	20	29	45	57	67	69

Table 25: optimal PV array inclination in Oban
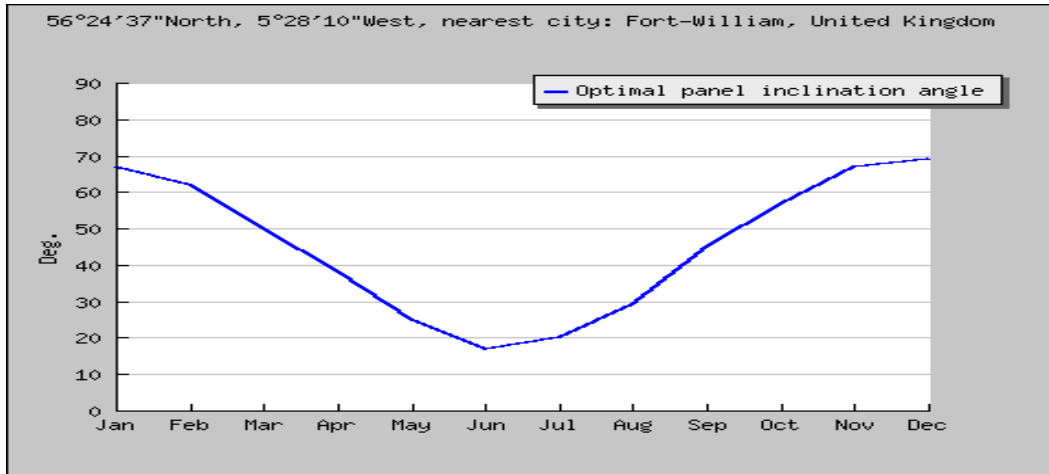
Figure 82: optimal PV array inclination in Oban [101]

➢ **Excel tool**

Array inclination φ from the horizontal plane

As it is already mentioned, array inclination affects the PV performance. PV system faced south and the tilt angle was altered from φ=0° up to φ=90°, meaning horizontal and vertical inclined PV system. In addition, φ varied from 35° to 45° with a 1° step to conceive what occurs around the optimal inclination angle. The following table and graph demonstrates the obtained results.

γ=0 Φ [Degrees]	Annual Global Solar Radiation on Surface [kWh/m^2]	Annual output for a 0.96kWp PVarray [kWh]	Annual PV array output [kWh/kWp]	Annual PV System Output with PR=0.75 [kWh/KWp]
0	854.6	851.7	887.2	665.4
35	921.9	914.4	952.5	714.4
36	920.3	912.8	950.9	713.2
37	918.6	911.1	949.1	711.8
38	916.6	909.2	947.1	710.3
39	914.5	907.1	944.9	708.7
40	912.1	904.9	942.6	706.9
41	909.6	902.4	940	705
42	906.8	899.8	937,3	702.9
43	904	897	934.3	700.7
44	900.9	894	931.2	698.4
45	897.6	890.8	927.9	695.9
60	826.3	822.2	856.4	642.3
90	580.6	584.3	608.6	456.5

Table 26: Annual total radiation and PV performance in Oban regarding tilt angle φ

from the horizontal plane
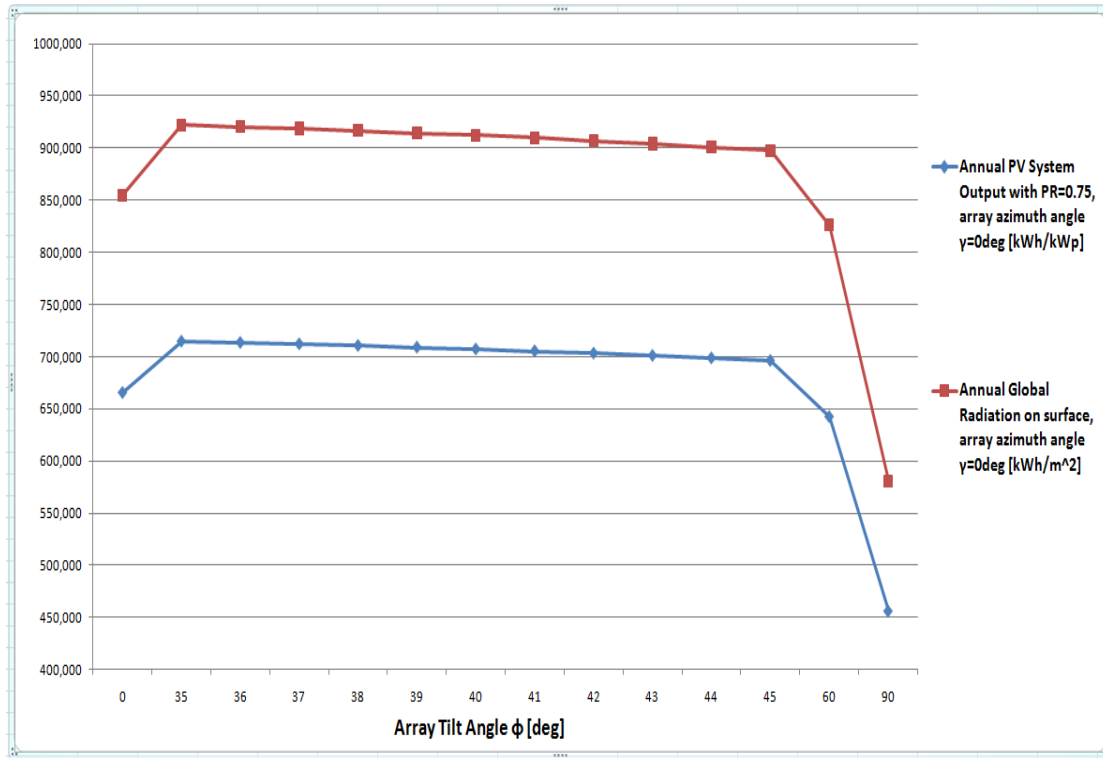
Figure 83: Annual total radiation and PV system output in Oban regarding tilt angle φ from the horizontal plane

A PV system inclined at 35° from the horizontal plane generates (optimal inclination) 714.4kWh. As it can be noticed from the above graph, the generated electricity reduces at a very low rate around that optimal inclination as the inclination angle increases. It is almost a straight line with a very little slope. A 40°/45° inclined PV system produces 706.9kWh and 695.9kWh respectively. The energy yield decreases significantly for a vertical inclined PV system. It produces only 456.5kWh, when a horizontal one generates 665.4kWh. So as to evaluate the performance of the Excel tool, we compare its results with the PVGIS site.

Annual PV System Output with PR=0.75 [kWh/kWp]			
Inclination	Horizontal	Vertical	Optimal
PVGIS site	645	497	726
Excel tool	665.4	456.5	714.4

Table 27: Comparison of PVGIS and Excel tool for Oban

The deviations between the Excel tool and the PVGIS are 3%, 8.14% and 1.6% concerning a horizontal, vertical and optimal inclined PV system. The conclusion is that the tool has almost an excellent performance.

128

Array orientation

Then, in order to estimate the influence of the array's orientation upon the PV system performance, the tilt angle φ from the horizontal remained constant at its optimum value and the surface azimuth angle γ was varied from 0° to -90° with -10° intervals. An angle γ equal to 0°/-45°/-90° refers to PV facing south, south-east and east respectively. The results are shown in the following table and graph.

φ=35	Annual Global Solar Radiation on Surface [kWh/m^2]	Annual output for a 0.96kWp PV array [kWh]	Annual PV array output [kWh/kWp]	Annual PV System Output with PR=0.75 [kWh/KWp]
γ=0	921.9	914.4	952.5	714.4
γ=-10	915.4	908.1	946	709.5
γ=-20	904.2	897.4	934.8	701.1
γ=-30	889.2	883.1	919.9	689.9
γ=-40	870.7	865.4	901.4	676.1
γ=-50	849.3	844.9	880.1	660.1
γ=-60	825.5	822.1	856.4	642.3
γ=-70	800.7	798.4	831.6	623.7
γ=-80	774.6	773.4	805.7	604.3
γ=-90	748.4	748.3	779.5	584.6

Table 28: Annual total radiation and PV performance in Oban regarding orientation
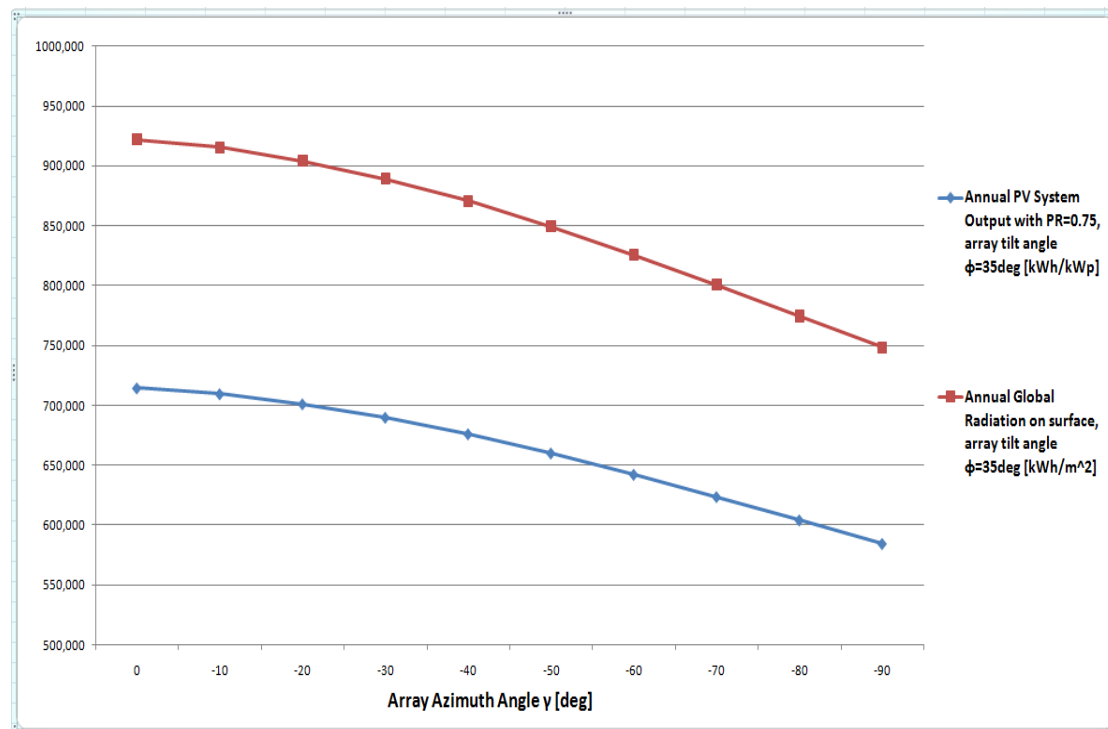
Figure 84: Annual total radiation and PV system performance in Oban regarding orientation

The PV system energy yield falls steadily as the array azimuth angle γ increases. A PV system facing south generates 18.2% more electricity than one facing east (584.6kWh instead of 714.4kWh). If γ=-40° meaning almost south-east facing PV, the generated electricity is decreased in a much smaller level; equal to 5.4% (676.1kWh instead of 714.4). Moreover, if γ=-50° the decrease is 7.6% concerning the optimal (south) orientation.

➢ **Merit**

The Oban climatic data (diffuse horizontal and direct normal solar radiation, ambient temperature, wind speed and direction, relative humidity) was introduced into Merit database. Merit was used in order to prove that the acquired results from the Excel tool are valid and accurate. A comparison concerning the energy yield of a PV array facing south and inclined at 35° from the horizontal was undertaken. The following graphs show some important parameters of the climatic conditions as well as the potential annual PV array output.
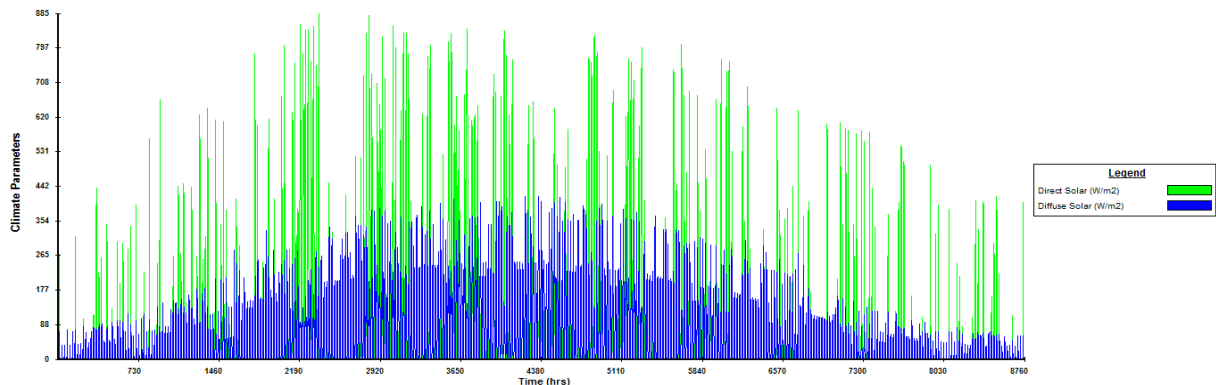
Figure 85: Direct normal and diffuse horizontal solar radiation in Oban
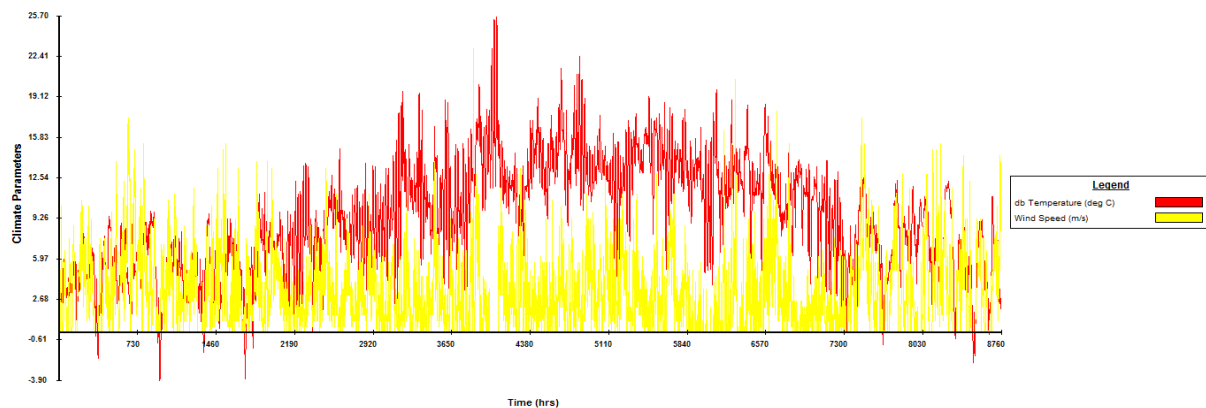
Figure 86: Ambient temperature and wind speed in Oban
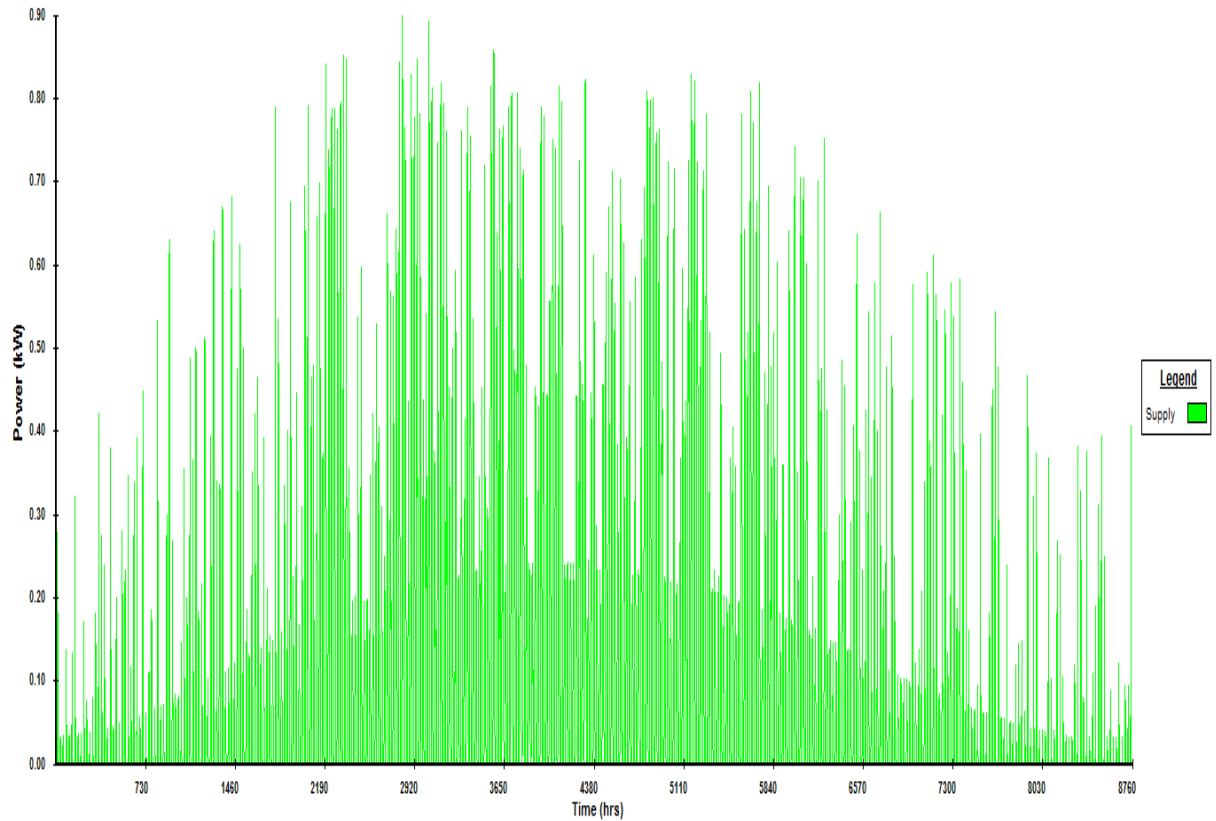
Figure 87: Annual output for a PV array of 0.96kWp in Oban

The peak power point of this 0.96kWp PV array is 0.88kW. It generates **965.05kWh** of electricity, while the acquired Excel tool result is 914.4kWh. Therefore, the Merit's result is **5.25% greater** than the Excel tool one.

7.3   Jersey

Jersey is a city situated in a small island that is very close to the Northern coast of France. Its geographical coordinates are; latitude=49°12'49" North and longitude=2°8'8" West. The optimal inclination angle for a PV installation is 36° [101]. The following table and graph demonstrate how this optimal angle is altered per month for a whole year time interval according to PVGIS.

Month	JAN	FEB	MAR	APR	MAY	JUNE	JUL	AUG	SEPT	OCT	NOV	DEC
Optimal inclination [deg]	64	59	46	33	20	12	16	28	43	54	64	67

Table 29: optimal PV array inclination in Jersey
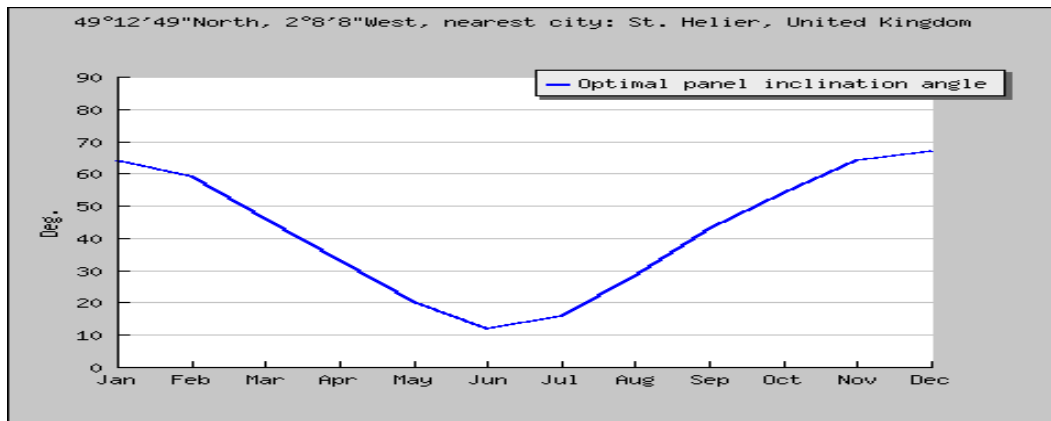
Figure 88: optimal PV array inclination in Jersey [101]

➤ **Excel tool**

Array inclination φ from the horizontal plane

As it occurred in Glasgow and in Oban the best array orientation was selected and the tilt angle φ from the horizontal varied in order to estimate its effect upon the PV system performance. Therefore the PV were facing south and angle φ was modified around the optimum inclination with 1° intervals (from φ=35° to φ=45°). In addition, φ=0° (horizontal inclined PV) and φ=90° (vertical inclined PV) were considered. The table and graph below show the acquired results.

γ=0° φ [degrees]	Annual Global Solar Radiation on Surface [kWh/m^2]	Annual output for a 0.96kWp PV array [kWh]	Annual PV array output [kWh/kWp]	Annual PV System Output with PR=0.75 [kWh/KWp]
0	1161.1	1153.5	1201.6	901.2
35	1242	1231.6	1282.9	962.2
36	1239.2	1229	1280.2	960.2
37	1236.2	1226.1	1277.2	957.9
38	1232.9	1223	1273.9	955.4
39	1229.3	1219.6	1270.3	952.8
40	1225.4	1215.8	1266.5	949.9
41	1221.3	1211.9	1262.4	946.8
42	1216.9	1207.6	1258	943.5
43	1212.2	1203.2	1253.3	940
44	1207.2	1198.4	1248.3	936.3
45	1202	1193.2	1243.1	932.3
60	1092.7	1088.5	1133.8	850.4
90	730.9	736.4	767.1	575.4

Table 30: Annual total radiation and PV performance in Jersey regarding tilt angle φ

from the horizontal plane

132
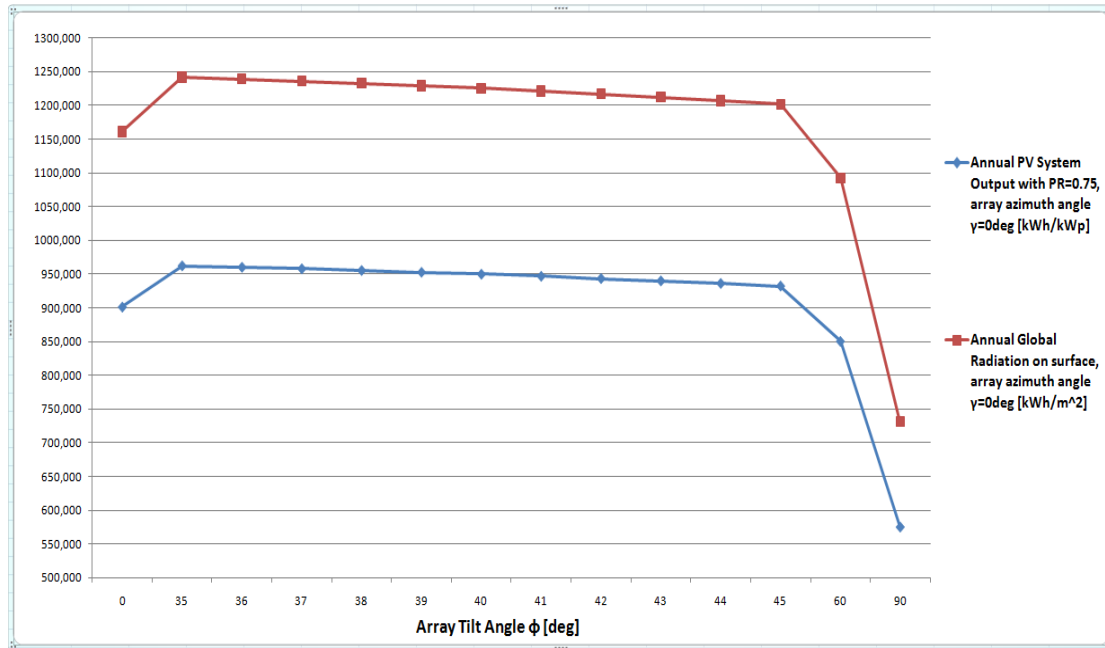
Figure 89: Annual total radiation and PV system output in Jersey regarding tilt angle φ from the horizontal plane

The graph proves that PV orientated around the optimal inclination generate about the same amount of electricity. The difference between 35° (optimal inclination) and 45° orientated PV is only 3.1%.

According to the developed Excel tool, the potential energy yield of a PV system installed horizontally / vertically / optimally is 901.2kWh / 575.4kWh / 962.2kWh respectively. Therefore an optimal inclined PV system generates 6.34% / 40.2% more electricity than a horizontal / vertical one. The difference between the vertical and the optimal inclined seems huge. These percentages are compared with the values from PVGIS site. According to PVGIS, the generated electricity (967kWh) by PV with optimal inclination is 12.31% / 30.71% larger regarding horizontal / vertical inclination. The deviation among PVGIS and tool percentages is neither big nor small but in logical margins and thus acceptable. Comparing again PVGIS with the tool, the divergence concerning the energy yield produced by optimally inclined PV is almost negligible, only 0.5%

Annual PV System Output with PR=0.75 [kWh/kWp]			
Inclination	**Horizontal**	**Vertical**	**Optimal**
PVGIS site	848	670	967
Excel tool	901.2	575.4	962.2

Table 31: Comparison of PVGIS and Excel tool for Jersey

133

Array orientation

Array orientation can be examined through variation of the array azimuth angle γ. An angle γ equal to 0° represents PV facing south which is the best possible orientation. Therefore, a due south PV installation, inclined at φ=35° is the best combination. In this sub-chapter, orientation varied from south to east (γ=-90°) with -10° steps, while inclination remained stable at 35°. The results are presented in the following table and graph.

φ=35° γ [degrees]	Annual Global Solar Radiation on Surface [kWh/m^2]	Annual output for a 0.96kWp PVarray [kWh]	Annual PV array output [kWh/kWp]	Annual PV System Output with PR=0.75 [kWh/KWp]
0	1242	1231.6	1282.9	962.2
-10	1225.6	1215.7	1266.3	949.7
-20	1203.8	1194.7	1244.4	933.3
-30	1176.8	1168.5	1217.2	912.9
-40	1145.7	1138.3	1185.8	889.3
-50	1112.	1105.6	1151.7	863.7
-60	1076.3	1070.9	1115.5	836.7
-70	1039.4	1035	1078.2	808.6
-80	1001.8	998.5	1040.2	780.1
-90	964.9	962.7	1002.8	752.1

Table 32: Annual total radiation and PV performance in Jersey regarding orientation
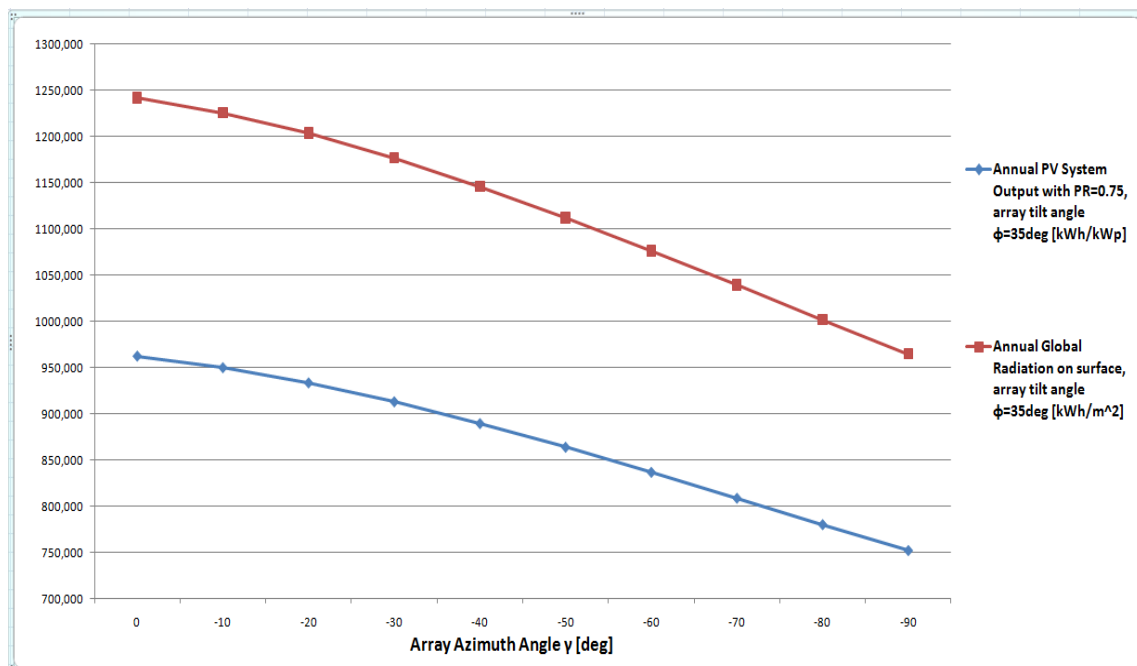
Figure 90: Annual total radiation and PV system performance in Jersey regarding orientation

It is noticeable from the graph that as surface azimuth angle increases; the potential energy yield reduces according to a slight slope curve. An average decrease of 2.5% every -10° step exists. An east orientated PV system generates about 21.83% less electricity than a south one (752.1kWh instead of 962.2kWh).

➢ **Merit**

The potential output of a 0.96kWp PV array according to software tool Merit and the Excel tool was compared in order to investigate tool's reliability. The Jersey climatic file was introduced into Merit database. The following graphs (derived from Merit) present the direct normal and diffuse horizontal solar radiation, the wind speed, the ambient temperature and the annual potential PV array output.
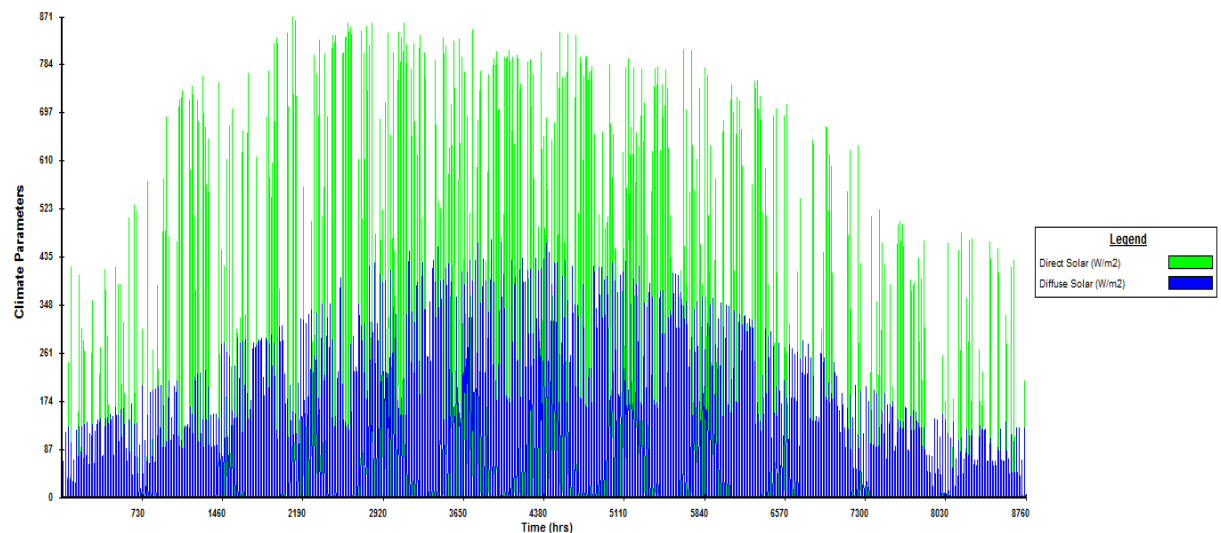
Figure 91: Direct normal and diffuse horizontal solar radiation in Jersey
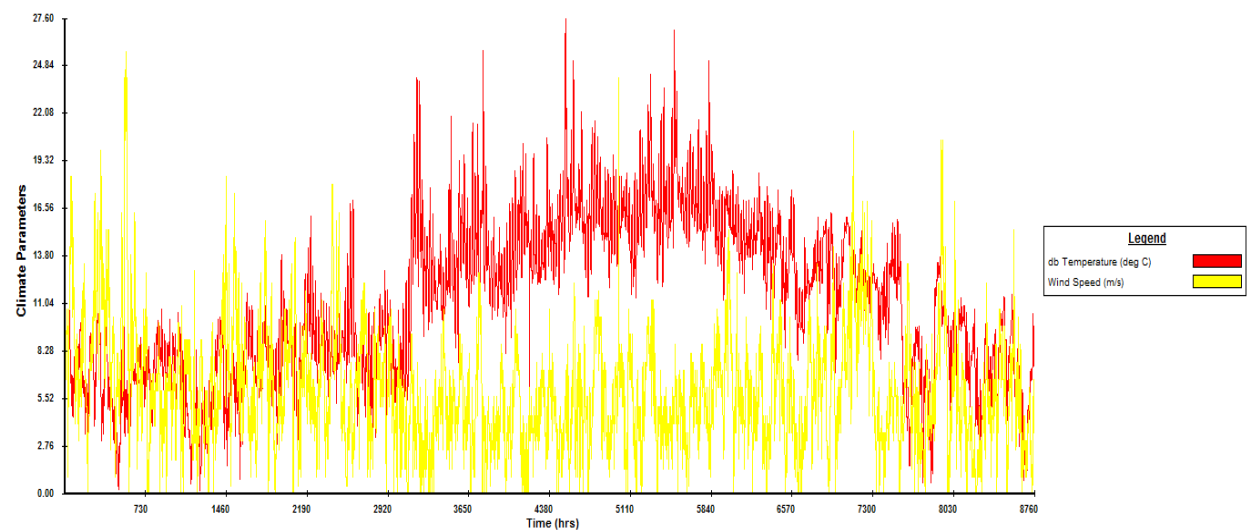
Figure 92: Ambient temperature and wind speed in Jersey
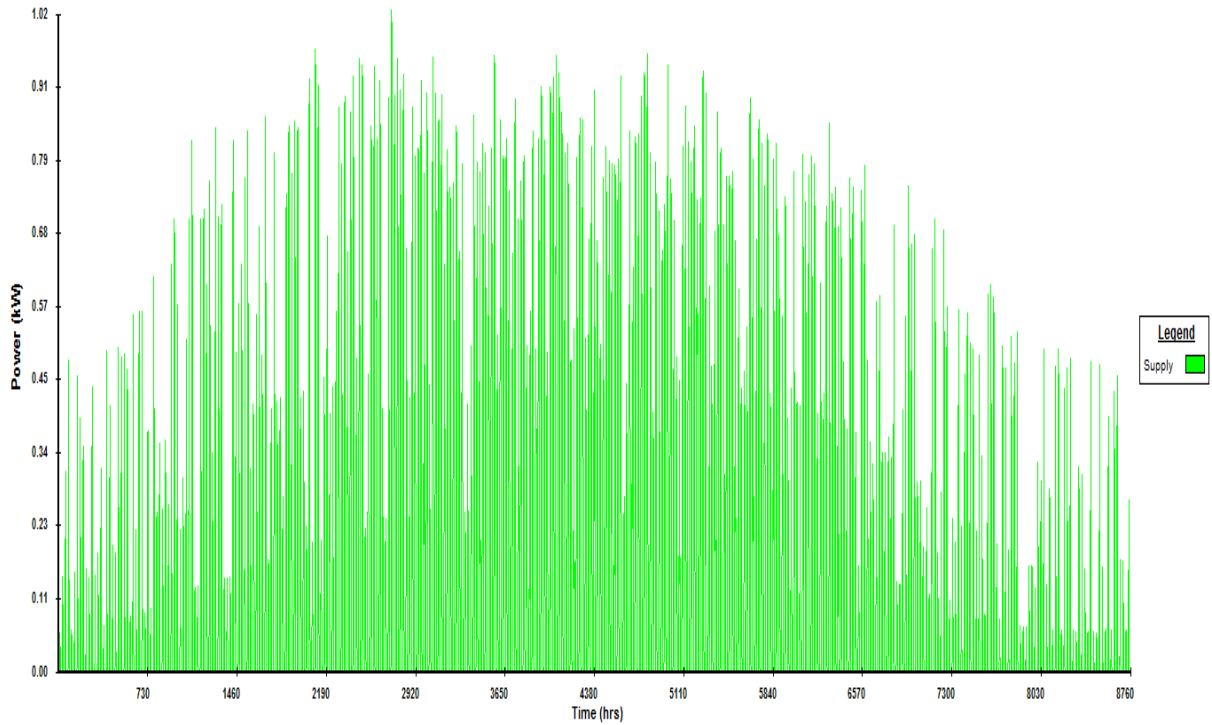
Figure 93: Annual output for a PV array of 0.96kWp in Jersey

The examined PV array generates **1.31MWh** annually and its peak power point is 1.02kW. Thus, Merit's result concerning the annual energy yield is **5.98% greater** than the 1231.6kWh obtained by the excel tool.

7.4 Athens

Athens is the capital of Greece and was selected in order to investigate how a hot warm southern Mediterranean climate affects the PV performance. Its geographical coordinates are; latitude=37°58'45" North and longitude=23°42'59" East. Its latitude declares that PV must be installed at a swallower angle compared to the previously mentioned regions. Thus, the optimal inclination angle is equal to 31° according to PVGIS [101] and it varies throughout the year in a way the following table and graph presents.

Month	JAN	FEB	MAR	APR	MAY	JUNE	JUL	AUG	SEPT	OCT	NOV	DEC
Optimal inclination [deg]	59	50	39	25	13	6	9	20	36	48	56	61

Table 33: optimal PV array inclination in Athens
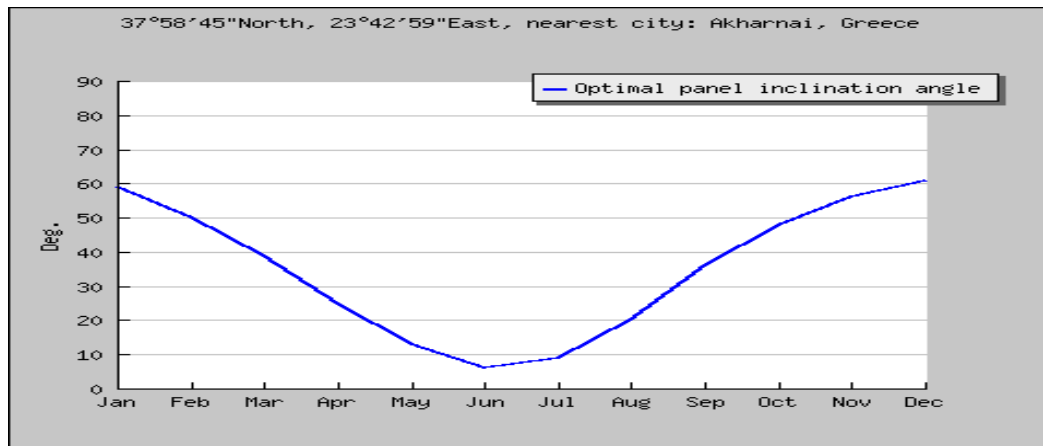
Figure 94: optimal PV array inclination in Athens [101]

➢ **Excel tool**

Array inclination φ from the horizontal plane

The array inclination angle φ from the horizontal was varied from 30° to 40° with a 1° step so as to examine the degree of influence of small deviations around the optimal inclination. In addition, results for φ=0° and φ=90° referring to horizontal and vertical inclined PV were acquired since the divergence of the energy yield among those inclinations as well as optimal is of great interest.

γ=0° φ [degrees]	Annual Global Solar Radiation on Surface [kWh/m^2]	Annual output for a 0.96kWp PV array [kWh]	Annual PV array output [kWh/kWp]	Annual PV System Output with PR=0.75 [kWh/KWp]
0	1613.6	1514	1577.1	1182.8
30	1720.9	1614.3	1681.6	1261.2
31	1717.8	1611.7	1678.8	1259.1
32	1714.2	1608.7	1675.7	1256.8
33	1710.6	1605.3	1672.2	1254.1
34	1705.7	1601.5	1668.2	1251.2
35	1700.8	1597.3	1663.9	1247.9
36	1695.4	1592.8	1659.1	1244.3
37	1689.7	1587.8	1654	1240.5
38	1683.5	1582.5	1648.4	1236.3
39	1676.8	1576.8	1642.4	1231.8
40	1669.7	1570.6	1636.1	1227.1
60	1443.8	1371.5	1428.6	1071.5
90	865.4	841.6	876.6	657.5

Table 34: Annual total radiation and PV performance in Athens regarding tilt angle φ from the horizontal plane

137
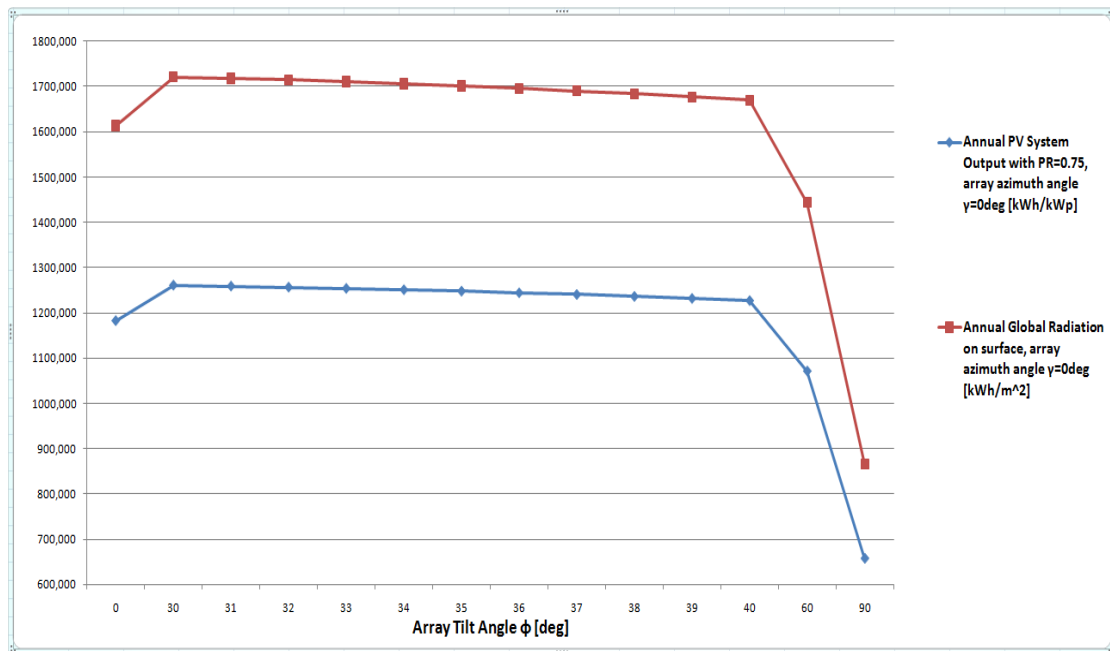
Figure 95: Annual total radiation and PV system output in Athens regarding tilt angle φ from the horizontal plane

The graph illustrates that there isn't such a huge difference in the energy yield between a PV system installed horizontally and optimally. Also the output is modified in a very small degree for inclinations similar to the optimum. However, its potential energy yield falls dramatically when it is horizontally installed.

A 30° inclined PV system (optimal inclination) generates 1261.2kWh electricity, while a horizontal and optimal one produce 1182.8kWh and 657.5kWh respectively. The above values interpreted in percentages mean a decrease of 6.21% and 47.87% respectively. The acquired results from the tool are then compared to the PVGIS site. According to PVGIS 1282kWh / 1161 kWh / 782 kWh are generated by a PV system which is optimally / horizontally and vertically inclined. Therefore a decrease of 9.44% instead of 6.21% and 39% instead of 47.87% exists.

Annual PV System Output with PR=0.75 [kWh/kWp]			
Inclination	**Horizontal**	**Vertical**	**Optimal**
PVGIS site	1161	782	1282
Excel tool	1182.8	657.5	1261.2

Table 35: Comparison of PVGIS and Excel tool in Athens

In other words, the deviations between the Excel tool and the PVGIS are 1.84%, 15.92% and 1.6% concerning a horizontal, vertical and optimal inclined PV system.

To sum up, the developed tool performs significantly well regarding PV inclined horizontally and optimally but a high divergence occurs regarding the vertically.

Array orientation

The array azimuth angle γ refers to array orientation. As in the previously mentioned regions, it was altered from γ=0° (due south) to γ=-90° (due east) with -10° steps, while the array inclination φ from the horizontal remained constant at 30° (optimal inclination).

φ=30° γ [degrees]	Annual Global Solar Radiation on Surface [kWh/m^2]	Annual output for a 0.96kWp PV array [kWh]	Annual PV array output [kWh/kWp]	Annual PV System Output with PR=0.75 [kWh/KWp]
0	1720.9	1614.3	1681.5	1261.2
-10	1711.2	1604.5	1671.3	1253.5
-20	1694.3	1588.1	1654.2	1240.7
-30	1672.3	1567.3	1632.6	1224.4
-40	1644.2	1541	1605.2	1203.9
-50	1610.3	1509.6	1572.4	1179.3
-60	1572.2	1474.6	1536.1	1152
-70	1531.2	1437.2	1497.1	1122.8
-80	1487.1	1397.1	1455.4	1091.5
-90	1440.7	1355.1	1411.6	1058.7

Table 36: Annual total radiation and PV performance in Athens regarding orientation
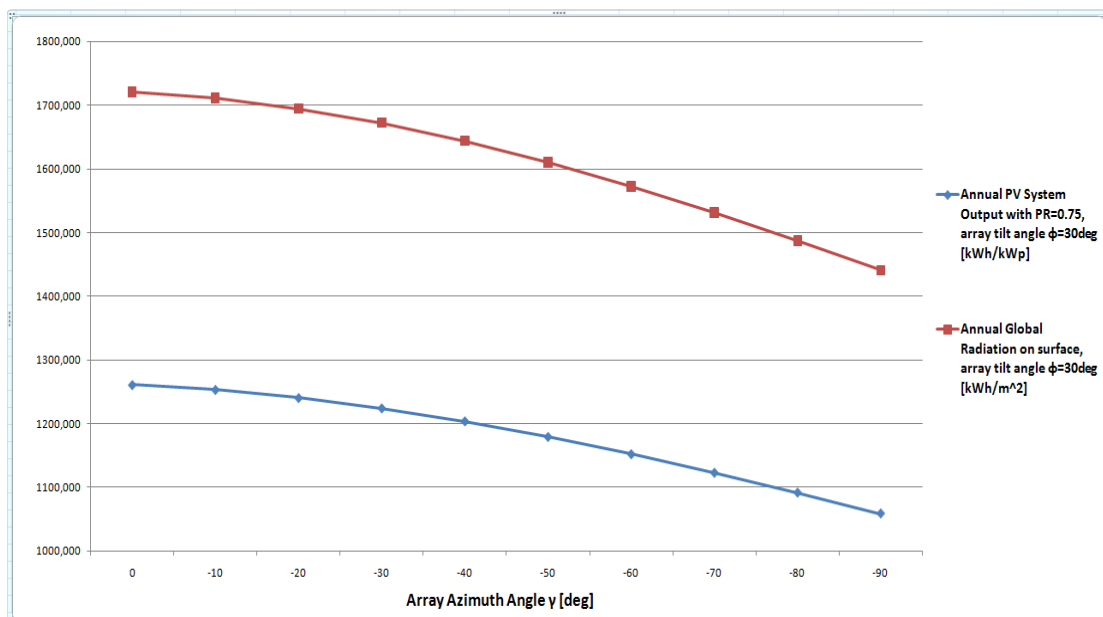
Figure 96: Annual total radiation and PV system performance in Athens regarding orientation

139

As the array's orientation further deviates from due south the potential energy yield is reduced steadily according to a slight sloped curve. A due east PV system generates 1058.7kWh, when one that faces south produces 1261.2kWh. Therefore, 16.06% more electricity is generated by optimally orientated PV.

➢ **Merit**

Merit was utilised as another means of evaluating the performance of the developed Excel tool concerning the PV array output. All the parameters (some shown in the first 2 graphs below) of Athens climatic data were introduced into its database and a 0.96kWp PV array was compared.
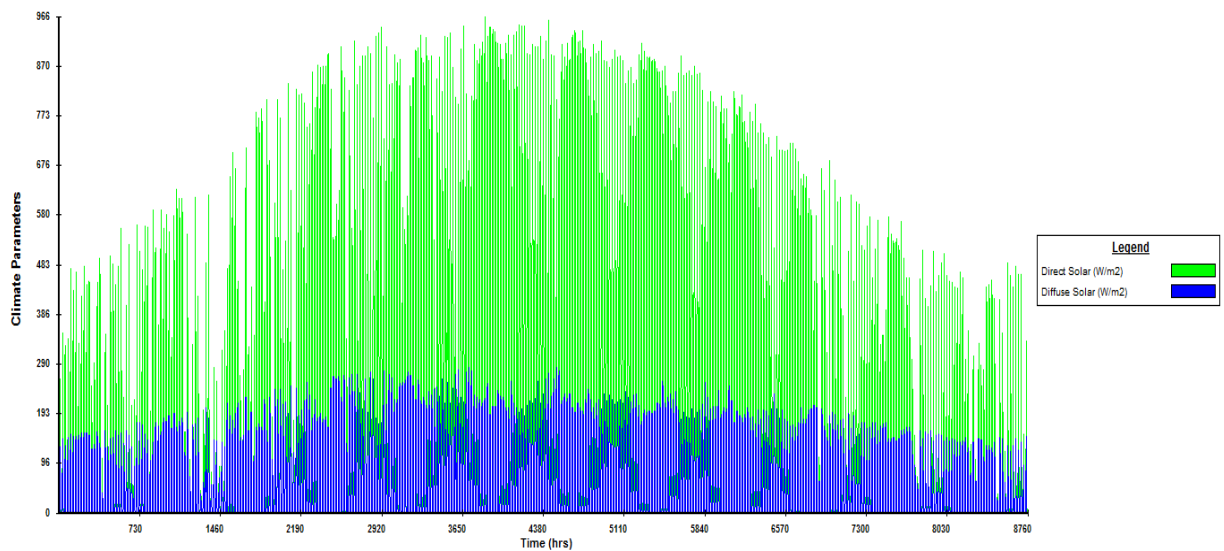
Figure 97: Direct normal and diffuse horizontal solar radiation in Athens
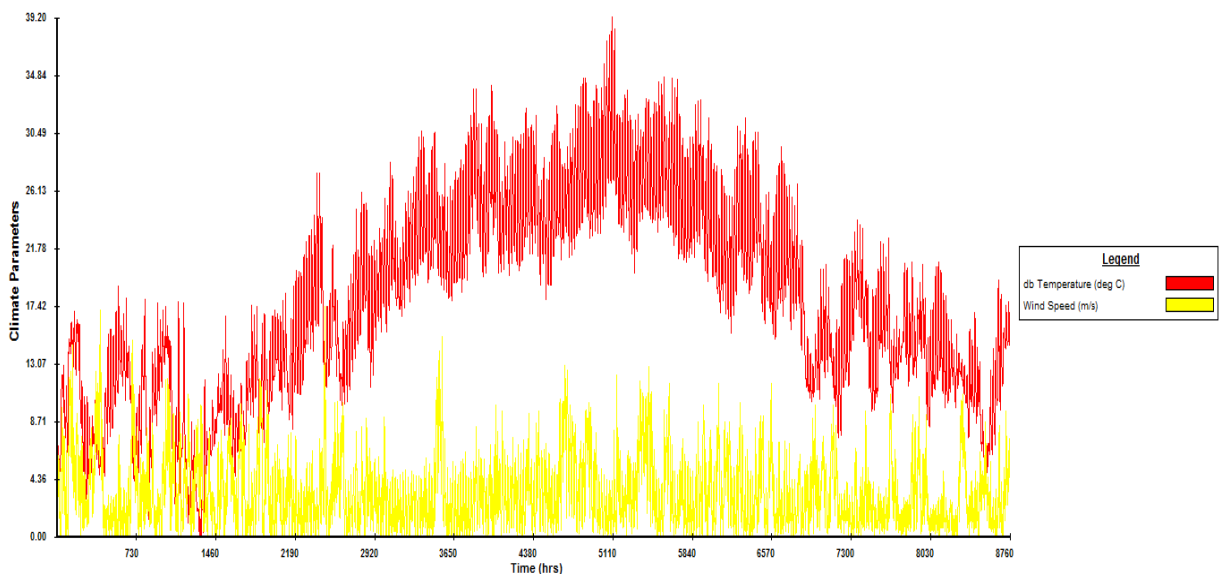
Figure 98: Ambient temperature and wind speed in Athens
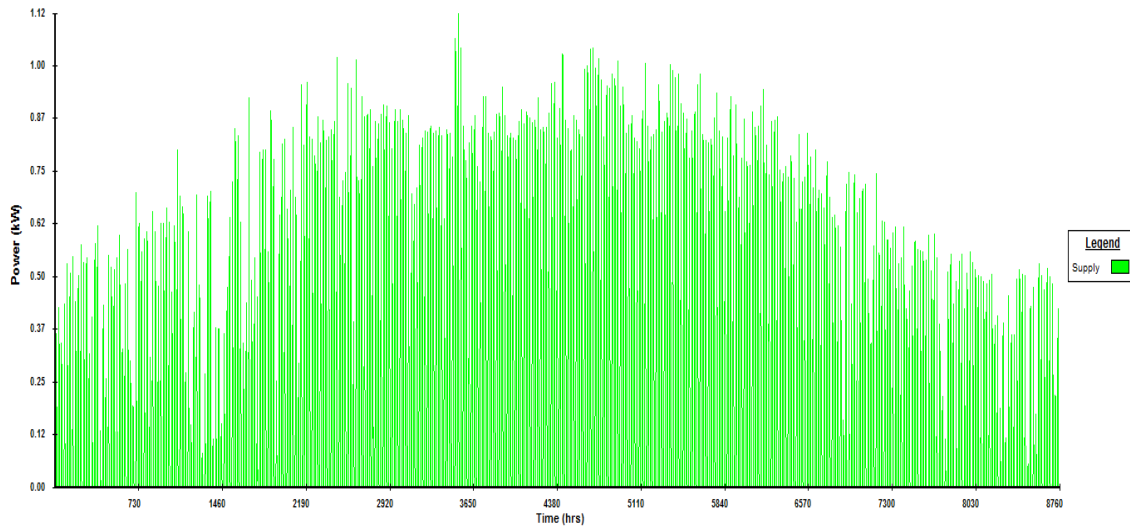
Figure 99: Annual output for a PV array of 0.96kWp in Athens

The investigated PV array generates annually **1.62MWh** and the peak power point is 1.12kW. This result is almost the same regarding the annual electricity yield of 1614.3kWh, acquired via the developed tool. Only a **0.35% deviation exists.**

7.5　Comparison of the 4 different regions

In the previous chapters (7.1, 7.2, 7.3, 7.4) the 4 selected European regions were analysed separately. Now, a comparison between these four sites would be made regarding their annual PV system output (results acquired by the Excel tool). Therefore, it would be analysed how the geographical coordinates of a location affect the potential energy yield concerning inclination as well as orientation.

Array inclination

The following table presents the PV performance in the 4 different regions concerning inclination (tilt angle φ) from the horizontal plane (the due south orientation kept fixed).

Annual PV System Output with PR=0.75 [kWh/kWp]			
γ=0° - Inclination φ	**Horizontal**	**Vertical**	**Optimal**
Glasgow	690.1	471.3	757.8
Oban	665.4	456.5	714.4
Jersey	901.2	575.4	962.2
Athens	1182.8	657.5	1261.2

Table 37: Comparison of PV performance in 4 regions concerning tilt angle φ from the horizontal plane

The conclusions drawn from the above table are:

- As it is anticipated, a PV installation in Athens generates the greatest amount of electricity among the investigated sites independently of its inclination angle provided that the same tilt angles are considered.

- An optimal inclined system in Athens generates 23.7% / 39.9% / 43.36% more electricity than in Jersey / Glasgow / Oban respectively.

- These percentages remain quite similar for horizontal inclined PV systems. They are modified into 23.81% / 41.65% / 43.74%, comparing Athens with Jersey / Glasgow / Oban respectively.

- A perceptible diversification is noticed in the rates per cent when the PV are mounted vertically. An appreciable decrease exists. The potential energy yield in Athens is now 12.49% / 28.32% / 30.5% greater compared to Jersey / Glasgow / Oban respectively.

It must be mentioned that the results emerging from the tool concerning the generated electricity by vertical inclined PV systems are always lower than the values provided by PVGIS. More specifically, the tool results in comparison with PVGIS are 15.38%, 8.15%, 14.13%, 15.92% lower in Glasgow / Oban / Jersey / Athens. This deviation may be attributed partially to the varying ground reflectance.

Array orientation

The table below shows how the annual PV system output is altered in the same 4 locations regarding the orientation γ. The optimal inclination angle was selected and remained stable for each site according to its latitude.

Annual PV System Output with PR=0.75 [kWh/kWp]				
Orientation γ	$\gamma=0°$ (south)	$\gamma=-40°$	$\gamma=-50°$	$\gamma=-90°$ (east)
Glasgow ($\varphi=35°$)	757.8	729.7	712.5	618.8
Oban ($\varphi=35°$)	714.4	676.1	660.1	584.6
Jersey ($\varphi=35°$)	962.2	889.3	863.7	752.1
Athens ($\varphi=30°$)	1261.2	1203.9	1179.3	1058.7

Table 38: Comparison of PV performance in 4 regions concerning orientation γ

According to the above table it is evident that:

- The highest amount of electricity is generated in Athens for every probable orientation angle

- As it is already stated several times, PV facing south produce the highest possible energy yield for all the different regions since they are all situated in the northern hemisphere.

- The further the divergence from the south, the less amount of electricity is generated.

- As it is pointed before, PV due south installed at the optimal inclination angle generate 23.7% / 39.9% / 43.36% more electricity in Athens in comparison with Jersey / Glasgow / Oban.

- A PV system with orientation angle γ=-40° in Athens has a 26.13% / 39.38% / 43.84% greater potential energy yield than one in Jersey / Glasgow / Oban.

- A due east PV installation located in Athens generates 28.96% / 41.54% / 44.77% more electricity compared to Jersey / Glasgow / Oban respectively.

- The final conclusion is that the percentages deviation among the 4 examined locations remains almost the same (1% - 2% difference) between the different orientation angles taking always into account that equal angles are compared each time.

8 Discussion & concluding remarks

8.1 General

In chapter 6 and 7 a large range of results have been presented based on equations, graphs and tables. To sum up, the most significant outcomes emerging from Troon case study and the comparison of the 4 European locations are the following:

➢ The majority of the available solar data provide the broadband solar irradiance on a horizontal surface measured by a pyranometer. The developed tool is very important since it divides the total amount of global irradiance into the direct and diffuse components (through the usage of clearness index) enabling the evaluation of incident radiation on a planar surface at any orientation and inclination angle. The calculated and measured radiation are very similar concerning their values as well as the shape, proving in that way the validity of the developed tool

➢ The peak values of solar radiation are presented at noon both in winter and summer but in summer the daytime is longer, the sky "clearer", and thus the intensity of the radiation higher.

➢ The absorbed solar energy by the PV array is converted into electricity and thermal losses to the surrounding environment. The radiated exchange to the neighbor surfaces and the sky are neglected.

➢ The PV array temperature is of great significance since it affects the PV efficiency and thus the generated electricity as well as the thermal losses to the surrounding environment. The most complex equation is selected for calculating the cell temperature since it provides more accurate and realistic results. Therefore, the PV array temperature T_{array} depends mainly upon the incident solar radiation and the heat exchange coefficient U_{PV}. U_{PV} is better estimated when both wind speed and wind direction are taken into account. The measured T_{array} is about 10°C / 15°C higher than the ambient temperature in winter / summer during daytime and 1°C - 2.5°C less during night. The estimated T_{array} is almost similar but always higher than the measured and rarely the divergence can even reach the 5°C in summer at noon time. The proportional deviation increase of calculated vs measured T_{array} regarding daytime hours with ambient temperature could provide

144

some insight on the significance of further researching cell temperature estimations accuracy especially in the case of southern European regions (cell efficiency may be drastically decreased mainly in summer).

➤ The PV array in Troon case study is tilted at an angle of 45° from the horizontal plane and orientated 17° east of south. The PV array output is proportional to the incident solar radiation. As a consequence, it is maximized at noon both in winter and in summer but summer's maximum is about 30% greater. Apart from the greater maximum the day time is longer in summer. These 2 factors lead to about 2.5 times higher potential energy yield during summer compared to winter. The most representative calculated PV array output (calculated with the help of calculated radiation and efficiency based upon the complex equation for T_{array}) is 0.19% smaller during the winter week and 10.44% larger during the summer week than the measured one. In general the calculated PV array output is 9.44% greater than the measured on a yearly basis (957.9kWh compared to 867.5kWh). Moreover, Merit's results concerning PV array output are higher than the measured both during the winter and the summer week. The deviation between Merit and tool results can be partially attributed to the neglect of radiant exchange between the PV array and the sky as well as to the existing inaccuracy in the division of global radiation to its diffuse and direct normal components. During the winter / summer week Merit estimates a PV array output of 14.42kWh / 38.41 kWh compared to the measured 11.858kWh / 30.246kWh. Another useful information provided by Merit is the poor demand supply matching rate in Troon case study; 42.29% and 33.09% during summer and winter week respectively.

➤ The installed inverter in Troon operated quite well. It was very reliable and its efficiency was most of the times equal or very close to the 93% specified by the manufacturer.

➤ The several parameters affecting the PV performance are analysed exhaustively in chapter 4. The effect of the array inclination and orientation angle regarding the potential energy yield is investigated in depth for Troon case study as well as for the 4 different selected climatic regions.

The tilt angle at which a PV array must be installed is of great relevance to the location's latitude. The optimal inclination angle varies throughout the year. In

general, shallower / steeper angles than the local latitude provide a higher energy yield in summer / winter respectively. This may be ascribed to solar elevation angle; low solar elevation angles in winter are responsible for higher planar inclination angles delivering higher yields, when as in summer higher solar elevation angles require modules installed at shallower angles. The results from the developed excel tool in Troon confirm this rule. The majority of PV systems are inclined at a fixed stable inclination. Therefore, the best choice is to install the PV systems at a specific angle that maximizes the potential energy yield during the whole year. This optimal inclination angle is equal to an intermediate value between the different optimal summer / winter angles. In latitudes between 45°-55° the optimal inclination angle increases modestly from 33°-36°. According to PVGIS this optimal angle in Troon (55°32'36" North) / Glasgow (55°51'56" North) / Jersey (49°12'49" North) is 37° / 37° / 36° respectively. Athens is situated in the southern, Mediterranean part of Europe. Its geographical coordinates are; latitude=37°58'45" North and longitude=23°42'59" East and that's why the optimal inclination is 31° (regarding PVGIS again). The relatively small deviation is justified by the fact that Southern regions absorb energy spread more uniformly around the year in contrast to the Northern climatic regions. The latter absorb energy mainly in summer (longer summer days compared to smaller latitudes - sky constantly overcast in winter time).

With regard to the array orientation all the investigated regions are in the northern hemisphere, therefore they must face south since the general acceptable rule is that PV face north in the southern hemisphere and south in the northern. It is evident from the tool results (regarding all the examined locations) that the further the deviation from due south, the higher the decreases in the potential energy yield. In addition, it is also proven through the Troon case study that this decrease is much larger in winter than in summer. The summer/winter divergence may be attributed to the different sun's orbit between summer and winter; the solar azimuth angle γ_s has a larger daily variation in summer.

➤ In Troon case study the PV array is orientated 17° east of south and inclined 45° from the horizontal plane. If the inclination angle is modified to 35° (provided that the orientation angle remained constant), an increase of 3.85% in the PV array output would appear. Additionally, if the PV array is installed due south (with

inclination angle equal to 45°), the potential energy yield would have increased by 8.67%.

➢ An optimal inclined and orientated PV system in Glasgow generates 757.8kWh according to the developed Excel tool. Merit's result is 3.97% higher. Assuming that PV face south, 8.93% / 37.8% more electricity is generated at optimal inclined compared to horizontal /vertical. Moreover, a due south PV system generates 18% more electricity than a due east, supposing optimal inclination.

➢ In Oban, PV generate 714.4kWh at optimal inclination and orientation, while Merit provides 5.25% higher output. Supposing optimal inclination, a due east PV system generates 18.2% less electricity in comparison with due south. Additionally, optimal inclined PV have a 6.86% / 36.1% greater energy yield than horizontal / vertical inclined (PV facing south).

➢ In Jersey the PV system output of an optimal orientated and inclined PV is 962.2kWh regarding the developed tool. Merit's result diverges by 5.98% (greater than the tool result). A horizontal / vertical inclined PV generated 6.34% / 40.2% less electricity than optimal inclined, presuming PV facing south. With regard to array orientation, a PV system facing south generates 21.83% more electricity than a PV system facing east (optimal inclination).

➢ The potential energy yield of an optimal inclined and orientated PV system in Athens is 1261.2kWh. The corresponding Merit result deviates only by 0.35%. A 6.21% / 47.87% divergence exists between optimal and horizontal / vertical PV respectively, taking into account that PV orientated due south. A due east PV system generates 16.06% less electricity than a due east one, comparing them at optimal inclination angle.

➢ The developed tool performs significantly well regarding the estimation of the potential energy yield of optimal and horizontal inclined PV. Its results are in great agreement with PVGIS. However, the values provided by PVGIS are much greater when vertical inclined PV systems are compared. Particularly, PVGIS values are 15.92% / 14.13% / 8.15% / 15.38% greater concerning Athens / Jersey / Oban / Glasgow respectively. This deviation may be explained partially by the varying ground reflectance.

➢ It is evident that the percentages deviation among the 4 investigated regions are almost equal (about 1% - 2% divergence) when optimal and horizontal inclined PV systems are compared. This conclusion is also valid concerning the undertaken comparison between the array inclination angles.

8.2   Future work

Equations focused on fully integrated PV installations

Equations applied in this project in order to estimate cell temperature are based on PV systems not fully integrated. BIPV /BIPV-T technologies shall become more popular in the near future as costs drop further (they shall become a more mature part of the PV market).

Thus it would be useful to introduce equations to the project's calculation tool further looking into the PV module's thermal envelope in case of fully integrated systems i.e. when PV cells are part of the roof or the wall building structure. Under these circumstances cell overheating may prove to be considerably higher leading to noticeable efficiency drops.

Exploitation of module thermal loads

On the other hand surplus heat gains may be utilized through heat exchange to warm up a building's interior in winter or dissipated outdoors in summer either through passive / mechanical ventilation or refrigerant liquid circulation after necessary modifications on their rear surfaces. Consequently it would be useful to research further optimum convective heat transfer scenarios and their effectiveness regarding BIPV system efficiency [90], [108].

In the latter case solar cooling might be a further option when temperature comfort levels are exceeded through the connection with solar adsorption / absorbtion chillers. Further work on estimating the efficiency of such hybrid systems would be appreciated especially in warmer climatic regions.

Thermal losses due to sky radiation

A parameter mentioned in the literature review but not introduced in the Excel tool's current state is heat radiated to the surrounding environment and sky dome Q_{sky}. Thus it would be interesting to include this parameter in a future upgraded version of the tool as heat emitted mostly to the sky may reduce noticeably the temperature deviation with the measured data.

Tool comparison to southern European case studies

Furthermore it would be very useful to compare tool estimations to actual PV system output data from grid connected partially or fully building integrated installations in central and southern Greece. Sunnyboy inverters have provided a web interface for energy producers to publish their energy yield and other output data for comparison reasons that could provide a first impression concerning the tool's accuracy level.

PV soiling effect

The evaluation of the effect of dust and pollutants soiling the modules external surfaces especially in urban environments should be looked into firstly in literature and then further researched upon.

Urban effect on diffuse – direct solar radiation and BIPV system output

Solar PV can decrease considerably the amount of energy required from conventional sources concerning the urban environment. In addition significant energy losses when distributing energy to the grid may be avoided when energy is consumed directly by buildings on site.

Researchers generally agree that air pollution may vary considerably the amounts of diffuse, direct and global radiation incident on building surfaces on an urban environment. It would be very useful to further research the frequency of days per year that such a phenomenon drastically alters the amount of solar diffuse and direct gains to a PV system. This may have significant impact on PV cell performance. More detail studies and annual high resolution databases concerning local microclimate conditions - local urban canyon wind velocities as well as building cell temperatures (2 parameters greatly affecting cell temperatures and thus PV system

performance) would lead to more accurate energy yield predictions regarding cities where smog is a common issue.

Some cell technologies' potential due to varying percentages between diffuse – direct radiation, wind speed and direction as well as neighbouring surfaces temperatures in an urban environment might lead to the recognition of currently underestimated PV cell types potential in the newly developed BIPV market. Therefore, further research on this subject constitutes an interesting challenge.

9   References

[1] UK Energy in Brief, July 2006, A national statistics publication, Department of Trade and Industry, London, Crown Copyright. DTI/Pub 8340/4.5k/07/06/NP. URN 06/220,http://webarchive.nationalarchives.gov.uk/+/http://www.berr.gov.uk/files/file32387.pdf

[2]   http://www.europarl.europa.eu/sides/getDoc.do?type=TA&reference=P6-TA-2007-0038&language=EN

[3] http://www.managenergy.net/buildings.html

[4] http://www.hm-treasury.gov.uk/prebud_pbr06_press01.htm

[5] http://www.info.gov.za/speeches/2007/07022115261001.htm

[6] http://www.sbsa.gov.uk/epc.htm

[7] Zaxarias Thomas, 2006, "*Renewable Energy Sources I*", University of Patras, Department of electrical and computer engineering, page 1, Patra

[8] Zaxarias Thomas, 2006, *"Renewable Energy Sources I"*, University of Patras, Department of electrical and computer engineering, page 69, Patra

[9] Duffie, Beckman, 1971, "*Solar Engineering of Thermal Process*", Second Edition, page 5, John Wiley & Sons, Inc

[10] Dr N Kelly, 2009 – 2010, "*Solar Energy Conversion*", slides from module 16915 Energy Resources and Policy, University of Strathclyde

[11] Zaxarias Thomas, 2006, *"Renewable Energy Sources I"*, University of Patras, Department of electrical and computer engineering, pages 72-73, Patra

[12] Duffie, Beckman, 1991, "Solar Engineering of Thermal Process", Second Edition, pages 81-82, John Wiley & Sons, Inc

[13] Santamouris, M. Asimakopulos, D. Asimakopoulos, 2001, *"Energy and Climate in the Urban Built Environment",* James & James Ltd

[14] A. Landsberg H.E., 1981, *"The urban climate"*, Academic press, New York and London.

[15] B. Oke T.R., 1988, *'The urban energy balance"*, Progress in physical Geography, Vol. 12, page 471.

[16] Hufty A., 1970, "*Les conditions de Rayonnement en Ville"*, In urban climates, WMO Techn. Note No. 108, pages 65-69, World meteorological station, Geneva.

[17] Chandler T.J., 1965, *"The climate of London"*, page 122, Hutschinson, London

[18] Unsworth, M. H. and Montheith, J. L., 1976, *"Aerosol and solar radiation in Britain"*, Quarterly journal of the royal meteorological society, Vol. 98, pages 778-797.

[19] East C., 1968, *"Comparison du Rayonnement Solaire en Ville et a la Campagne"*, Cahiers de geographie du Quebec, Vol. 12, pages 81-89.

[20] Nishizawa T. and Yamashita S., 1967, *"On attenuation of solar radiation in the largest cities"*, Japanese progress in climatology, Tokyo, pages 66-70.

[21] Davenport A.G., 1968, *"The dependences on wind loads on meteorological parameters"*, In proceeding of symposium of wind effects on structure, National physical laboratory, pages 53-102. HMSO, London.

[22] Wald L., 2006, Available Databases, Products and Services. In: Dunlop E., Wald L., Suri M. (Eds.), *"Solar Energy Resource Management for Electricity Generation from Local to Global Scale",* Nova Science Publishers., Hauppauge.

[23] Zaxarias Thomas, 2006, *"Renewable Energy Sources II"*, University of Patras, Department of electrical and computer engineering, page 150, Patra

[24]   http://upload.wikimedia.org/wikipedia/commons/8/8d/SolarCell-IVgraph3-E.PNG

[25] http://www.joju.co.uk/products.php

[26]http://www.n-e-renewables.org.uk/page/technologies/photovoltaics/pv_variations.cfm

[27] Christian N. Jardine, Gavin J. Conibeer and Kevin Lane, *"PV-COMPARE: Direct comparison of eleven PV Technologies at Two Locations in Northern and Southern Europe"*, Environmental Change Institute, Department of Physics, University of Oxford

[28] Martin A. Green, 1992, *"Solar Cells: Operating Principles, Technology and System Applications"*

[29] J.A. Eikelboom, M.J. Jansen, 2000, *"Characterisation of PV Modules of New Generations"*, ECN report ECN-C-00- 067

[30] ASTM E 892, *"Terrestrial Solar Spectral Irradiance at Air Mass 1.5 for a 37° Tilted Surface"*

[31] David L. King, William E. Boyson, and Jay A. Kratochvil, *"Analysis of Factors Influencing The Annual Energy Production of Photovoltaic Systems"*, Sandia National Laboratories, Albuquerque, NM. 87185-0752

[32] J.Wohlgemuth and S. Ransome, 2002 *"Performance of BP Solar Tandem Junction Amorphous Silicon Modules"*, New Orleans.

[33] http://www.solaressence.co.uk/Solar-Electric-PV-System-Schematic.html

[34] Kenji Otani, Koichi Sakuta, Tadatoshi Sugiura and Kosuke Kurokawa, *"Performance Analysis and Simulation on 100 Japanese Residential Grid-Connected PV Systems Based on Four Year Experience"*, 17th European Photovoltaic Solar Energy Conference and Exhibition 22-26 Oct. 2001, Munich, Germany

[35] Omer, SA, Riffat, SB and Wilson, R, 2000, *"BIPV design study for Renewable Energy Centre and Eco-Energy House"*, ETSU S/P2/00325/REP1.

[36] Electricity Association, 1998, *"Load profiles in the 1998 electricity supply market"*, Electricity Association, http://www. Electricity.org.uk/

[37] http://re.jrc.ec.europa.eu/pvgis/cmaps/eu_opt/pvgis_Europe-solar_opt_publication.png

[38] Marcel Suri, Thomas A. Huld, Ewan D. Dunlop, Heinz A. Ossenbrink, *"Potential of solar electricity generation in the European Union member states and candidate countries"*, European Commission, DG Joint Research Centre, Institute for Environment and Sustainability, Renewable Energies Unit, TP 450, via E. Fermi 1, I-21020 Ispra (VA), Italy

[39] IEC 61724, 1998, *"Photovoltaic System Performance Monitoring – Guidelines for Measurement, Data Exchange and Analysis"*, International Electrotechnical Commission, TC 82 – Solar photovoltaic energy systems

[40] M. van Cleef, P. Lippens, J.Call, *"Superior Energy Yields of UNI-SOLAR® Triple JunctionThin Film Silicon Solar Cells compared to Crystalline Silicon Solar Cells under Real Outdoor Conditions in Western Europe"*, - Bekaert ECD Solar Systems Europe

[41] E. Bura, N. Cereghetti, D. Chianese, A. Realini and S. Rezzonico *"PV Module Behavior in Real Conditions: Emphasis on Thin Film Modules"*, LEEE-TISO, CH-Testing Centre for PV-Modules, University of Applied Sciences of Southern Switzerland (SUPSI)

[42] David L. King, Jay A. Kratochvil, and William E. Boyson, *"Stabilization and Performance Characteristics of Commercial Amorphous Silicon PV Modules"*, Sandia National Laboratories, Albuquerque

[43] http://vivliothmmy.ee.auth.gr/58/1/diplomatiki.pdf

[44] Buchet E, 1988, *"Etude du dimensionnement et developpement d' un logiciel d' aide a la conception de systemes de production d' energie utilisant la conversion photovoltaıque de l' energie solaire"*, MS Thesis, University of Saint Jerome, Marseille, France.

[45] http://en.wikipedia.org/wiki/File:I-V_Curve_T.png

[46] Andreev VM, Grilikhes VA, Rumyantsev VD, 1967, *"Photovoltaic conversion of concentrated sunlight"* , London: Wiley, ISBN: 0471967653.

[47] Nolay P, 1987, *"Developpement d' une methode generale d' analyse des systemes photovoltaıques"*, MS Thesis, Ecole des Mines, Sophia-Antipolis, France

[48] Emery K, Burdick J, Caiyem Y, Dunlavy D, Field H, Kroposki B, et al., *"Temperature dependance of photovoltaic cells, modules and systems"* ,In: Proceeding of the 25th IEEE PV specialists conference, Washington, USA; 13–19 May 1996, pages 1275–1278.

[49] King DL, Eckert PE, *"Characterizing (rating) the performance of large photovoltaic arrays for all operating conditions"*, In: Proceeding of the 25th IEEE PV specialists conference, Washington, USA, 13–19 May 1996, pages 1385–1388.

[50] Wilshaw AR, Bates JR, Pearsall NM, *"Photovoltaic module operating temperature effects"*, In: Proceeding of Eurosun'96, Munich, Germany; 1996, pages 940–944.

[51] Krauter S, Araujo RG, Schroer S, Hanitsch R, Salhi MJ, Triebel C, Lemoine R., *"Combined photovoltaic and solar thermal systems for facade integration and building insulation"* , Solar Energy 1999; 67(4–6):239–48.

[52] Del Cueto JA., *"Comparison of energy production and performance from flat-plate photovoltaic module technologies deployed at fixed tilt"*, In: Proceeding of the 29th IEEE PV specialists conference, New Orleans, USA; 20–24 May 2002.

[53] Photon International, *"Market survey on solar modules"*, February 2004, pages 46–55.

[54] M. Mattei, G. Notton, C. Cristofari, M. Muselli, P. Poggi, 2006, *"Calculation of the polycrystalline PV module temperature using a simple method of energy balance"*, Laboratoire Systemes Physiques de l' Environnement, Universite de Corse Pascal Paoli, France, Renewable Energy, pages 553-567, available on line at linkinghub.elsevier.com/retrieve/pii/S096014810500073X

[55] Evans DL., 1981, *"Simplified method for predicting photovoltaic array output"*, Mechanical and Energy Systems Engineering, Arizona State University, U.S.A.; Solar Energy, Vol. 27, Issue 6, pages 555-560

[56] Evans DL, Florschuetz LW, 1977, *"Cost studies on terrestrial photovoltaic power systems with sunlight concentration"*, Mechanical Engineering Faculty, Arizona State University, U.S.A.; Solar Energy, Vol. 19, Issue 3, pages 255-262

[57] Nolay P, 1987, *"Developpement d' une methode generale d' analyse des systemes photovoltaıques"*, MS Thesis, Ecole des Mines, Sophia-Antipolis, France

[58] ASTM, 1998, *"Standard test methods for electrical performance of non concentrator terrestrial photovoltaic modules ad arrays using reference cells, standard E1036"*, West Conshohocken, PA: American Society for Testing and Materials

[59] Myers DR, Emery K, Gueymard C, *"Revising and validating spectral irradiance reference standards for photovoltaic performance"*, In: ASES/ASME solar 2002 conference proceeding, Reno, Nevada, 15–20 June 2002

[60] Furler G, Beckman WA, Klein SA, Modeling of a photovoltaic powered refrigeration system, personal communication of authors M. Mattei, G. Notton*, C. Cristofari,M.Muselli,P.Poggi, available on line *linkinghub.elsevier.com/retrieve/pii/S096014810500073X* .

[61] Sandnes B, Rekstad J, *"A photovoltaic/thermal (PV/T) collector with a polymer absorber plate, experimental study and analytical model"*, Solar Energy 2002, 72(1):63- 73.

[62] Jones AD, Underwood CP, 2001, *"A thermal model for photovoltaic systems"*, School of the Built Environment, University of Northumbria, Newcastle, UK; Solar Energy, Vol 70, Issue 4, pages 349–359.

[63] Schott T., *"Operational temperatures of PV modules"*, In: Proceeding of the 6th PV solar energy conference; 1985, pages 392–396.

[64] Pratt AW, 1981, *"Heat transmission in buildings"*, London: Wiley.

[65] Duffie JA, Beckman WA., 1974, "Solar energy thermal processes", London: Wiley, ISBN: 0-471-22371-9

[66] McAdams WC, 1954, *"Heat transmission"*, 3rd edition, New York: McGraw-Hill.

[67] R.J. Cole and N.S. Sturrock, 1977 *"The convective heat exchange at the external surface of buildings"*, Building and Environment, Vol. 12, Issue 4, pages 207–214.

[68] Barker G, Norton P, *"Predicting long-term performance of photovoltaic arrays using short-term test data and an annual simulation tool"*, NREL Report, CP-550-33601 presented at the Solar 2003 Conference: America's Secure Energy, Austin, Texas, 2003.

[69] Ingersoll JG, May 1986 *"Simplified Calculation of Solar Cell temperatures in Terrestrial Photovoltaic Arrays",* J. Solar Energy Eng. 1986, Vol. 108, Issue 2, pages 95–101.

[70] S. Krauter and R. Hanitsch, June 1996,*"Actual optical and thermal performance of PV-modules"*, University of Technology Berlin, Electrical Machines Institute; Solar Energy Materials and Solar Cells, Vol. 41-42, pages 557-574

[71] Dr. Siddig, A. Omer, Dr. R. Wilson & Professor S. B. Riffat, *"PV in Practice: A case study of Two PV Systems Installed on a Domestic and an Educational Buildings",* Institute of Building Technology, School of The Built Environment, The University of Nottingham, UK

[72] Meyer E.L., Ernest van Dyk E., *"The effect of reduced shunt resistance and shading on photovoltaic module performance",* Department of Physics, Fort Hare University, Alice, South Africa, In: Photovoltaic Specialists Conference, 2005. Conference Record of the Thirty-first IEEE

[73] Van Dyk, E.E. Meyer, E.L. Vorster, F. J. Leitch and A. W. R. Leitch, 2002, *"Long term monitoring of photovoltaic devices",* Renewable Energy, Vol. 25, pages 183-197

[74] Woyte A., Islam S, Belmans R., Nijs, J., *"Two years analytical monitoring results of an experimental photovoltaic system set-up under determined shadowing conditions"*, PV in Europe, Rome, Italy, October 7-11, 2002

[75] A.M. Reis, N.T. Coleman, M.W. Marshall, P.A. Lehman, and C.E. Chamberlin, *"Comparison of PV Module Performance Before and After 11-Years of Field Exposure",* Schatz Energy Research Center, Humboldt State University, Arcata, from the Proceedings of the 29th IEEE Photovoltaics Conference New Orleans, Louisiana, May 2002

[76] A.W. Czanderna and F.J. Pern, September 1966*"Encapsulation of PV modules using ethelyne vinyl acetate copolymer as a pottant: A critical review"*, Measurements and Characterization Branch, National Renewable Energy Laboratory, Golden, U.S.A; Solar Energy Materials and Solar Cells, Vol. 43, Issue 2, pages 101-181

[77] N.G. Dhere, N.R Raravikar, 2001, *"Adhesional shear strength and surface analysis of a PV module deployed in a harsh coastal climate"*, Solar Energy Materials and Solar Cells, Volume 67, pages 363-367

[78] D.L. King, J.A. Kratchovil, M.A. Quintana, and T.J. McMahon, *"Applications for infrared imaging equipment in photovoltaic cell, module, and system testing"*, Twenty-eighth IEEE PVSC, 2000, pages 1487-1490

[79] K. Machida, T. Yamazaki, and T. Hirasawa, *"Secular degradation of crystalline photovoltaic modules"*, Solar Energy Materials and Solar Cells, Volume 47, 1997, pages 149-153

[80] Allan Gregg, Terence Parker, and Ron Swenson, *'A "Real World" Examination of PV Systems Design and Performance"*, IEEE, Photovoltaic Specialist Conference and Exhibition, January 3-7, 2005, Lake Buena Vista, Florida USA

[81] Honsberg C., Bowden S., Photovoltaics CD ROM http://pvcdrom.pveducation.org/celloper/shunt.htm

[82] B. Decker, U. Jahn, 1997, *"Performance of 170 grid connected PV plants in Northern Germany-Analysis of yields and optimization potentials"*, Institut fur Solarenergieforshung Hameln-Emmertal/ISFH, Emmerthal, Germany; Solar Energy, Vol.59, Issues 4-6, April – June 1997, pages 127-133

[83] H. Haeberlin, C. Beutler, *"Normalised representation of energy and power for analysis of performance and on line error detection in PV systems"*, Proceedings 13th European Photovoltaic solar energy conference, Nice, France, 1995

[84] IEA-PVPS Task 2, *"Analysis of photovoltaic systems"*, Report IEA-PVPS T2-01:2000 (2000).

[85] M. C. Russell, *"Grid-Tied PV System Modeling: How and Why"*, 1st WCPEC, 1994, pages 1040-1043

[86] Decker B., Grochowski J. and Jahn U., 1993, *"Results and experience from the German 1000-Roof-Photovoltaic Programme- 140 Grid connected PV systems in Lower Saxony"*, linkinghub.elsevier.com/retrieve/pii/S0038092X96001326

[87] Basant Agrawal , G.N. Tiwari, *"Optimizing the energy and exergy of building integrated photovoltaic thermal (BIPVT) systems under cold climatic conditions"*, Centre for Energy Studies, Indian Institute of Technology Delhi, Hauz Khas, New Delhi India; Applied Energy, Vol. 87, Issue 2, February 2010, pages 417-426

[88] Swapnil Dubey, G.S. Sandhu and G.N. Tiwari, 2008, *"Analytical expression for electrical efficiency of PV/T hybrid air collector"*, Centre for Energy Studies, Indian Institute of Technology Delhi, Hauz Khas, New Delhi, India: Applied Energy, Vol. 86, Issue 5, May 2009, pages 697-705

[89] http://www.springerlink.com/content/n30m34rm24001630/fulltext.pdf

[90] G. Fraisse, C. Menezo and K. Johannes, *"Energy performance of water hybrid PV/T collectors applied to combisystems of Direct Solar Floor type"*, Solar Energy, Vol. 81, Issue 11, November 2007, pages 1426-1438, www.Elsevier.com

[91]http://www.renewableenergyworld.com/rea/news/article/2010/02/2010-french-tariffs-raise-price-for-solar-geothermal-and-biomass

[92] http://oxfordsolar.energyprojects.net/links/tech_pv.htm

[93]http://www.energygrants.co.uk/solar_power/solar-pv-feed-in-tariffs.html?gclid=COjv0Kyv9aQCFVBc4wod4ECZhA

[94]http://www.pv-tech.org/news/_a/helapco_outlines_change_in_greek_feed-in_tariff_laws/

[95] http://oxfordsolar.energyprojects.net/links/tech_pv.htm

[96]http://www.n-e
renewables.org.uk/page/technologies/photovoltaics/PV_costs_benefits.cfm

[97] EPIA European Photovoltaic Industry Assossiation, "Solar Generation IV - 2007, Solar electricity for over one billion people and two million jobs by 2020", http://www.epia.org

[98] http://www.solarbuzz.com/Moduleprices.htm

[99] T. Oozeki, T. Izawa, K. Otani, K. Kurokawa, *"An evaluation Method of PV systems",* 12th International photovoltaic science and engineering conference (PVSEC-12), Cheju, Korea 2001; Solar Energy Materials and Solar Cells, Vol.75, Issues 3-4, February 2003, pages 687-695

[100] Francesca Jane Born, 2001, *"Aiding Renewable Energy Integration through Complimentary Demand – Supply matching",* page 206,
www.esru.strath.ac.uk/Documents/PhD/**born_**thesis.pdf

[101] http://re.jrc.ec.europa.eu/pvgis/apps/radmonth.php?lang=en&map=europe

[102] http://re.jrc.ec.europa.eu/pvgis/cmaps/eu_hor/pvgis_solar_horiz_GB.png

[103] http://re.jrc.ec.europa.eu/pvgis/cmaps/eu_opt/pvgis_solar_optimum_GB.png

[104] http://re.jrc.ec.europa.eu/pvgis/cmaps/eu_hor/pvgis_solar_horiz_FR.png

[105] http://re.jrc.ec.europa.eu/pvgis/cmaps/eu_opt/pvgis_solar_optimum_FR.png

[106] http://re.jrc.ec.europa.eu/pvgis/cmaps/eu_hor/pvgis_solar_horiz_GR.png

[107] http://re.jrc.ec.europa.eu/pvgis/cmaps/eu_opt/pvgis_solar_optimum_GR.png

[108] http://www.springerlink.com/content/n30m34rm24001630/fulltext.pdf

[109] Francesca Jane Born, 2001, *"Aiding Renewable Energy Integration through Complimentary Demand – Supply matching",* page 319, www.esru.strath.ac.uk/Documents/PhD/**born_**thesis.pdf

[110] Vasiliki Perraki, 2004, *"Photovoltaic System Physics",* University of Patras, Department of electrical and computer engineering, Patra

[111] Vasiliki Perraki, 2006, *"New Photovoltaic Technologies"*, University of Patras, Department of electrical and computer engineering, Patra

[112] Tomas Markvart, *"Solar Electicity"*, University of Southampton, Second Edition, John Wiley & sons LTD, ISBN 0-471-98853-7

[113] Tom Markvart & Luis Castaner, *"Practical Handbook of Photovoltaic Fundamentals and Applications"*, 2003 ELSEVIER Ltd, ISBN 1-85617-390-9